Appendix I: The Predicted Three-Dimensional Structure of the Human D_2 Dopamine Receptor and the Binding Site and Binding Affinities for Agonists and Antagonists

The predicted 3D structure of the human D2 dopamine receptor and the binding site and binding affinities for agonists and antagonists

M. Yashar S. Kalani, Nagarajan Vaidehi, Spencer E. Hall, Rene J. Trabanino, Peter L. Freddolino, Mazhyar A. Kalani, Wely B. Floriano, Victor Wai Tak Kam, and William A. Goddard III*

Materials and Process Simulation Center, Beckman Institute, California Institute of Technology, Pasadena, CA 91125

Contributed by William A. Goddard III, January 6, 2004

Dopamine neurotransmitter and its receptors play a critical role in the cell signaling process responsible for information transfer in neurons functioning in the nervous system. Development of improved therapeutics for such disorders as Parkinson's disease and schizophrenia would be significantly enhanced with the availability of the 3D structure for the dopamine receptors and of the binding site for dopamine and other agonists and antagonists. We report here the 3D structure of the long isoform of the human D2 dopamine receptor, predicted from primary sequence using first-principles theoretical and computational techniques (i.e., we did not use bioinformatic or experimental 3D structural information in predicting structures). The predicted 3D structure is validated by comparison of the predicted binding site and the relative binding affinities of dopamine, three known dopamine agonists (antiparkinsonian), and seven known antagonists (antipsychotic) in the D2 receptor to experimentally determined values. These structures correctly predict the critical residues for binding dopamine and several antagonists, identified by mutation studies, and give relative binding affinities that correlate well with experiments. The predicted binding site for dopamine and agonists is located between transmembrane (TM) helices 3, 4, 5, and 6, whereas the best antagonists bind to a site involving TM helices 2, 3, 4, 6, and 7 with minimal contacts to TM helix 5. We identify characteristic differences between the binding sites of agonists and antagonists.

With the implication of G protein-coupled receptor (GPCR) in many diseases (1, 2), the need to solve the high-resolution 3D structure of this class of integral membrane proteins to enable structure-based drug design is an important problem in structural biology. Despite the importance of solving the structure of the GPCRs, the only experimental 3D structure available for a GPCR is bovine rhodopsin. This lack of structures is because the GPCRs are bound to the membrane, making it difficult to express in sufficient quantities for crystallization.

To provide structural and ligand binding information on GPCRs, we have been developing first-principles computational techniques for predicting the 3D structure of GPCRs using only the amino acid sequence (MembStruk) and for predicting binding site and binding energy of various ligands to GPCRs (HierDock). Using these techniques, we have reported the structure of olfactory receptors (3, 4), bovine rhodopsin (4, 5), and other GPCRs (4).

Dopamine neurotransmitter plays a critical role in cellular signaling processes responsible for information transfer in neurons functioning in the nervous system (6, 7). Dopamine receptors (DR) belong to the superfamily of GPCRs, and to date there are five reported sequences for the human DR with multiple isoforms for each. The DRs may be subdivided based on their pharmacological behavior into the D1-like and the D2-like subfamilies, and these are ideal targets for treating schizophrenia and Parkinson's disease; therefore, development of improved remedies would be significantly enhanced with the availability of the 3D structure for the DR and of the dopamine-binding site. We report here the 3D structure of the long isoform of human D2 DR, hereafter referred to as D2DR, predicted from primary sequence using the MembStruk (3–5) and HierDock (3) first-principles theoretical and computational techniques. The structure is validated by predicting the binding site and relative binding affinities of dopamine, three known dopamine agonists, and seven known antagonists. The predicted binding site for dopamine and agonists is located between transmembrane (TM) helices 3, 4, 5, and 6, whereas the best antagonists bind to a site involving TM helices 2, 3, 4, 6, and 7 with minimal contacts to TM helix 5. The predicted binding sites contain the critical residues for binding dopamine and several antagonists that have been identified by mutation studies and give relative binding affinities that correlate well with experiment.

Computational Methods

All calculations for the protein used the DREIDING force field (FF) (8) with charges from CHARMM22 (9) unless specified otherwise. The non-bond interactions were calculated by using the cell multipole method (10) in MPSim (11). The ligands were described with the DREIDING FF using Gasteiger charges (12). For the lipids we used the DREIDING FF with QEq charges (13). All of the calculations treated the solvent (water) using the analytical volume generalized born approximation to the Poisson–Boltzmann solvation model (14).

MembStruk Structure Prediction Method for D2DR. The MembStruk procedure (MembStruk3.5), used to predict the 3D structure of D2DR, is described in ref. 5. Here we detail the steps that are relevant to the prediction of D2DR. The various steps of the MembStruk3.5 as applied to D2DR are as follows.

TM prediction. The seven TM boundaries of the human D2DR were predicted by using the TM2nd5 (5) procedure. Seven sequences with bit score >200 in the BLAST (15) search of D2DR were aligned by using multiple sequence alignment program CLUSTALW (16). This alignment was used to predict the TM regions using TM2nd5. It is shown that the seven TM helices in D2DR are of different lengths and also are different in length from the corresponding TM helices of bovine rhodopsin.

Optimization of the relative translation of helices. TM2nd5 also predicts the hydrophobic center along each helix used for optimizing the relative translational position of the TM helices. The seven canonical α-helices were built and the helical axes were positioned based on the 7.5-Å 3D density map of frog rhodopsin (17). Relative translational orientation of the helices was optimized by fitting the hydrophobic center of each helix predicted using TM2nd5 to a plane.

Optimization of rotational orientation of the TM regions. The rotational orientation of the canonical helices was also optimized by using

Abbreviations: GPCR, G protein-coupled receptor; FF, force field; TM, transmembrane; DR, dopamine receptor.

*To whom correspondence should be addressed. E-mail: wag@wag.caltech.edu.

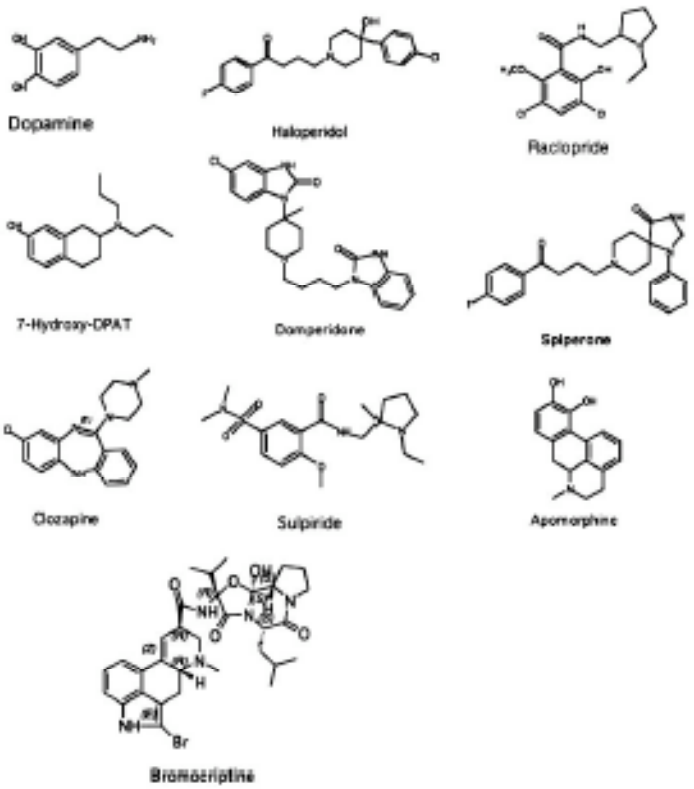

Fig. 1. Ten agonists and antagonists studied for the human dopamine D2 receptor.

the multisequence hydrophobicity moments of the middle third of each helix about their maximum hydrophobic center. This analysis yielded a clear consensus on which residues should contact the membrane and which residues should face the receptor interior.

Optimization of helical bends and kinks. The kinks and bends in each canonical helix was optimized with Newton–Euler inverse mass operator (NEIMO) torsional dynamics (18, 19) or Cartesian dynamics (described with the Dreiding FF and Charmm22 charges) for 500 ps at 300 K constant temperature, and we picked the minimum energy conformation from the dynamics. The helical bundle now has helices with bends and kinks. The rotational orientation of these noncanonical helices was further optimized by using both the procedure in step 4 followed by energy-based optimization called "Roumin" described in ref. 5. In the energy-based rotational orientation optimization, we performed systematic rotations on all of the seven helices over 5° at a time and over a small grid of rotation angles −50° to 50°. At each rotation angle the side chains were added by using the side chain placement program SCWRL 5.0 (20) followed by potential energy minimization using conjugate gradients to 0.1 kcal/mol per Å rms deviation in force per atom. Steps 3, 4, and 6 are part of a systematic search algorithm for optimum translational and rotational orientation, and these steps allow conformational search and aid in getting over large energy barriers between various conformations of the TM barrel.

Equilibration of the optimized TM barrel. The optimized TM barrel structure from the previous step was then equilibrated by immersing it in a bilayer barrel of dilauroylphosphatidyl choline, and the full system was optimized with rigid body quaternion molecular dynamics, treating each molecule as a rigid body for 50 ps at a constant temperature of 300 K using the MPSim code (11).

Loop addition and final optimization. The interhelical loops were built by using WHATIF (21), and disulfide bonds were formed between Cys-107 in TM3 and Cys-182 in extracellular loop 2. This full system was then optimized with the conjugate gradient minimization technique to 0.1 kcal/mol per Å rms in force.

Prediction of Ligand Binding Sites and Binding Energies. *Ligand structure preparation.* The 10 ligands shown in Fig. 1, were built with CHEMDRAW, and the 2D structure was converted to 3D structures by using POLYGRAF software. These ligands consist of agonists dopamine, 7-hydroxydipropylaminotetralin, apomorphine, and bromocriptine and antagonists like clozapine, domperidone, haloperidol, etc. We have categorized the antagonists

studied here into two classes: (*i*) class I, clozapine-like bulky antagonists; and (*ii*) class II antagonists that have two aromatic or ring moieties connected by a flexible linker with a protonated amine group as in haloperidol. Hydrogens were added, and Gasteiger charges were assigned to all of the ligands with appropriate protonated states. We then minimized the potential energy of each ligand using conjugate gradients to an rms deviation in force of 0.1 kcal/mol per Å.

Receptor prediction method for D2DR. HierDock protocol is a hierarchical strategy ranging from coarse grain docking to fine grain optimization for docking ligands in proteins and determining their putative binding site. This method has been tested for various GPCRs (3–5, 22), outer membrane protein A (23), and globular proteins (24–28). (The protocol has been described in detail in these references.) The version of HierDock used in this study is described in ref. 4. In brief, the various steps of HierDock version 2.0 protocol is as follows:

1. First we carried out a coarse grain docking procedure to generate a set of conformations for ligand binding in the receptor. Here we used DOCK4.0 (29) to generate and score 500 conformations, of which 50 (10%) were selected by using a buried surface area cutoff of 90% and energy scoring from DOCK4.0 for further analysis. The options used in DOCK4.0 are flexible ligand docking with torsion drive and allowing four bumps with the protein.
2. The 50 best conformations selected for each ligand from step 1 were subjected to all-atom minimization keeping the protein fixed but the ligand movable. The solvation energy of each of these 50 minimized conformations was calculated by using analytical volume generalized born continuum solvation method (14). Then the five best scoring conformations based on the potential energy of the ligand in the protein were selected from these 50 conformations for the next step.
3. Next we optimized the structure of the receptor/ligand complex allowing the structure of the protein to accommodate the ligand. This was essential to identify the optimum conformations for the complex. The all-atom receptor/ligand energy minimization was performed on the 10 structures from the previous step. Using these optimized structures, we calculated the binding energy (BE) using the equation

$$BE = PE\ (\text{ligand in protein}) - PE\ (\text{ligand in solvent}) \quad [1]$$

as the difference between the potential energy (PE) of the ligand in the protein and the potential energy of the ligand in water. The energy of the ligand in water is calculated by using DREIDING FF and analytical volume generalized born continuum solvation method.
4. Next we selected, from the five structures from step 3, the one with the maximum number of hydrogen bonds between ligand and protein. For this structure we used the SCREAM side chain replacement program (V.W.T.K., N.V., and W.A.G., unpublished observations) to reassign all side chains for the residues within 5 Å in the binding pocket. (This uses a side-chain rotamer library of 1,478 rotamers with 1.0-Å resolution, with the all-atom DREIDING energy function to evaluate the energy for the ligand–protein complex.) The binding energy of all of the five optimized complexes was calculated by using Eq. 1.

Locating the putative binding site. To locate the binding site of dopamine, other agonists, and antagonists, we scanned the entire D2DR structure without any knowledge of the binding site. The molecular surface of the entire receptor structure was mapped by using autoMSutility of DOCK4.0. Spheres were generated to fill up the void regions of the entire receptor using the sphgen utility of DOCK4.0. The program PASS (30) was then used to locate plausible centers of large void regions in the receptor. The spheres that were within 5.0 Å of these centers were clustered for docking of ligands. For D2DR we obtained nine regions where we applied the only steps 1 and 2 of the HierDock protocol. The best energy conformation for each ligand in each region was selected based on (*i*) location of the binding site (those in the intracellular loop or completely in the extracellular loop regions were omitted for D2DR), (*ii*) buried surface area (90% cutoff value was used), and (*iii*) interaction energy of the ligand with the protein. If more than one region scanned had similar energies within a certain tolerance factor, then both those regions were chosen as putative binding regions. A tolerance of 30 kcal/mol was used because the minimization of the ligand with the fixed receptor structure was done for only a fixed number of 50 conjugate gradient steps. Using this procedure we found similar putative binding sites for agonists and class I antagonists whereas, the predicted binding sites for class II antagonists were different. Class II antagonists had three contiguous regions with the best bound conformation having ligand–receptor interaction energies within 30 kcal/mol of each other. Hence, for these long antagonists we merged the spheres of these three regions together as the putative binding site. Because the number of spheres in the merged region was high (>300), the sphere density was thinned to ~100 spheres. Details of these energies will be published elsewhere.

Prediction of binding sites and binding energies. Once the putative binding sites were determined for agonists and antagonists, all of the agonists and antagonists were docked into their respective putative binding regions using HierDock protocol steps 1–4, and the best five bound structures for each ligand was chosen. Herein we performed iterative docking: the structure with side chains replaced and minimized was used in the generation of a new sphere set, and the target ligands were redocked to this optimized binding structure by performing HierDock procedure steps 1–4. This iterative HierDock procedure optimizes the side chain conformation of the residues in the binding site for ligand binding.

Results and Discussion

Fig. 2 shows the 3D structure of the human D2 DR predicted by using MembStruk3.5 and the predicted binding site of dopamine determined by using HierDock. During the scanning procedure to determine the binding site, only one site was found to be favorable for binding dopamine and other agonists studied. Thus, the predicted binding site of dopamine is located in the top third of the 7-TM barrel involving TM domains 3–6. The amino acid residues within 5.5 Å of the dopamine binding site in D2DR are shown in Fig. 3. We found the following residues to be essential for binding of dopamine in the human D_2 receptor.

1. Asp-114 in TM3. The carboxyl group of the aspartate forms a tight salt bridge (2.6 Å) with the primary amino group of dopamine. This residue is conserved over all five human DRs, as well as in all human biogenic amine receptors. Mutation studies have implicated this residue in the direct binding of the dopamine to D2DR (31).
2. Ser-193 and Ser-197 in TM5. These residues hydrogen-bond to the metahydroxyl (2.7 Å) and parahydroxyl (2.7 Å) groups, respectively, of the catechol ring of dopamine, playing an essential role in recognizing dopamine. These two residues are conserved over all five human DRs and have been shown to be involved in direct binding of ligand through mutation studies (31). Ser-194 is also conserved over all five human DRs, and mutation studies indicate that it is involved in binding of the ligand. In our structure, Ser-194 is hydrogen-bonded to the backbone nitrogen of residue 192 rather than dopamine. However, Ser-194 might serve as an alternate to Ser-193 in hydrogen bonding to the metahydroxyl group of the catechol for the slightly modified structure of the receptor that might result from activation.

BIOPHYSICS

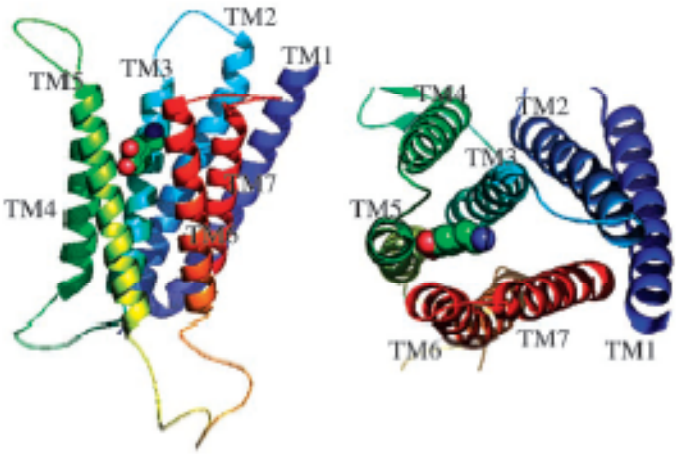

Fig. 2. Predicted binding site of dopamine (shown in spheres) in the predicted structure of human dopamine D2 receptor.

3. Phe-110, Met-117, Cys-118 (TM3), Phe-164 (TM4), Phe-189, Val-190 (TM5), Trp-386, Phe-390, and His-394 (TM6) form a mostly hydrophobic pocket for dopamine. We find Trp-386 and Phe-390 of the conserved WXXFF motif on TM6 to be within the 4.5-Å binding pocket, but Phe-389 is 7.2 Å away from dopamine.

Thus, the predicted binding site (involving TM domains 3–6) is in excellent agreement with the residues determined experimentally to be involved in binding (31–38). This provides a good validation of the predicted structure for D2DR and of the predicted binding site of dopamine. We also carried out full HierDock predictions for the binding sites of three other known agonists: apomorphine, 7-hydroxydipropylaminotetralin, and bromocriptine, and we found very similar active sites. In particular, all dopamine agonists bind tightly to both Ser-193 and Ser-197 in TM5 in addition to Asp-114 in TM3 just as in dopamine. These predicted structures can be further tested by selective mutation of some of the additional residues we have identified in the active site.

To further validate the predicted structure for D2DR, we used the HierDock procedure to predict the binding conformation and the binding energy for seven well-studied antagonists. We found two classes of antagonists.

Class I antagonists (exemplified by clozapine) occupy the region between TM3, TM4, TM5, and TM6 (the agonist binding pocket). Thus, clozapine makes (*i*) a 2.8-Å salt bridge to Asp-114 (TM3); (*ii*) a hydrogen bond to Ser-193 (TM5) (3.2 Å) but not to Ser-194 or Ser-197; (*iii*) heteroatom interactions with Trp-386 (TM6) (3.1 Å); and (*iv*) a mostly hydrophobic pocket shown in Fig. 4 formed by Val-87 and Trp-90 (TM2), Phe-110, Leu-113, Val-115, Met-117, and Cys-118 (TM3), Phe-164 (TM4), Phe-189, Val-190, Ser-194, and Ser-197 (TM5), Phe-382, Trp-386, Phe-389, and Phe-390 (TM6), and Thr-412, Trp-413, Tyr-416, and Ser-419 (TM7).

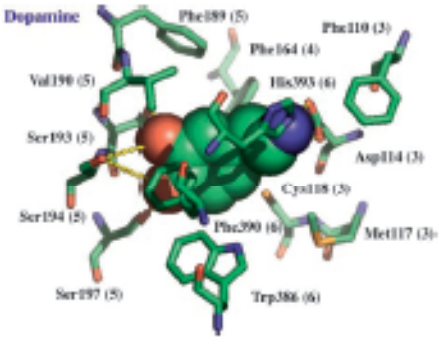

Fig. 3. Residues within 5.5 Å of the dopamine binding site in the human dopamine D2 receptor. The numbers shown in parentheses are the TM helix to which the residue belongs. The distance between Asp-114 and the primary amine group in dopamine is 2.6 Å. Ser-193 on TM5 makes a 2.7-Å hydrogen bond with the *m*-etahydroxyl group, and Ser-197 makes a 2.7-Å hydrogen bond to the parahydroxyl group of dopamine.

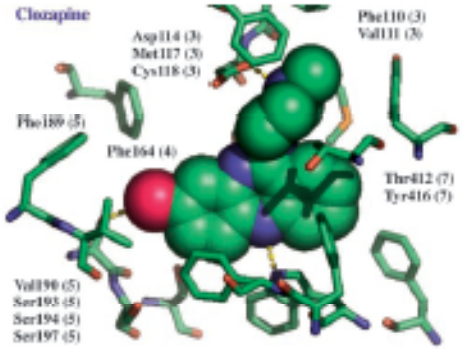

Fig. 4. Residues within 5.5 Å of clozapine bound to human D2DR.

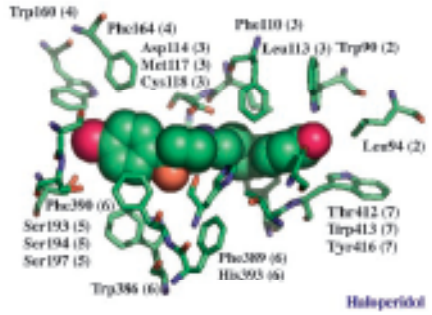

Fig. 5. Residues within 5.5 Å of haloperidol bound to human D2DR.

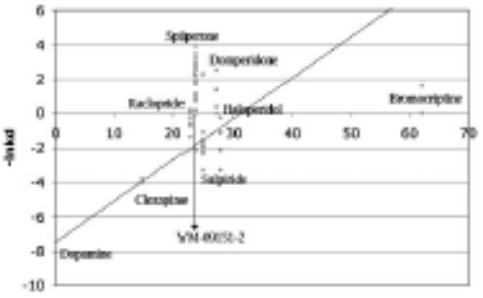

Fig. 6. Comparison of calculated dissociation energies of known agonists and antagonists with the experimental dissociation constants (40–45, 1) for the D2r receptor. Here, a more positive energy indicates stronger binding. No corrections to the binding energies were made for zero-point energy, dynamics, or entropy.

Class II antagonists, exemplified by haloperidol, occupy the region between TM2, TM3, TM6, and TM7, with minimal contacts to TM4 and TM5. Thus, haloperidol makes (*i*) a 2.8-Å salt bridge to Asp-114 (TM3); (*ii*) a hydrogen bond (3.2 Å) to Ser-197 (TM5) (3.2 Å) but not to Ser-193 or Ser-194; (*iii*) heteroatom interactions with Trp-386 (TM6) at 3.8 Å and Trp-90 (TM2) at 3.0 Å; and (*iv*) a mostly hydrophobic pocket (as shown in Fig. 5) provided by Val-87, Val-91, and Leu-94 (TM2), Phe-110, Leu-113, Val-115, Met-117, and Cys-118 (TM3), Trp-160 and Phe-164 (TM4), Phe-189, Val-190, and Val-196 (TM5), Trp-386, Phe-389, Phe-390, and His-393 (TM6), and Ser-409, Thr-412, Trp-413, Tyr-416, and Val-417 (TM7). Other class II antagonists with very similar binding sites include spiperone and sulpiride. Interestingly, many class II antagonists have been shown to cross-react with other aminergic receptors and other class A GPCRs. In some GPCRs, CCR1 for example, the conserved TM3 Asp is replaced with a longer-chain Glu. From distant restraints and structural considerations it appears that a longer linker alkyl chain in the ligand would push the protonated amino group of the ligand closer to the TM2 and TM7, and this would alleviate binding to those GPCRs with a conserved Asp in this position on TM3. However, this longer alkyl chain ligand would bind better and be specific to GPCRs with Glu in this position.

The residues we found to be important for binding of agonists and antagonists are consistent with all available data from substituted cysteine accessibility method, radiolabeling, and mutation experiments (31) on these receptors. All seven antagonists make a tight contact to Asp-114 in TM3, but none forms strong contacts to both Ser residues in TM5, in contrast with our observation that all agonists have strong coupling to Asp in TM3 and both Ser in TM5. This finding suggests that strong coupling between TM3 and TM5 is essential for dopaminergic transduction (consistent with experiments showing that hydrogen bonds to both conserved serines of TM5 are essential for dopamine activation) (31–38). The predicted structures for antagonists lead to a weakening of the coupling between TM3 and TM5 and (particularly for class II antagonists) prevent motion between TM3 and TM6.

Based on the criteria that a salt bridge to TM3 and two hydrogen bond contacts to TM5 are both essential for activation, whereas the salt bridge and one hydrogen bond are important for antagonists, we can categorize all ligands as agonists and antagonists. This criteria correctly predict the nature of all ligands studied here. Recently, an agonist in the dipropylaminotetralin series (39) has been reported with no hydroxyl group. This finding may indicate a more complicated criterion for agonists and will be studied later.

Fig. 6 shows the calculated binding energies (relative to dopamine), for the nine ligands with experimental dissociation constants. It is clear from Fig. 6 that the experimental dissociation constant varies over several orders of magnitude for a given ligand. However, we found that the calculated binding energies always fall within the range of experimental binding constants. Taking dopamine into account, the best correlation factor calculated is 0.92, with bromocriptine as an outlier to this fit. This good correlation provides additional validation for the predicted structure and function.

In summary, the predicted first-principles structure of D2DR leads to correct predictions of the critical residues for binding dopamine and several antagonists (as identified by mutation studies) and gives relative binding affinities that correlate fairly well with experiments. It should be noted that, given the approximations in the calculated binding energies, one can distinguish a very good binder from a very weak binder but cannot distinguish ligands with similar binding affinities. We found that the predicted binding site of dopamine and other agonists is located between TM helices 3, 4, 5, and 6 but that the strongest binding antagonists bind to a site involving TM helices 2, 3, 4, 6, and 7, with minimal contacts to TM5. We identify the characteristic differences between the binding sites of agonists and antagonists, because agonists involve tight binding between helices 3 and 5 whereas antagonists involve tight binding of ligand between TM helices 3 and 6.

The validation of the predictions for D2 justify carrying out similar studies to predict the structures and ligand binding to the other four human DRs. We hope that this study will provide a basis for designing agonists and antagonists selective to binding to just one of the five DR subtypes, which could be of tremendous value in treating dopamine-related diseases while minimizing side effects.

[1] Lee, T. & Seeman, P. (1979) *Soc. Neurosci. Abstr.* **5**, 652 (abstr.).

This research was initiated with support from the Army Research Office (ARO) Multidisciplinary University Research Initiative (MURI) and was completed with support from National Institutes of Health Grants BRGRO1-GM625525, R29AI40567, and HD36385. The computational facilities were provided by a Shared University Research grant from IBM and Defense University Research Instrumentation Program grants from ARO and the Office of Naval Research (ONR). The facilities of the

Materials and Process Simulation Center are also supported by the Department of Energy in addition to the National Science Foundation, ARO-MURI, MURI-ONR, General Motors, ChevronTexaco, Seiko-Epson, the Beckman Institute, and Asahi Kasei.

1. Pierce, K. L., Premont, R. T. & Lefkowitz, R. J. (2002) *Nat. Rev. Mol. Cell Biol.* 3, 639–650.
2. Schoneberg, T., Schulz, A. & Gudermann, T. (2002) *Rev. Physiol. Biochem. Pharm.* 144, 143–227.
3. Floriano, W. B., Vaidehi, N., Singer, M., Shepherd, G. & Goddard, W. A., III (2000) *Proc. Natl. Acad. Sci. USA* 97, 10712–10716.
4. Vaidehi, N., Floriano, W. B., Trabanino, R. J., Hall, S. E., Freddolino, P. L., Choi, E. J., Zamanakos, G. & Goddard, W. A., III (2002) *Proc. Natl. Acad. Sci. USA* 99, 12622–12627.
5. Trabanino, R. J., Hall, S. E., Vaidehi, N., Floriano, W. B., Kam, V. & Goddard, W. A., III (2004) *Biophys. J.*, in press.
6. Jackson, D. M. & Westfind-Danielsson, A. (1994) *Pharmacol. Ther.* 64, 291–369.
7. Strange, P. G. (1996) *Adv. Drug Res.* 28, 313–351.
8. Mayo, S. L., Olafson, B. D. & Goddard, W. A., III (1990) *J. Phys. Chem.* 94, 8897–8909.
9. MacKerell, A. D., Bashford, D., Bellott, M., Dunbrack, R. L., Evanseck, J. D., Field, M. J., Fischer, S., Gao, J., Guo, H., Ha, S., *et al.* (1998) *J. Phys. Chem. B* 102, 3586–3616.
10. Ding, H. Q., Karasawa N. & Goddard, W. A., III (1992) *J. Chem. Phys.* 97, 4309–4315.
11. Lim, K.-T., Brunett, S., Iotov, M., McClurg, R. B., Vaidehi, N., Dasgupta, S., Taylor, S. & Goddard, W. A., III (1997) *J. Comput. Chem.* 18, 501–521.
12. Grubmüller, J. & Tavan, P. (1998) *Tetrahedron* 54, 3239–3250.
13. Rappé, A. K. & Goddard, W. A., III (1991) *J. Phys. Chem.* 95, 3358–3363.
14. Zamanakos, G. (2001) Ph.D. thesis (California Inst. of Technology, Pasadena).
15. Altschul, S. F., Madden, T. L., Schaffer, A. A., Zhang, J., Zhang, Z., Miller, W. & Lipman, D. J. (1997) *Nucleic Acids Res.* 25, 3389–3402.
16. Thompson, J. D., Higgins, D. G. & Gibson, T. J. (1994) *Nucleic Acids Res.* 22, 4673–4680.
17. Schertler, G. F. X., Villa, C. & Henderson, R. (1998) *Nat.* 12, 508–518.
18. Vaidehi, N., Jain, A. & Goddard, W. A., III (1996) *J. Phys. Chem.* 100, 10508–10517.
19. Jain, A., Vaidehi, N. & Rodriguez, G. (1993) *J. Comp. Phys.* 106, 258–268.
20. Bower, M., Cohen, F. E. & Dunbrack, R. L., Jr. (1997) *J. Mol. Biol.* 267, 1268–1282.
21. Vriend, G. (1990) *J. Mol. Graphics* 8, 52–56.
22. Freddolino, P. L., Kalani, M. Y. S., Vaidehi, N., Floriano, W. B., Trabanino, R. J., Kam, V. & Goddard, W. A., III (2004) *Proc. Natl. Acad. Sci. USA*, in press.
23. Datta, D., Vaidehi, N., Floriano, W. B., Kim, K. S., Pramanik, N. V. & Goddard, W. A., III (2002) *Proteins Struct. Funct. Genet.* 50, 213–221.
24. Datta, D., Vaidehi, N., Xu, X. & Goddard, W. A., III (2002) *Proc. Natl. Acad. Sci. USA* 99, 2636–2641.
25. Zhang, D., Vaidehi, N., Goddard, W. A., III, Danner, J. F. & Debe, D. (2002) *Proc. Natl. Acad. Sci. USA* 99, 6579–6584.
26. Wang, P., Vaidehi, N., Tirrell, D. A. & Goddard, W. A., III (2002) *J. Am. Chem. Soc.* 124, 14442–14443.
27. Kobayashi-Inskay, P. M., Vaidehi, N., Floriano, W. B. & Goddard, W. A., III (2003) *J. Phys. Chem B* 107, 11549–11557.
28. Floriano, W. B., Vaidehi, N., Zamanakos, G. & Goddard, W. A., III (2004) *J. Med. Chem.* 47, 56–71.
29. Ewing, T. A. & Kuntz, I. D. (1997) *J. Comput. Chem.* 18, 1175–1189.
30. Bandy, G. P., Jr., & Stouten, P. F. (2000) *J. Comput. Aided Mol. Des.* 14, 383–401.
31. Shi, L. & Javitch, J. (2002) *Annu. Rev. Pharmacol. Toxicol.* 42, 437–467.
32. Shi, L., Simpson, M. M., Ballesteros, J. A. & Javitch, J. A. (1999) *Biochemistry* 38, 12339–12348.
33. Hu, D., Ballesteros, J. A., Weinstein, H., Chen, J. & Javitch, J. A. (1999) *Biochemistry* 38, 11278–11285.
34. Javitch, J. A., Ballesteros, J. A., Weinstein, H. & Chen, J. (1998) *Biochemistry* 37, 998–1006.
35. Simpson, M. M., Ballesteros, J. A., Chiappa, V., Chen, J., Suehiro, M., Hartman, D. S., Godel, T., Snyder, L., Sakmar, T. P. & Javitch, J. A. (1998) *Mol. Pharmacol.* 56, 1116–1126.
36. Javitch, J. A., Shi, L., Simpson, M. M., Chen, J., Chiappa, V., Vukica, I., Weinstein, H. & Ballesteros, J. A. (2000) *Biochemistry* 39, 12190–12199.
37. Dijkstra, D., Rodenhuis, N., Vermeulen, E. S., Pugsley, T. A., Wise, L. D. & Wikstroem, H. V. (2002) *J. Med. Chem.* 45, 3022–3031.
38. Tozer, M. M., Frolunowitz, N., Stec, B. & DuHaud, C. J. (1994) *J. Med. Chem.* 37, 2874–2888.
39. Payne, S. L., Johansson, A. M. & Strange, P. G. (2002) *J. Neurochem.* 82, 1106–1117.
40. Bandy, M., Martres, M. P. & Schwartz, J. C. (1979) *Naunyn-Schmiedeberg's Arch. Pharmacol.* 308, 221–227.
41. Leysen, J. E., Gommeren, W. & Laduron, P. M. (1978) *Biochem. Pharmacol.* 27, 307–316.
42. Burt, D. R., Creese, I. & Snyder, S. H. (1976) *Mol. Pharmacol.* 12, 800–812.
43. Seeman, P. (1992) in *Receptor Tables: Drug Dissociation Constants for Neurotransmitters and Transmitters* (SZ Research, Toronto).
44. Watson, S. & Arkinstall, S. (2001) *The G Protein-Linked Receptor Factsbook* (Academic, London), Vol. 2.
45. Seeman, P. & Tallerico, T. (1998) *Mol. Psychiatry* 3, 123–134.

Appendix II: Predicted 3-D Structure for Human β2 Adrenergic Receptor and the Binding Site for Agonists and Antagonists

Predicted 3D structure for the human β2 adrenergic receptor and its binding site for agonists and antagonists

Peter L. Freddolino, M. Yashar S. Kalani, Nagarajan Vaidehi, Wely B. Floriano, Spencer E. Hall, Rene J. Trabanino, Victor Wai Tak Kam, and William A. Goddard III*

Materials and Process Simulation Center, California Institute of Technology, Pasadena, CA 91125

Contributed by William A. Goddard III, January 5, 2004

We report the 3D structure of human β2 adrenergic receptor (AR) predicted by using the MembStruk first principles method. To validate this structure, we use the HierDock first principles method to predict the ligand-binding sites for epinephrine and norepinephrine and for eight other ligands, including agonists and antagonists to β2AR and ligands not observed to bind to β2AR. The binding sites agree well with available mutagenesis data, and the calculated relative binding energies correlate reasonably with measured binding affinities. In addition, we find characteristic differences in the predicted binding sites of known agonists and antagonists that allow us to infer the likely activity of other ligands. The predicted ligand-binding properties validate the methods used to predict the 3D structure and function. This validation is a successful step toward applying these procedures to predict the 3D structures and function of the other eight subtypes of ARs, which should enable the development of subtype-specific antagonists and agonists with reduced side effects.

The adrenergic receptors (ARs) are the class of G protein-coupled receptors (GPCR) responsible for mediating the effects of the catecholamines epinephrine and norepinephrine. There are currently nine known human ARs, partitioned into three subclasses: α1 (three subtypes located in vascular smooth muscle, the digestive tract, liver, and postsynaptically in the CNS), α2 (three subtypes located pre- and postsynaptically in the CNS, and in a wide variety of peripheral sites), and β (three subtypes located primarily in cardiac, vascular, and adipose tissues, respectively).

The members of this receptor class mediate a wide variety of physiological responses, including vasodilation and vasoconstriction, heart rate modulation, regulation of lipolysis, and blood clotting. These diverse and important functions make the adrenergic receptors a tempting pharmaceutical target, but attempts to create effective and specific drugs acting on these receptors have been slowed down by the lack of a 3D structure for any GPCR other than the bovine photoreceptor rhodopsin. The focus of this paper is the β2AR, which is targeted by agonist therapy in the treatment of asthma. Unfortunately, β2 agonists also exhibit cross-reactivity with the other βARs, causing side effects such as increased heart rate and blood pressure (1). Three-dimensional models of the ARs would be extremely useful in the design of subtype-specific pharmaceutical compounds. In addition, the ARs have been thoroughly studied experimentally so that there are ample data for validating the structural predictions, which may in turn provide improved understanding for the superfamily of GPCRs.

We report here the predicted 3D structure of β2AR, which we use to predict detailed binding sites of agonists and antagonists to β2AR. This is an excellent case for validation because there is a wealth of experimental data on ligand-binding sites and mutational analysis with which to compare our results (2, 3).

We use the MembStruk computational method to predict the atomic level tertiary structure of GPCRs using only the primary sequence, and we use the HierDock method to predict the binding site and binding energy of ligands binding to the protein (4, 5). These methods have been validated for bovine rhodopsin (5, 6) where the predicted binding site is in good agreement with the experimental results. In addition, recent results for human D2 dopamine receptor (unpublished data) lead to predicted binding sites and energies for dopamine and D2 agonists and antagonists that are in good agreement with experimental data.

Materials and Methods

Structure Prediction of GPCRs: The MembStruk Method. The MembStruk method (version 3.5) for predicting the structure of transmembrane proteins consists of the following steps (5, 6). All energy and force evaluations use the DREIDING force field, CHARMM22 (7) charges for the protein, and QM charges for the ligands.

Transmembrane (TM) prediction (TM2ndS). First, we predict the seven TM domains by using hydropathicity analysis combined with information from sequence alignments. The extent of each TM region is predicted by using sequence alignments of 14 input sequences having sequence identities ranging from 40% to over 90%. Then, we calculate the average hydrophobicity for every residue position over all these sequences in the multiple sequence alignment while averaging over a window size 12 to 20 residues. The baseline for this profile serves as the threshold value for determining the TM regions.

Position of maximum hydrophobicity. For each TM region, we identify lipid-accessible residues from the sequence alignments (less conserved residues) and from analysis of the hydrophobicity maxima in the sequence. This position of maximum hydrophobicity is used to estimate the relative translational orientation of the helices. We use the Eisenberg scale for hydrophobicity (8).

Assembly of the helix bundle and optimization of the translational orientation of the helices. The helical axes are oriented according to the 7.5-Å electron density map of frog rhodopsin (9). The initial relative translational orientation of each helix is optimized on placing into the same fitting plane all of the hydrophobic centers obtained from step 2.

Optimization of helical bends and kinks. We construct canonical helices for the predicted TM segments and optimize the structures of the individual helices using energy minimization followed by fast torsional Newton–Euler inverse mass operator method (NEIMO) dynamics (10, 11) for 500 ps. This procedure optimizes the bends and kinks in each helix.

Monte Carlo optimization of rotational orientation of the helices. The initial rotational orientation of each helix (about its axis) is determined by setting the direction of the net hydrophobic moment of the middle one-third of each helix (about its hydrophobic center). Because molecular dynamics is not likely to surmount the barriers that might separate one good rotational state from another, we carry out a systematic search in which each helix is rotated through a grid of rotational angles, for each value of which the other six helices are optimized sequentially.

Abbreviations: AR, adrenergic receptor; GPCR, G protein-coupled receptor; TM, transmembrane; CRMS, rms deviation in alpha carbon coordinates.

*To whom correspondence should be addressed. E-mail: wag@wag.caltech.edu.

www.pnas.org/cgi/doi/10.1073/pnas.0308075101

This sampling allows the system to surmount rotational energy barriers to sample various possible rotational minima for each helix. This rotational optimization is carried out for each helix in turn (over the same grid) until there is no longer a change.

Optimization of the assembled helical bundle with an explicit lipid environment. The optimized helix bundle is further equilibrated by immersing the protein into a lipid bilayer and performing rigid body molecular dynamics (12, 13). The helix bundle surrounded by a lipid bilayer was optimized by using rigid body dynamics.

Loop building. We construct the full GPCR protein by adding interhelical loops and disulfide bridges to the helix bundle using WHATIF (14). In β2AR, the second intracellular loop (60 residues between TM5 and TM6) was truncated by 23 residues in the middle of the loop (residues 241–264) because such large loops are quite flexible, leading to a multiplicity of conformations with similar energies. Because this deletion is in the middle of a 60-residue loop region and because this loop is on the intracellular side, these changes should have little effect on the structure of the TM region. Currently, we omit modeling the amino and carboxyl terminal regions.

Optimization of the final model. We optimize the final structure by using conjugate gradient minimization of all atoms in the structure but with lipid fixed.

Validation: Structure prediction for bovine rhodopsin. The only GPCR with an experimental 3D crystal structure is bovine rhodopsin (15, 16), making this the best structure for validating MembStruk. Trabanino *et al.* (6) showed that the TM regions of the MembStruk-predicted structure for rhodopsin agree with the crystal structure, to 2.85 Å CRMS (rms deviation in alpha carbon coordinates) for all of the main chain atoms. This good agreement with the crystal structure indicates that the MembStruk procedure predicts the helical regions reasonably well, without using any knowledge of the crystal structure.

Functional Prediction of GPCRs: The HierDock Protocol. The HierDock ligand-screening protocol follows a hierarchical strategy for examining ligand-binding conformations and calculating their binding energies. The steps are as follows.

Scanning. We carry out a coarse grain docking procedure to generate a set of conformations for ligand binding in the receptor. Here, we use DOCK 4.0 (17) to generate and score 1,000 configurations, of which 10% were selected by using a buried surface area cutoff of 85% and by using energy scoring from DOCK 4.0, for further analysis.

Ligand relaxation. The 100 best conformations selected for each ligand from step 1 are subjected to all-atom minimization, keeping the protein fixed but the ligand movable. The solvation of each of these 100 minimized structures was calculated by using the analytical volume generalized born (AVGB) continuum solvation method (18). The binding energies (BE) were calculated by using BE = [PE (ligand in solvent) − PE (ligand in protein)] where PE is the potential energy. Then, the 10 structures based both on binding energies and buried surface areas were selected from these 100 structures for the next step.

Complex relaxation. We optimize the structure of the receptor/ligand complex allowing the structure of the protein to accommodate the ligand. This relaxation is essential to identify the optimum conformations for the complex. The all-atom receptor/ligand energy minimization was performed on the 10 structures from the previous step. Using these optimized structures, we calculate the binding energy as the difference between the energy of the ligand in the protein and the energy of the ligand in water. The energy of the ligand in water is calculated by using DREIDING force field and the analytical volume generalized born (AVGB) continuum solvation method (18).

Side-chain optimization. We select, from the 10 structures from the previous step, the one with the maximum number of hydrogen bonds between ligand and protein. For this structure, we use the SCREAM side-chain replacement program to reassign all side-chain rotamers for the residues within 4 Å in the binding pocket [SCREAM uses a side-chain rotamer library (1,478 rotamers with a 1.0-Å resolution) with the all-atom DREIDING energy function to evaluate the energy for the ligand–protein complex].

Scanning the entire receptor for binding sites. To locate the binding site, we scan the entire protein for potential binding regions. The entire molecular surface of the predicted structure of β2AR is mapped, and spheres representing the empty volume of the receptor are generated by using the Sphgen program in the DOCK 4.0 suite of programs. The entire set of receptor spheres is divided into six overlapping regions, and epinephrine is used to scan for a putative binding site. This first pass is carried out by performing only the first 2 steps of the HierDock protocol described above.

Determination of binding site and binding energy for all ligands. In the second pass, we then take a 10 × 10 × 10-Å cube surrounding the putative binding site and perform all of the steps of the HierDock protocol as described above for all ligands in the study.

Validation for function prediction protocol. The HierDock protocol has been validated by using it to predict the binding site for aminoacyl t-RNA synthetases (19, 20) and 37 other co-crystals of globular proteins (21, 22). We also validated HierDock for binding of a ligand to a GPCR by docking 11-*cis*-retinal to bovine rhodopsin (5, 6). The CRMS between crystal structure and the docked structure for *cis*-retinal is 0.6 Å, which is excellent considering that no information of the binding site was assumed. We have also used HierDock to predict binding to olfactory receptors and to other GPCRs (4, 5).

Results

Predicted Structure of Human β2AR. Our predicted β2AR structure shows the same general topology as bovine rhodopsin. There are kinks at the conserved prolines of TM2 and TM6 and minor bends in several other helices. The overall β2AR structure deviates from rhodopsin by 3.96 Å coordinate rms in the alpha carbons ($CRMS_\alpha$) of the TM region (8.49 Å $CRMS_\alpha$ over the entire structure). We suspect that this 3D structure represents the inactive state of the receptor because it seems to predict binding of agonist and antagonist equally well.

Predicted Binding Site of Epinephrine in β2AR. From the HierDock protocol described above, the predicted binding site of epinephrine is shown in Fig. 1 where epinephrine is nestled between TM3, 4, 5, and 6 as shown in the top view (Fig. 1*B*). This figure also shows the details of the 5.0-Å binding site of epinephrine, which suggests that the following residues are critical in binding the epinephrine.

Asp-113 (TM3). Asp-113 forms a salt bridge with the amine (2.9 Å) of epinephrine and accepts a hydrogen bond from the alkyl OH group (3.0 Å). The Asp at this position is conserved across all biogenic amine receptors (whose endogenous ligands all include a similar amine), and numerous binding studies have shown that this residue interacts with the amine in epinephrine (2), validating our predicted binding site. The second oxygen of the carboxylate of Asp-113 is 3.8 Å from the amine, making the interaction with this part of the side chain much weaker.

Ser-203, -204, and -207 (TM5). We find that all three serines form a hydrogen-bonding network with the two catechol OH groups of epinephrine as shown in Fig. 2. The four hydrogen bond distances are 3.1 Å (Ser-203-meta OH), 2.9 Å (Ser-204-meta OH), 3.0 Å (Ser-203-para OH), and 3.1 Å (Ser-207-para OH). Detailed mutational studies have shown that Ser-204 interacts specifically with the meta hydroxyl whereas Ser-207 interacts specifically with the para hydroxyl (2), validating our predicted binding site. In addition, a recent study indicates that Ser-203 (previously thought not to be involved in binding) is quite important to agonist binding, interacting with the meta OH of epinephrine (23). Our results indicate that Ser-203 interacts with both the meta and para OH groups to form the elegant hydrogen-bonding

BIOCHEMISTRY

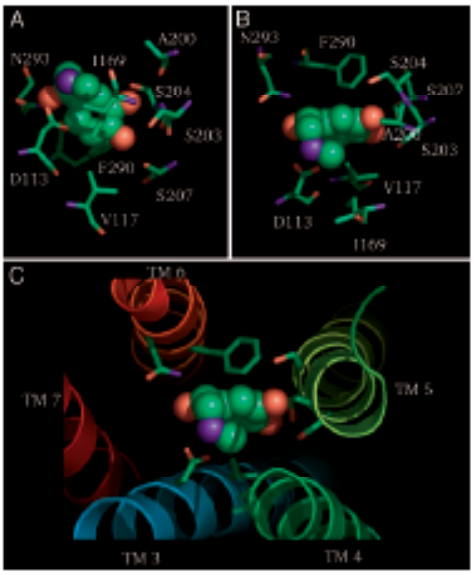

Fig. 1. Five-angstrom predicted binding site of epinephrine in the predicted structure for β2AR. Complete amino acids are shown in the side view (*A*) and top view (*B*) whereas only side chains are shown in (*C*). Protein model figures generated by using RASMOL software (21).

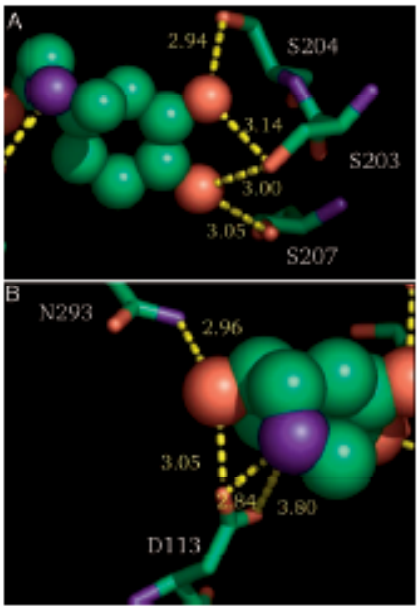

Fig. 2. Important hydrogen bond contacts in the predicted binding site of epinephrine to human β2AR. (*A*) The hydrogen-bonded network formed between both catechol hydroxyl groups with all three highly conserved TM5 serines (S203, S204, and S207). (*B*) The hydrogen-bonded network involving the highly conserved TM3 aspartic acid and N293 with binding to the amine of the ligand.

network shown in Fig. 2. The Ser-203-meta OH interaction is conserved across all agonists in our study whereas the Ser-203-para OH interaction was not, indicating that the meta interaction is probably functionally important whereas the network including the para OH may not be vital to agonist recognition. This conclusion agrees with mutation data indicating that binding of phenylephrine (epinephrine without the para OH) is not substantially affected by mutation of Ser-203 (23).

Asn-293 (TM6). This residue donates a hydrogen bond (3.0 Å) to the alkyl OH of epinephrine, which is also coupled to Asp-113. Recently, point mutational studies by Shi *et al.* (24) showed that Asn-293 is important for binding, and it has been speculated to recognize the alkyl OH of epinephrine (24). A detailed picture of the ionic and hydrogen bond interactions between Asp-113, Asn-293, and the ligand is shown in Fig. 2*B*.

Ile-169 (TM4). This residue provides a hydrophobic interaction with the *N*-methyl group of epinephrine. It is established experimentally that epinephrine binds more strongly to β2AR than norepinephrine, and this methyl group is the only difference between these two ligands. Thus, it is plausible that Ile-169 is responsible for this selectivity

Val-117 (TM3) and Phe-290 (TM6). These residues provide hydrophobic interactions (favorable van der Waals interactions) with the ring of epinephrine. Phe-290 is in a hydrophobic region that also includes Phe-289 and Trp-286, collectively termed the WXXFF motif. This motif is conserved throughout the biogenic amine receptors (24). In our structure, only Phe-290 seems to be directly involved in binding the ligand, but the other two residues may act to position it properly while contributing to the hydrophobicity of this region of the binding pocket.

Binding Sites of Other Ligands. Predicted binding sites of all other ligands in the study are shown in Fig. 7 (which is published as supporting information on the PNAS web site). The predicted binding site of each ligand is described below; the structures of these ligands are shown in Fig. 3.

Norepinephrine (native ligand). The predicted binding site is broadly similar to that of epinephrine, with two exceptions. Ile-169 interacts with the ring of norepinephrine because there is no *N*-methyl group in norepinephrine; this change allows the tail of norepinephrine to have a slightly different shape than in epinephrine. Additionally, in binding to norepinephrine, Asp-113 interacts only with the amine group (not with the hydroxyl group in the alkyl chain of norepinephrine), but both oxygens of the carboxylate of Asp-113 are strongly involved (distances of 2.9 Å and 3.2 Å). Fig. 4 compares the binding conformations of epinephrine and norepinephrine, along with the location of

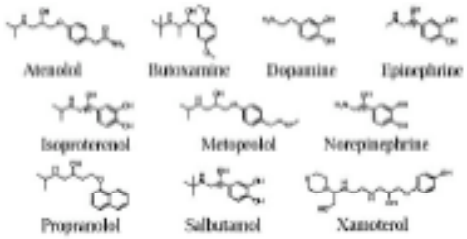

Fig. 3. Structures of all ligands docked to the β2AR in this study.

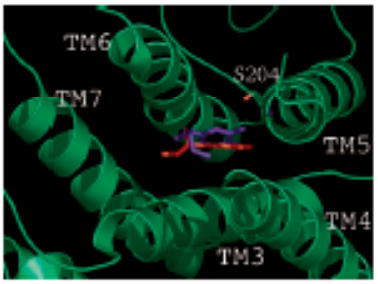

Fig. 4. Comparison of the predicted binding sites of epinephrine (blue) and norepinephrine (red) to the β2AR. Epinephrine is tilted toward S204 (making a strong contact) whereas norepinephrine is tilted slightly away (making a weak contact).

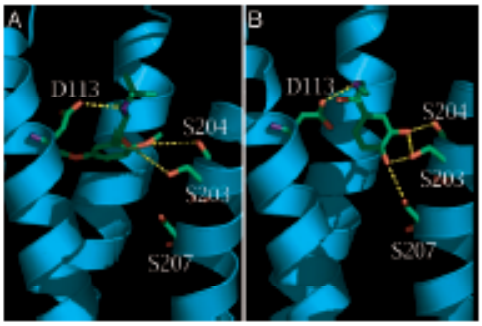

Fig. 5. Critical hydrogen-bonding contacts in the binding of butoxamine (*A*) and epinephrine (*B*) to β2AR. Note that butoxamine does not contact S207 (6 Å away) whereas epinephrine has a strong hydrogen bond (2-Å contact).

Ser-204. We see that epinephrine has a stronger interaction with this serine than norepinephrine, but a counterclockwise rotation of helix 5 by ≈20° could improve the interaction with both ligands. It is possible that our predicted structure has small errors in rotational orientation of the helices, or that this potential for rotation is indicative of domain-level movements that occur during activation, as will be discussed below.

Isoproterenol (synthetic agonist). All interactions found in the binding of epinephrine are also found in the binding site for isoproterenol. However, isoproterenol has a larger alkyl group than epinephrine, which interacts with additional residues. Thus, Trp-109 has a direct hydrophobic interaction with this isopropyl tail whereas Ile-169 seems to interact more strongly. Additionally, Trp-173 (EC2) seems to close over the top of the binding site to interact with the isopropyl group of isoproterenol.

Salbutamol (β2AR-specific agonist). Salbutamol seems to form interactions similar to those of epinephrine and isoproterenol. However, there is sufficient space in the binding cavity for the *t*-butyl group of salbutamol to fit in the same location as the methyl of epinephrine, interacting with Ile-169, His-172, and Trp-173. The bulky hydrophobic tails of these three ligands cause them to bind in a slightly different conformation than norepinephrine and dopamine, which may contribute to βAR subtype specificities and differences in affinity between adrenergic and dopamine receptors.

Dopamine (native ligand for dopaminergic receptors; weak agonist for β2AR). The predicted binding site of dopamine seems broadly similar to that of norepinephrine, with two important exceptions. First, the catechol OHs of dopamine seem to interact only with Ser-203 and Ser-207 (Ser-204 is over 4.8 Å away). This result may be due to the lack of a hydrogen bond with Asn-293, which would otherwise pull the ligand in the direction of Ser-204. Second, because there is no alkyl OH, Asn-293 does not interact with this part of the ligand and instead seems to interact weakly with the amine.

Propranolol (synthetic antagonist). Propranolol binds in the same pocket as the other ligands, but in a substantially different conformation. Most notable is that the ligand hydroxyl group forms a bifurcated hydrogen bond with Ser-203 and Ser-204, but there is no interaction with Ser-207. In addition, it seems that the Cβ of Ser-203 is also involved in a hydrophobic interaction with the backbone and ring system of propranolol. The amine of propranolol seems to interact with Asp-113 (as do the other ligands), but here the aromatic ring system of the ligand sits much closer to TM6. As a result the aromatic ring interacts strongly with Phe-289, Phe-290, and Ile-294. The isopropyl tail seems to be in the same conformation as for isoproterenol, interacting with Trp-109. Ile-169 seems to be involved in a hydrophobic interaction with the alkyl backbone of the ligand.

Butoxamine (β2-selective antagonist). Butoxamine binds in a conformation almost identical to that of propranolol, with an aromatic system interacting with TM6 and a *t*-butyl group on the amine that binds in exactly the same position as the same portion of salbutamol. Oxygens on butoxamine are involved in hydrogen-bonding interactions with Ser-203 and Ser-204, but there is no interaction between butoxamine and Ser-207. Although there is no interaction with Asn-293 in our initially predicted structure, we find that a 180° rotation of the asparagine side chain allows a strong interaction between the asparagine amine and a methyl ether oxygen of butoxamine. This interaction improves the binding energy by ≈2.5 kcal/mol. The *N*-isopropyl group seems to make the same interactions as the hydrophobic tails of salbutamol and isoproterenol.

Metoprolol (β1-selective antagonist). Metoprolol binds to the β2AR in a conformation that allows its amine group to interact with Asp-113, while allowing a pair of oxygens in the ligand to interact with Ser-203 and Ser-204. A third oxygen in metoprolol interacts with the amine of Trp-109 whereas hydrophobic portions of the ligand have strong interactions with Phe-290 and Ile-169. Although metoprolol is marketed as a specific β1AR blocker, its side effect profile indicates it could have some antagonistic cross-reactivity with β2AR, as will be discussed below.

Xamoterol (β1-selective agonist) and Atenolol (β1-selective antagonist). The predicted binding sites are shown in Fig. 7, but our calculations showed that they do not bind appreciably to β2AR.

Discussion

Difference in Agonist and Antagonist Binding Sites. Of the eight most strongly bound molecules in our calculations, some are known to act as agonists whereas others act as antagonists. We find that the binding sites of the known agonists and antagonists described above show consistently different patterns in the binding site. Thus, the agonists epinephrine, norepinephrine, salbutamol, and isoproterenol all form hydrogen bonds with both Ser-204 and Ser-207, and the antagonists that bind strongly to the receptor form hydrogen bonds only with Ser-203 (or Ser-203 and Ser-204 for butoxamine), but never Ser-207. This difference between the binding of epinephrine and butoxamine is shown in Fig. 5. Both agonists and antagonists have a strong bond to the Asp-113 of TM3. Based on these results, we suggest that an agonist must couple strongly to TM5 with both Ser-204 and Ser-207 while also bonding to TM3 through Asp-113. On the other hand, the antagonists need to recognize the same site (to block the agonist) but lead to a more flexible coupling of TM3 and TM5 so that they do not induce the transition to the activated state.

BIOCHEMISTRY

Ligand	Experimental Effect	Predicted Effect	Binding Energy (kcal/mol)	D113	S203	S204	S207	N293
Isoproterenol	Agonist	Agonist	-69.76	**2.91**	**2.91**	3.99	**2.85**	4.36
Epinephrine	Agonist	Agonist	-64.33	**2.85, 3.82**	**3.20, 3.00**	**2.93**	**3.03**	**3.00**
Salbutamol	Agonist (B2)	Agonist	-58.34	**2.81**, 3.70	**3.09, 3.28**	**2.93**	**3.45**	3.65
Dopamine	Weak Agonist	Weak Agonist	-50.12	**2.95, 3.18**	**2.82, 3.18**	4.82	4.92	**2.96**
Butoxamine	Antagonist (B2)	Antagonist	-47.32	**2.99**	-4.46	3.76	x	**(3.03)***
Norepinephrine	Agonist	Agonist	-44.37	**2.87, 3.16**	**2.87, 3.18**	4.18	**2.91**	3.61
Metoprolol	Antagonist (B1)	Antagonist	-38.55	**2.85**	**2.89**	**3.07**	x	x
Propranolol	Antagonist	Antagonist	-32.17	**2.89**	**3.30**	4.04	x	x
Atenolol	Antagonist (B1)	N/A	-4.80	**2.89, 3.67**	**3.13**	4.47	x	x
Nanoterol	Agonist (B1)	N/A	-42.67	**2.77**	**2.71**	**2.81**	x	x

Fig. 6. Predicted binding energies and contact distances (hydrogen-bonding and ionic) for the ligands of Fig. 4 to β2AR (all distances are heavy atom–heavy atom). A more positive energy signifies stronger binding. Based on the TM5 criteria described in the text, ligands were classified as either agonists or antagonists; their experimentally recognized effects are also indicated. Hydrogen bond lengths and electrostatic interactions between the receptor are also shown for each of five key residues of the protein; strong interactions (contacts <3.5 Å) are shown in bold. An x indicates no interaction. The hydrogen bond in butoxamine marked with an asterisk indicates a contact that is made only with the side chain of N293 flipped 180° from the simulated conformation, as described in the text.

Difference in Agonist-Binding Sites. Among the agonists in this study, we find two slightly different binding conformations. Isoproterenol, salbutamol, and epinephrine (the stronger agonists for β2AR) bind in a conformation that allows them to form a strong hydrogen-bonding network with all three of the conserved TM5 serines (as shown in Fig. 2). In contrast, the weaker agonists norepinephrine and dopamine form strong contacts only with Ser-203 and Ser-207, lying rather far from Ser-204. On the other hand, for both cases, only a small rotation of TM5 would bring Ser-204 into an excellent hydrophilic interaction with the ligand, while also improving the hydrogen bond angles to the other two residues. These results suggest that β2AR activation may be mediated by a rotation of TM5 to optimize hydrogen bonding with agonist ligands. A small counterclockwise (as viewed from the extracellular side) rotation of TM5 would greatly improve the interactions of norepinephrine and dopamine with Ser-204 (and also Ser-207 for dopamine). It would also improve the interaction of salbutamol with Ser-207 and that of isoproterenol with Ser-204. Although the hydrogen-bonding interactions with epinephrine seem optimal in the docked conformation, it is so close to Ser-203 that it has a minor van der Waals clash with the Cβ hydrogens of this side chain; a slight rotation of TM5 could relieve this clash while also allowing some improvement in the hydrogen bond angles to Ser-203. The underlying trend behind these interactions is that all of the agonists seem to bind with their catechol hydroxyls much closer to the beta carbon position of Ser-203 than those of Ser-204 or Ser-207, even in cases (such as epinephrine) where hydrogen bond distances to Ser-204 and Ser-207 are optimal in these structures. This conformation is possible because the rotamers of Ser-204 and Ser-207 are fully extended toward the ligand whereas that of Ser-203 is more parallel with the ring of the ligand (perpendicular to the cytoplasmic plane). This feature makes it possible for interactions with all agonists to be improved by a rotation of TM5 to improve the hydrogen bonding network that they form with the serines of TM5. This TM5 rotation will improve the binding to ligand with little or no motion of the ligand, allowing the binding interactions with TM3 and TM6 to be preserved through this rotation (we believe that anchoring interactions with TM3 and TM6 may be what causes the ligand to fall into a slightly nonoptimal conformation with respect to its TM5 contacts). Thus, we postulate that all β adrenergic agonists bind strongly to the three conserved serines in TM5 and exert activating effects by inducing a rotation of TM5 that may have broad-reaching effects elsewhere in the protein. In contrast, antagonists do not form this network of interactions with the TM5 serines, making them incapable of inducing the conformational changes leading to activation.

Recent experimental studies indicate that activation of the β2AR involves a movement of TM6 relative to TM5 and TM3 (25), causing disruption of an ionic lock between the cytoplasmic ends of TM3 and TM6 (26). Detailed interhelical-linkage studies on the β2AR have shown that modifications that maintain close contact between the cytoplasmic ends of TM3 and TM6 completely block receptor activation (27). These results, combined with Ghanouni's fluorescence experiments (25), have led to the conclusion that, on activation, TM6 either rotates slightly counterclockwise (as viewed from the extracellular region) or tilts its intracellular end toward TM5. It is possible that a small rotation of TM5 is the critical step in causing the protein to transition to the activated state. Clearly, the linkage of TM5 and TM6 by the IL-3 loop must play some key role in this. A recent study on bacteriorhodopsin showed that a potential-based change in the conformation of the IL-3 loop may be directly responsible for an outward tilting of TM6 occurring at the end of the M segment of the photocycle (28). Although the function of bacteriorhodopsin is quite different from that of the β2AR, this experiment illustrates that manipulating the conformation of IL-3 in a seven-TM protein can cause a meaningful spatial movement of TM6. A similar mechanism may be involved in activation of the β2AR (and potentially other GPCRs as well), with the agonist-induced rotation of TM5 causing the IL-3 loop to change conformations, and thus leading to a translation of TM6 and a full transition to the activated state. More detailed studies will be required to determine the exact relationship between these activation events.

Binding Energies and Interactions of the Various Ligands. *Classification as agonist or antagonist.* The analysis of hydrogen-bonding contacts described above to classify each binding ligand as either an agonist or antagonist leads to the classifications shown in Fig. 6. This criterion correctly classifies all ligands as either agonists or antagonists. We classify dopamine as a weak agonist because it makes the appropriate serine contacts, but its contact to S204 is quite weak, and thus dopamine may not be as effective in inducing the activating conformational change (described above) as the other agonists in this study.

Comparison of predicted binding energies and effects with experimental data. The binding energies for all ligands in this study are shown in Fig. 6. These results are in qualitative agreement with experiment. Thus, it is known that isoproterenol exhibits the

strongest binding affinity among the common agonists to β2AR and that epinephrine binds more strongly than norepinephrine (2), all in agreement with our calculations. We also find that salbutamol (known to be a β2-specific agonist) binds quite strongly, on par with other strong agonists for this receptor. With only one exception, the results for the agonists, and their relative ordering, are perfectly in accord with experimental affinities (29). Only for dopamine is there a deviation between our results and the known relative affinities for β2AR. Dopamine is known to bind less strongly than norepinephrine, but we predict it to bind more strongly. We do not have an explanation for this result because we find an almost identical binding mode.

We should emphasize that the binding energies reported here come from energy minimization, corresponding to the binding enthalpy at 0 K (except that we do not include zero point energy). The calculations do include solvation effects (based on the properties of water at 300 K), but they do not include explicit entropic terms or the temperature corrections in the enthalpy. Nevertheless, these results provide valuable information about the active site, including an interpretation of difference between agonists or antagonists, and indeed the calculated binding energies show a very good correlation with experimental dissociation constants, particularly when agonists and antagonists are analyzed separately. A graph comparing our calculated binding energies with experimental energies is included in Fig. 8 (which is published as supporting information on the PNAS web site).

Our results suggest that both propranolol and butoxamine act as antagonists for this receptor. Butoxamine is known to be a selective antagonist for β2AR whereas propranolol is an unselective β antagonist. The other three ligands considered here (metoprolol, atenolol, and xamoterol) were designed to be specific for β1AR. Of these ligands, we find that only metoprolol binds appreciably to β2AR, and, because it does not interact with Ser-207, we expect metoprolol to act as an antagonist. This finding is consistent with the side effect profile for metoprolol, which indicates the occurrence of breathing problems consistent with β2AR antagonism (30).

Full analysis of the subtype selectivity of these compounds (agonists and antagonists) must await completion of similar studies for β1AR, but the current results are promising, both because salbutamol (a strong selective β2 agonist) was found to be strongly active and because two β1-specific compounds were found not to bind.

Conclusion

We find that the predicted 3D structure of the β2AR leads to predicted binding sites of various ligands that are in excellent agreement with all available experimental data. The predicted docking conformations for epinephrine and all other ligands with well characterized binding sites match very closely to experimental results. Most notably, all experimentally determined hydrophilic interactions are predicted successfully in our computational models.

The predicted binding site and energetics of other ligands to the predicted β2AR structure also lead to good agreement with experiment. Moreover, this analysis leads to a classification of ligands as either agonists or antagonists, based on whether or not they interact with both of the highly conserved TM5 serines of the receptor: Any ligand that binds but does not contact both serines will act as an antagonist whereas those ligands binding to both serines will act as agonists. This correlation allows us to successfully classify all ligands in the study as agonists or antagonists (or nonbinding), and it may prove useful in predicting the effects of novel ligands to β2AR or other GPCRs. We hope that detailed analyses of the reasons behind this correlation may aid in finding a detailed description of how receptor activation occurs, both in the β2AR and in other receptors in this family.

This study of β2AR, and other successful recent studies in other GPCRs, suggests that these *ab initio* predictions of the 3D structure and function may be useful for other GPCRs. We anticipate that these methods may also be useful for predicting the function of less well characterized GPCRs, such as lipid and peptide receptors, and may be useful in quickly assaying potential cross-reactivity effects of new compounds. Carrying out similar studies for the binding site of each ligand to the other eight adrenergic receptors should help develop an understanding of the origins of subtype specificities in the ARs.

This research was supported partially by National Institutes of Health Grants BRGRO1-GM625523, R29AI40567, and HD36385. The computational facilities were provided by a Shared University Research grant from IBM and Defense University Research Instrumentation Program grants from the Army Research Office (ARO) and the Office of Naval Research (ONR). The facilities of the Materials and Process Simulation Center are also supported by the Department of Energy, the National Science Foundation, the Multidisciplinary University Research Initiative (MURI)-ARO, MURI-ONR, General Motors, ChevronTexaco, Seiko-Epson, the Beckman Institute, and Asahi Kasei.

1. Giroux, M. & Ferriere, J. (2003) *J. AirAware* 40, 41–48.
2. Strader, C. D. (1994) *Annu. Rev. Biochem.* 63, 101–132.
3. Lotvall, J. (2002) *Rules. Pharmacol. Ther.* 15, 497–501.
4. Floriano, W. B., Vaidehi, N., Goddard, W. A., III, Singer, M. S. & Shepherd, G. M. (2000) *Proc. Natl. Acad. Sci. USA* 97, 10712–10716.
5. Vaidehi, N., Floriano, W. B., Trabanino, R. J., Hall, S. E., Freddolino, P., Choi, E. J., Zamanakos, G. & Goddard, W. A., III (2002) *Proc. Natl. Acad. Sci. USA* 99, 12622–12627.
6. Trabanino, R. J., Hall, S. E., Vaidehi, N., Floriano, W. B., Kam, V. & Goddard, W. A., III (2004) *Biophys. J.*, in press.
7. MacKerell, A. D., Bashford, D., Bellott, M., Dunbrack, R. L., Evanseck, J. D., Field, M. J., Fischer, S., Gao, J., Guo, H. & Ha, S. (1998) *J. Phys. Chem.* 102, 3586–3616.
8. Ebersberg, D., Weiss, R. M. & Terwilliger, T. C. (1984) *Proc. Natl. Acad. Sci. USA* 8, 140–144.
9. Schenker, G. F. X. (1993) *Eye* 12, 504–510.
10. Jain, A., Vaidehi, N. & Rodriguez, G. (1993) *J. Comp. Phys.* 106, 258–268.
11. Vaidehi, N., Jain, A. & Goddard, W. A., III (1996) *J. Phys. Chem.* 100, 10508–10517.
12. Ding, H. Q., Karasawa, N. & Goddard, W. A., III (1992) *J. Chem. Phys.* 97, 4309–4315.
13. Lim, K.-T., Brunett, S., Iotov, M., McClurg, R. B., Vaidehi, N., Dasgupta, S., Taylor, S., Goddard, W. A., III (1997) *J. Comput. Chem.* 18, 501–521.
14. Vriend, G. (1990) *J. Mol. Graphics* 8, 52–56.
15. Palczewski, K., Kumasaka, T., Hori, T., Behnke, C. A., Motoshima, H., Fox, B. A., Le Trong, I., Teller, D. C., Okada, T. & Stenkamp, R. E. (2000) *Science* 289, 739–745.
16. Teller, D. C., Okada, T., Behnke, C. A., Palczewski, K. & Stenkamp, R. E. (2001) *Biochemistry* 40, 7761–7772.
17. Ewing, T. A. & Kuntz, I. D. (1997) *J. Comput. Chem.* 18, 1175–1189.
18. Zamanakos, G. (2001) Ph.D. thesis (California Institute of Technology, Pasadena, CA).
19. Wang, P., Vaidehi, N., Tirrell, D. A. & Goddard, W. A., III (2002) *J. Am. Chem. Soc.* 124, 14442–14449.
20. Kolossvary, P. M., Vaidehi, N., Floriano, W. B. & Goddard, W. A., III (2003) *J. Phys. Chem. B* 107, 11549–11557.
21. Datta, D., Vaidehi, N. & Goddard, W. A., III (2002) *Proc. Natl. Acad. Sci. USA* 99, 2626–2661.
22. Floriano, W. B., Vaidehi, N., Zamanakos, G. & Goddard, W. A., III (2004) *J. Med. Chem.* 47, 56–71.
23. Liapakis, G., Ballesteros, J. A., Papachristou, S., Chan, W. X., Chen, X. & Javitch, J. A. (2000) *J. Biol. Chem.* 275, 37779–37788.
24. Shi, L. & Javitch, J. A. (2002) *Annu. Rev. Pharmacol. Toxicol.* 42, 437–467.
25. Ghanouni, P., Steenhuis, J. J., Farrens, D. L. & Kobilka, B.K. (2001) *Proc. Natl. Acad. Sci. USA* 98, 5997–5002.
26. Ballesteros, J. A., Jensen, D. J., Liapakis, G., Rasmussen, S. G. F., Shi, L., Gether, U. & Javitch, J. A. (2001) *J. Biol. Chem.* 276, 29171–29177.
27. Sheikh, S. P., Vilardarga, J.-P., Baranski, T. J., Lichtarge, O., Iiri, T., Meng, E. C., Nissenson, R. A. & Bourne, H. R. (1999) *J. Biol. Chem.*, 274, 17033–17041.
28. Aloia[illegible], U., Rimbo, I. & Pohlmann, T. (2000) *J. Mol. Biol.* 304, 705–719.
29. Seaman, P. (1993) *Receptor Tables: Drug Dissociation Constants for Neurotransmitters and Transporters* (SZ Research, Toronto), Vol. 2.
30. Prichard, A. M. & Redfield, M. M. (2002) *MM Mayo Clinic Proc.* 77, 830–846.
31. DeLano, W. L. (2003) *The PyMOL Molecular Graphics System* (DeLano Scientific, San Carlos, CA).

BIOCHEMISTRY

Appendix III: The Predicted Structure of the Human D_1 Dopamine Receptor

The Predicted Structure of the Human D_1 Dopamine Receptor

M. Yashar S. Kalani [§,*], Nagarajan Vaidehi[*] & William A. Goddard III[**]

* Materials and Process Simulation Center, Beckman Institute, California Institute of Technology, Pasadena, CA 91125

§ Johns Hopkins University School of Medicine, Baltimore, MD 21205

****To whom correspondence should be addressed (e-mail: wag@wag.caltech.edu)**

Results:

We have predicted the structure and binding site of 11 agonists and antagonists (Shown in **Figure 3-1**) in D_1DR using the methods detailed in the Methods and Materials section. **Figure 3-2** shows the 3D atomic resolution structure of the human D_1DR modeled based on the predicted D_2 structure using the Membstruk procedure and the predicted binding site of dopamine determined using the HierDock procedure. We refer to this predicted structure as D_1DR. Using the D_1DR structure, we have identified the agonist and antagonist-binding sites for a library of 11 ligands (**Figure 3-1**), calculated their binding energies, and the criteria for agonist and antagonist activation of the receptor. The antagonists studied in this publication are divided into two classes: 1) class I antagonists that are bulky and bind in a similar location as agonists, exemplified by Clozapine, and 2) class II antagonists that consists of two aromatic moieties connected by a flexible linker chain exemplified by Haloperidol. In this paper we give details of the residues in the binding site of all the 11 ligands and analyze the similarities and differences in their binding sites.

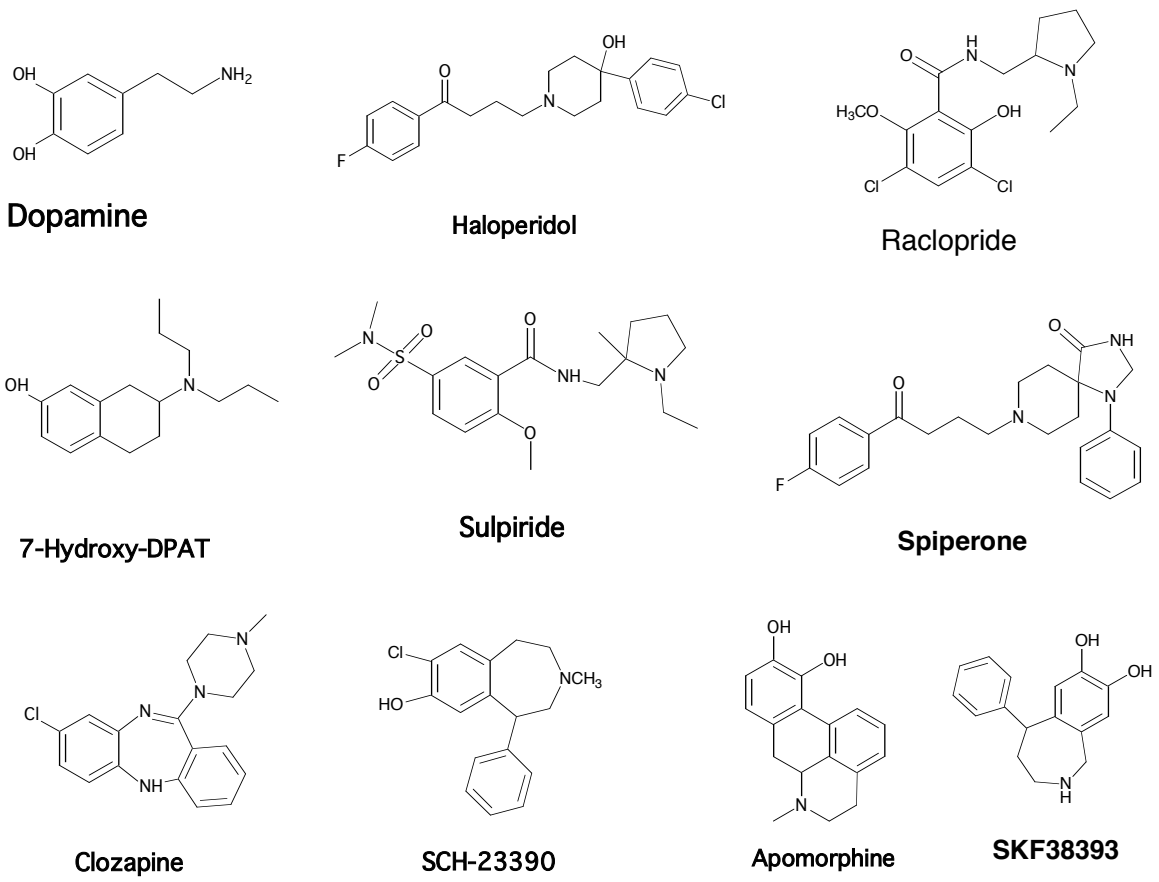

Figure 3-1. 10 agonists and antagonists studied for the human Dopamine D_1 receptor.

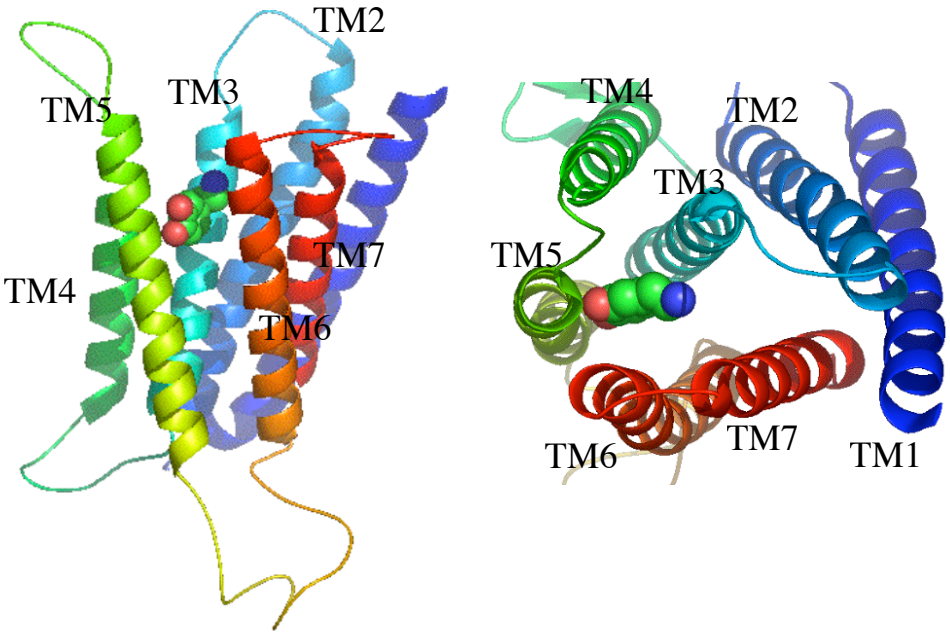

Figure 3-2. Predicted binding site of Dopamine (shown in sphere) in the predicted structure of human dopamine D_1 receptor.

In the preliminary studies, we have validated these methods for bovine rhodopsin, human ß-2 adrenergic receptor, human s1p (sphingolipid) and lpa (lysophosphatidic acid) receptors, the human D_2 dopamine receptor (Kalani 2003), and 10 mouse olfactory receptors (Vaidehi 2002, Floriano 2000, Floriano 2003, Hall 2003). The results are in good agreement with available experimental data, indicating a good description of the binding site and relative binding energies of various ligands.

Prediction of the Structure of Human D_1DR:

The Membstruk procedure used to predict the structure is detailed in Vaidehi 2002. The homology modeling procedure used to model the structure of the D_1 receptor based on the D_2 (MS) structure is outlined elsewhere. The TM2nDs procedure (Vaidehi 2002, Trabanino 2003) was utilized to identify the transmembrane (TM) spanning regions based on a hydrophobic analysis of the sequence. A seven helical motif was identified (below) ranging from 19-29 residues per helix. The highlighted residues represent TM helices, while the intervening sequences are loop regions. The same transmembrane predictions were used in the alignment to the human D_2 structure to perform homology modeling.

MRTLNTSAMDGTGLVVERDFSVRILTACFLSLLILSTLLGNTLVCAAVIRFRHLRS
KVTNFFVISLAVSDLLVAVLVMPWKAVAEIAGFWPFGSFCNIWVAFDIMCSTASI
LNLCVISVDRYWAISSPFRYERKMTPKAAFILISVAWTLSVLISFIPVQLSWHKAK
PTSPSDGNATSLAETIDNCDSSLSRTYAISSSVISFYIPVAIMIVTYTRIYRIAQKQIR
RIAALERAAVHAKNCQTTTGNGKPVECSQPESSFKMSFKRETKVLKTLSVIMGV
FVCCWLPFFILNCILPFCGSGETQPFCIDSNTFDVFVWFGWANSSLNPIIYAFNADF
RKAFSTLLGCYRLCPATNNAIETVSINNNGAAMFSSHHEPRGSISKECNLVYLIPH
AVGSSEDLKKEEAAGIARPLEKLSPALSVILDYDTDVSLEKIQPITQNGQHPT

Scheme 5-1. Predicted transmembrane regions are highlighted below in the human D_1 dopamine receptor. (the N-termini are not completely clear)

The TM prediction was utilized in building seven canonical α-helices and optimized using the procedure described in Vaidehi 2002. The helices were bundled in explicit bilayer of dilaurylphosphatidylcholine lipid molecules to mimic the biological membrane. The structural factors such as helical bend, helical tilt etc., of the predicted structure of D_1DR (homology) structure compared to the crystal structure of rhodopsin are summarized in **Table 3-1**.

TM Helix	Helical Bend	Plane Tilt	HPM Angle	HPM Mag.	HPM Fit	Plane CM Dist.	Plane CM Angle	CM Fit
1	9.3	40.7	9.3	1.1	-0.8	15.6	0.0	2.7662
2	12.2	37.9	55.8	3.5	-2.9	10.0	36.3	0.5758
3	4.6	12.3	-36.1	2.0	-0.6	4.5	120.3	2.2851
4	31.5	21.3	13.3	1.8	2.4	14.0	116.5	-4.5510
5	10.3	5.7	-68.9	1.4	-0.8	14.8	183	5.4926
6	23.3	11.1	-166.3	4.3	-5.0	11.5	238.5	2.6714
7	31.9	18.9	-31.3	2.0	9.7	13.0	295.9	-9.2401

Centered Comparison Table

TM Helix	HPM Angle	HPM Mag.	Helical Bend	P. Face Deg.
1	61.2	2.2	8.7	251
2	31.9	4.2	5.6	151
3	-11.0	2.6	2.0	59
4	8.1	2.8	8.9	244
5	-69.0	4.9	20.8	223
6	-159.7	4.9	18.2	174
7	-44.5	2.1	39.4	145

Table 3-1. Comparison of the D_1DR with the crystal structure of bovine rhodopsin.

RMS height of TMR: 31.2

RMS radius of TMR: 12.4

From **Table 3-1** it is clear that the helical bends are very different for D_1DR compared to rhodopsin. The volume of the TM barrel for D_1DR is 15111.9 $Å^3$. There is one disulfide bond between Cys96 and Cys186 in EC2. Rhodopsin has a volume of 11,807.7 $Å^3$. The calculated RMS in the coordinates of the $C_{\square}$ atoms of the D_1DR

structure compared to the crystal structure of rhodopsin is 4.78 Å and a total residue RMS of 6.32Å (all atoms).

Prediction of the putative binding site for dopamine in D_1DR: The Hierdock2.0 procedure (Vaidehi 2002) was utilized to scan all the D_1DR models as described in Materials and Methods section. We discuss the details of the predicted binding site in D_1DR (homology) model for all the 11 ligands studied in this paper to capture the same binding as those identified in the D_2 (MS) for comparison reasons and explanations of receptor specificity in future chapters.

Dopamine: Dopamine is the endogenous ligand of the dopamine receptors. It binds in the putative agonist binding site located between TM3, 4, 5, and 6. There are two main contacts that energetically stabilize dopamine in this docked conformation; 1) salt bridge between the TM3 Asp103 (bidentate, 2.8 Å and 2.9 Å), and 2) a network of hydrogen bonds to the TM5 Ser198, Ser199, and Ser202. In our structure Ser198 and Ser202 both have 3.2 and 3.1 Å interactions with the catechol hydroxyls. Ser199 is ~ 5 Å away and the interactions it has with the catechol hydroxyls are too far to be considered hydrogen bonds, although a rotation of TM5 will allow Ser199 to form excellent interactions with the catechol of dopamine. Under no circumstance can all three serines in TM5 form hydrogen bonds with reasonable distances and angles; at no time can there be more than 2 hydrogen bonds to the sequence of serines in TM5. Interaction between Ser198 and Ser199 may result during steps leading to or resulting from activation. Other residues in the binding pocket provide mostly hydrophobic packing for the ligand. These residues

include Trp99, and Ser107 (TM3), Phe156 (TM4), Tyr194, and Ala195 (TM5), Trp285, Phe289, and Asn292 (TM6). The first phenylalanine of the conserved WXXFF motif, Phe288 is slightly greater than 5.5 Å away from dopamine. Asn292 in TM6 is providing a very strong component of the binding energy of dopamine to the receptor. Assuming Asp103 forms a bidentate salt bridge, or a salt bridge and a hydrogen bond to the amino group of dopamine, the interaction with Asn292 fulfils the ability of the amino group to form favorable interactions with any other residues. It must be noted, however, that the

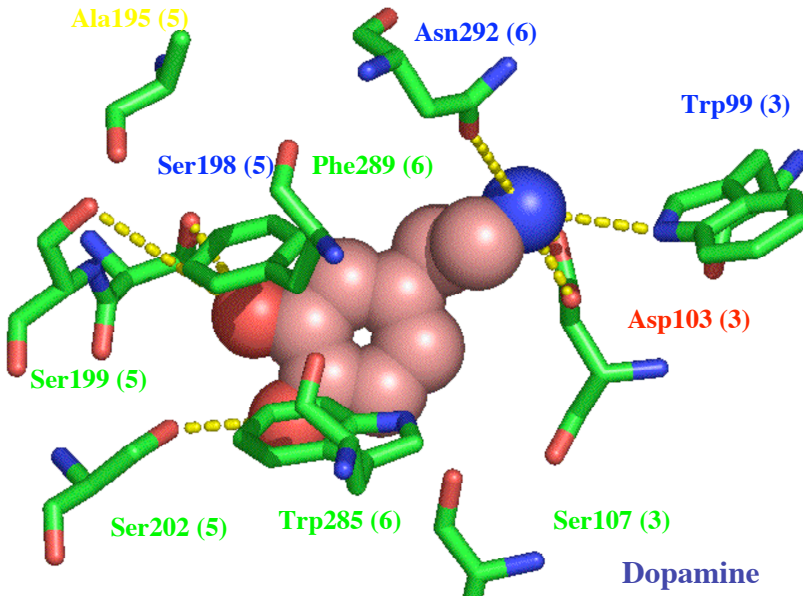

Figure 3-3. The 5.5 Å binding site of dopamine to the human D_1 dopamine receptor. The numbers in the brackets indicate the TM helices to which the residues belong to.

presence of Trp99 (3) may be the reason why dopamine exhibits reduced binding to the D_1 subtype of the receptor compared to the D_2 receptor. The presence of the Trp99 (3) provides Asp103 (3) an alternate hydrogen bond donor, meaning the aspartate will share its electron density between the protonated amino group and the indole and will not

interact as efficiently with the primary amino group. Interestingly, I predict that tertiary amino groups should have enhanced binding to this receptor since the presence of a single proton will not cause for competition for the aspartate electron density.

7-OH DPAT: The ligand binds in putative agonist binding site located between TM3, 4, 5, and 6. The protonated amino group of 7-OH DPAT is salt bridged to the TM3 Asp103 (2.9 Å). The other major polar contacts are to the conserved TM5 serines 198, 199 and 202. There are two hydrogen bonds, one 3.3 Å to Ser198 and 2.9 Å to Ser202. The interaction to Ser199 is $\sim$ 6 Å and is too long to be considered a hydrogen bond. The remainder of the residues in the cavity are mainly hydrophobic residues that provide stabilization for the aromatic and aliphatic rings of the ligand. The residues in close hydrophobic contact of the ligands are Trp99, Phe102, Cys106, Ser107 (all in TM3), Trp148 (TM4), Tyr194, Ile201 (both in TM5), Trp285, Phe288, Phe289, Asn292 (all TM6), Val317, Trp321 (both in TM7) (**Figure 3-4**) which provide a mainly hydrophobic pocket.

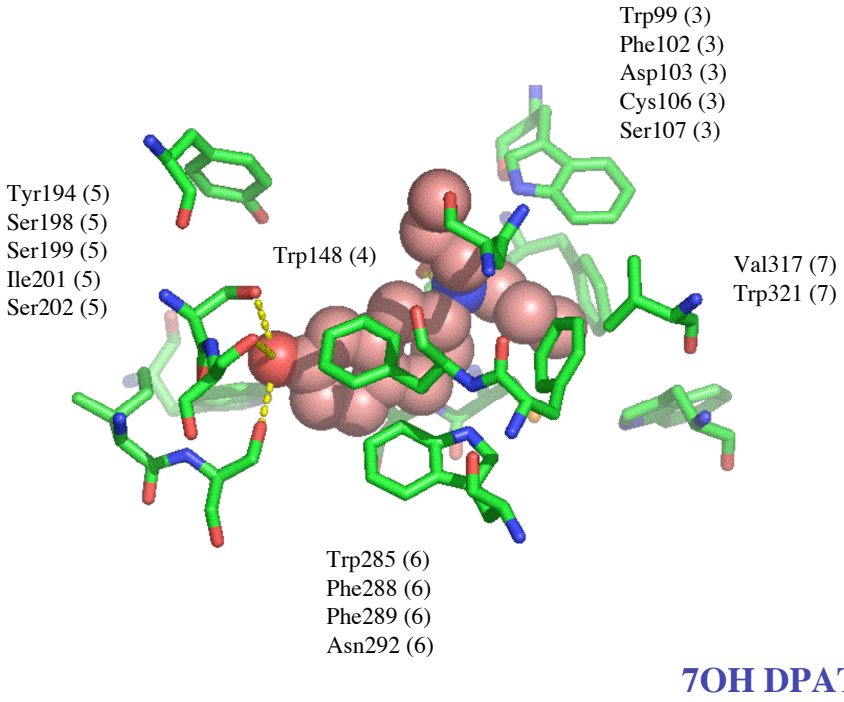

Figure 3-4. The 5.5 Å binding site of 7-OH DPAT to the human D_1 dopamine receptor. The numbers in the brackets indicate the TM helices to which the residues belong to.

Apomorphine: The ligand binds in the putative agonist binding site located between TM3, 4, 5, and 6. The protonated amino group of Apomorphine is salt bridged to the TM3 Asp103 (2.9 Å). The other major polar contacts are to the conserved TM5 serines198, 199 and 202. There are as previously two hydrogen bonds to Ser198 (3.8 Å) and Ser202 (3.1 Å) both to the lone hydroxyl group on Apomorphine. The contact to Ser199 is ~ 6 Å apart. Other residues form a most hydrophobic pocket around the ligand; these residues include: Trp99, Phe102, Cys106, Ser107, Ile111 (all TM3), Trp148, Phe156 (both TM4), Tyr194, Ile201 (TM5), Trp285, Phe288, Phe289, Asn292 (all TM6),

Val317 (TM7) (**Figure 3-5**). Mutational experiments have shown that Phe288Ala and Phe289Ala mutants show substantial reduction in binding constants for Apomorphine (Cho et al 1995). This shows that these residues are important in ligand recognition.

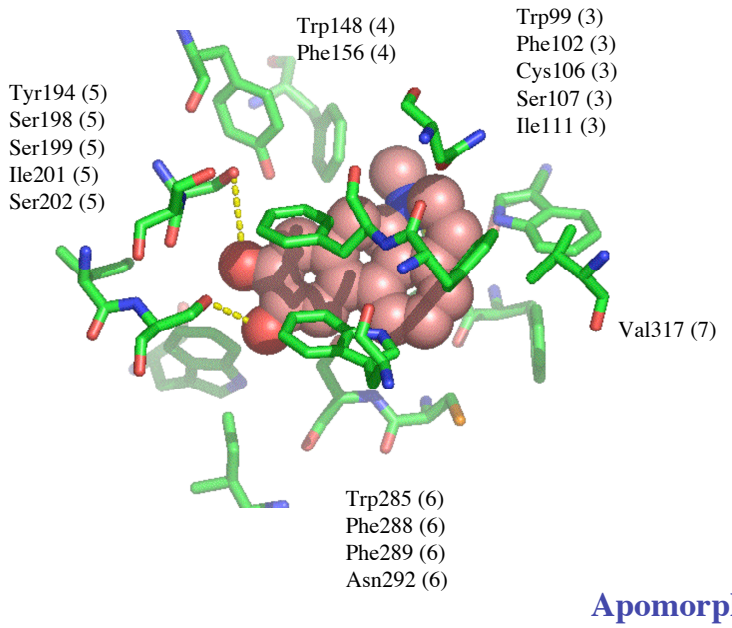

Figure 3-5. The 5.5 Å binding site of Apomorphine to the human D_1 dopamine receptor. The numbers in the brackets indicate the TM helices to which the residues belong to.

Clozapine: Clozapine is a class I antagonist, meaning it binds in the putative agonist binding site located between TM3, 4, 5, and 6. There is, as always, an amino group salt bridged to the TM3 Asp103 (2.8 Å). As is the case for all antagonists studied, there is a lone hydrogen bond to the sequence of TM5 serines. Although the hydrogen bond may be to either Ser198 or Ser202, in our structure, the more reasonable distance and angle are for the interaction between Ser198 and the heteroatom (3.3 Å). There is a third

interaction, which although cannot be categorized as a hydrogen bond, is energetically significant; this is a 3.1 Å interaction between Trp285 in TM6 and the hydrogen of the ring in Clozapine. Ser107 is 4.9 Å apart from the other nitrogen in the Clozapine ring. The remainder of the residues provide a mostly hydrophobic pocket for the ligand. There residues in close proximity of the Clozapine ligand are Trp99, Phe102, Cys106, Ser107 (TM3), Phe156 (TM4), Tyr194, Ala195 (TM5), Phe281, Phe288, Phe289, Asn292, (TM6), Val317, Trp321 (TM7) (**Figure 3-6**).

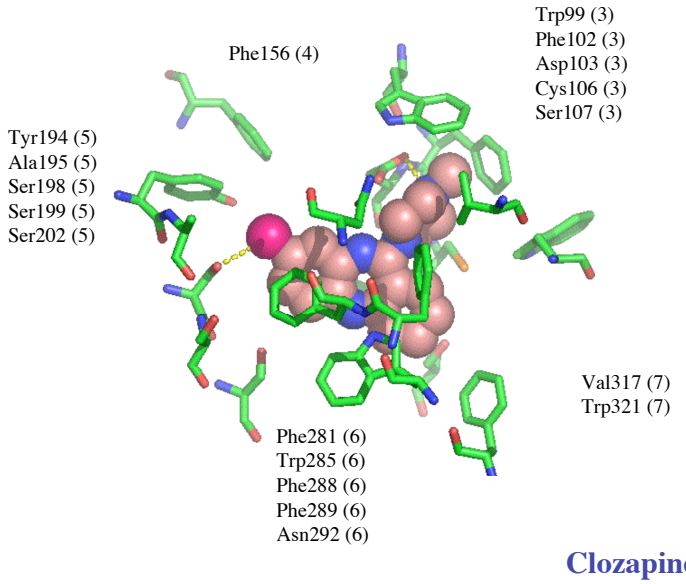

Figure 3-6. The 5.5 Å binding site of Clozapine to the human D_1 dopamine receptor. The numbers in the brackets indicate the TM helices to which the residues belong to.

Fenoldopam: Fenoldopam is an agonist, meaning it binds in the putative agonist binding site located between TM3, 4, 5, and 6. There is a bidentate salt bridge between Asp103 (TM3) with and the amino group with distances of 2.6 and 2.8 Å. Ser107 (TM3) is hydrogen bonded to heteroatom with a length of 3.3 Å. The catechol portion is hydrogen

bonded to the TM5 serine networks of Ser198, Ser199, and Ser202 (TM5). There is a 3.1 Å interaction and a 2.8 Å interaction to the catechol by Ser198 and Ser202, respectively. Ser199 is too far to form a hydrogen bond to the ligand. Interestingly, it is possible for the phenol group to be pi stacked between Phe288 and Phe289 (TM6) and for its hydroxyl group to interact via a hydrogen bond with Asn202 (TM6). The remainder of the residues in the cavity provide a mostly hydrophobic pocket for the drug. These residues include: Trp99, Ile104, Ile111 (TM3), Trp148 (TM4), Ala195, Ile201 (TM5), Phe281, Trp285 (TM6), Val317 (TM7) (**Figure 3-7**).

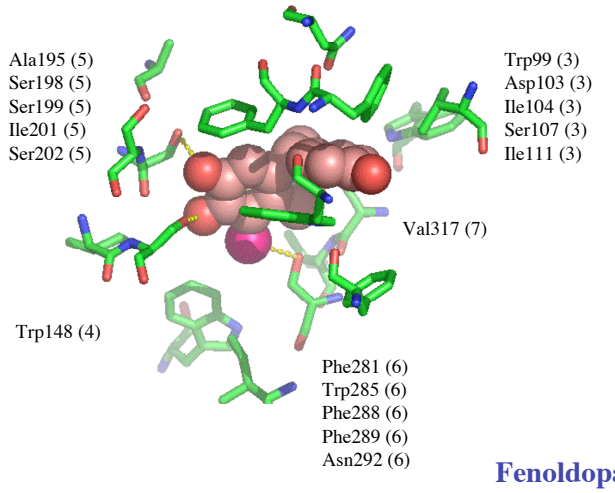

Figure 3-7. The 5.5 Å binding site of Fenoldopam to the human D_1 dopamine receptor. The numbers in the brackets indicate the TM helices to which the residues belong to.

Haloperidol: The ligand binds in the putative antagonist-binding site located between TM2, TM3, TM4, TM5, TM6, and TM7. Class II antagonists such as Haloperidol are

composed of two aromatic domains connected by a linker domain, which has a protonated amino group. The protonated amino group of Haloperidol is salt bridged to the TM3 Asp103 (2.8 Å). There are several heteroatom contacts that are typically too weak to be considered hydrogen bonds. There is a long hydrogen bond between the hydroxyl of Haloperidol and TM6 Trp285 (4.2 Å). Haloperidol and other class II antagonists are predicted to have low affinities to the D_1 receptor; and, indeed experimental studies are in accordance with this prediction. The presence of Phe102 (TM3) blocks the cavity usually occupied by the linker and the second aromatic domain. The blocking of the cavity causes the ligand to contort on itself and not fit properly in the cavity. As a result the interaction with the serine network is absent. The absence of contacts with the serine network is deemed unimportant for the function of the antagonist, and as a result haloperidol would continue to function as an antagonist, but it would have significantly reduced affinity to this receptor. The class I antagonist, apparently, would bind with a greater affinity to this receptor. Other residues form a mostly hydrophobic pocket around the ligand; these residues include: Trp80 (2), Lys81 (2), Trp99 (3), Cys106 (3), Ser107 (3), Trp148 (4), Val152 (4), Phe156 (4), Tyr194 (5), Ser198 (5), Ser199 (5), Ile201 (5), Ser202 (5), Trp285 (6), Phe288 (6), Phe289 (6), Asn292 (6), Asp314 (7), Val317 (7), Trp318 (7), Trp321 (7) (**Figure 3-8**).

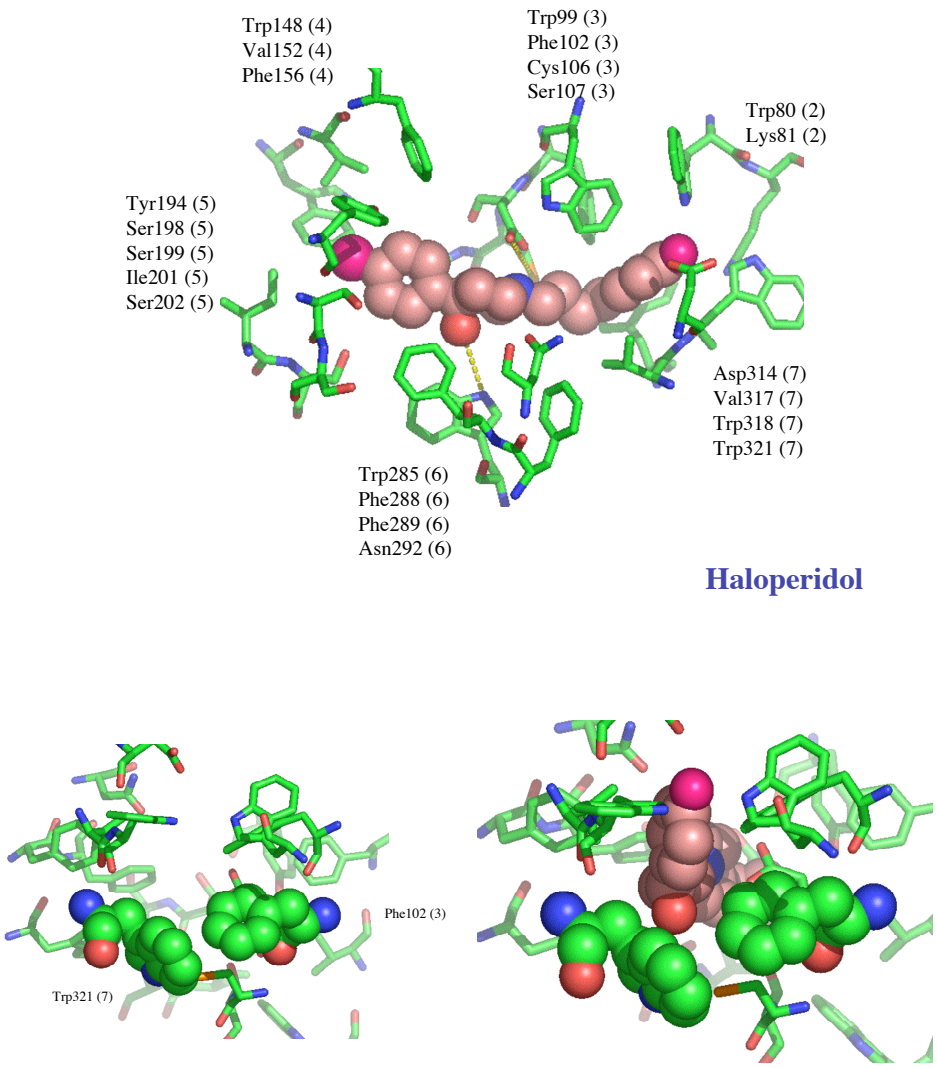

Figure 3-8. (a) The 5.5 Å binding site of Haloperidol to the human D_1 dopamine receptor. The numbers in the brackets indicate the TM helices to which the residues belong to. (b) The binding cavity without the ligand is presented on the left, and the cavity with the ligand present on the right. The presence of the TM3 Phe102 blocks the cavity for the class II antagonist to occupy the void between TM2 and TM7.

Raclopride: Raclopride binds in the class I antagonist-binding site, although it begins to extend to the TM2, and 7 aromatic micro-domain. The critical contact points are the salt bridge between TM3 Asp103 and the protonated amino group of the ligand (3.0 Å), and interactions with the TM3 Ser107 (3.9 Å) and Ser202 (4.0 Å), the latter of which is too long to be considered a hydrogen bond. Tyr194 in TM5 forms a hydrogen bond with the heteroatom on the ligand (3.3 Å). The remainder of the residues provide a mainly hydrophobic pocket for the remainder of the ligand. The residues in close proximity of the ligand include: Trp99 (3), Ile111 (3), Trp148 (4), Val152 (4), Phe156 (4), Ser197 (5), Ser198 (5), Ser199 (5), Trp285 (6), Phe288 (6), Phe289 (6), Asn292 (6), and Val317 (7) (**Figure 3-9**). Raclopride fits nicely into the cavity and does not clash with Phe102 in TM3. It is predicted that the shorter antagonists, Clozapine and the likes, will have higher affinity than the class II antagonists to this class of the receptors.

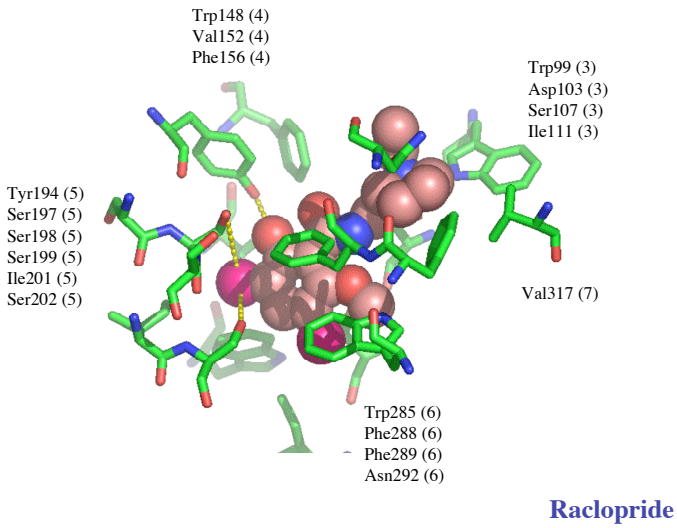

Figure 3-9. The 5.5 Å binding site of Raclopride to the human D_1 dopamine receptor. The numbers in the brackets indicate the TM helices to which the residues belong to.

SCH-23390: SCH-23390 is a class I antagonist. It forms a salt bridge with the TM3 Asp103 with a distance of 2.9 Å. There are two hydrogen bond contacts with the 5th transmembrane domain. There is a 3.0-Å interaction Tyr194 (5) and a 3.4 Å interaction with Ser202 (5). The remainder of the residues create a mostly hydrophobic pocket for the ligand, with Phe288 (6) and Phe289 (6) forming excellent Van der Waals interactions with the phenyl substituent of the ligand. Other amino acids in the cavity include: Trp99 (3), Phe102 (3), Ser107 (3), Trp148 (4), Val152 (4), Phe156 (4), Ala195 (5), Ser198 (5), Ser199 (5), Trp285 (6), Asn292 (6), Cys293 (6), and Val317 (7) (**Figure 3-10**). There is no clash between the ligand and Phe102 (3) since the ligand does not extend into the domain between TM2 and TM7.

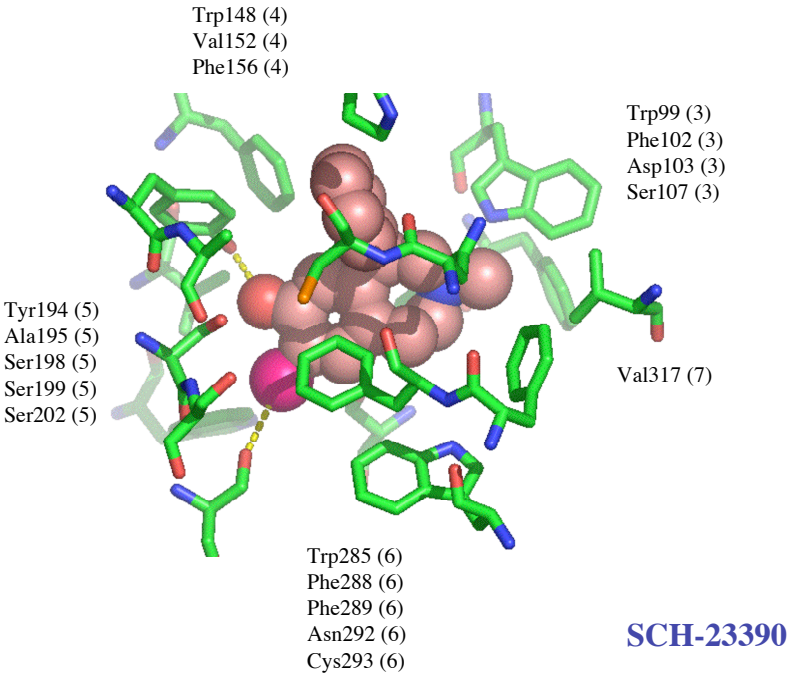

Figure 3-10. The 5.5 Å binding site of SCH-23390 to the human D_1 dopamine receptor. The numbers in the brackets indicate the TM helices to which the residues belong to.

SKF-38393: SKF-38393 is an agonist. It forms a bidentate salt bridge with Asp103 with a distance of 2.8 Å. There are two hydrogen bonds to Ser198 (3.1 Å) and Ser202 (3.5 Å). The phenyl substituent is pi stacked between Phe288 (6) and Phe289 (6). The remainder of the residues form a pocket around the ligand; these residues include: Trp99 (3), Ser107 (3), Phe156 (4), Tyr194 (5), Ala195 (5), Ser199 (5), Ile201 (5), Trp285 (6), Asn292 (6), and Cys293 (6) (**Figure 3-11**).

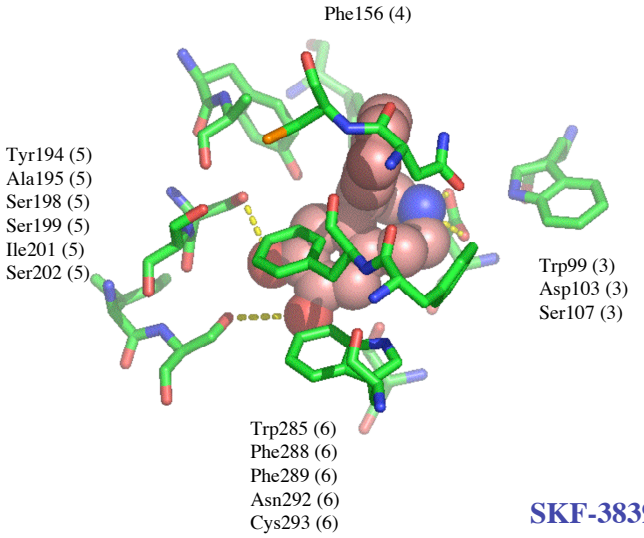

Figure 3-11. The 5.5 Å binding site of SKF-38393 to the human D_1 dopamine receptor. The numbers in the brackets indicate the TM helices to which the residues belong to.

Spiperone: Spiperone is a class II antagonist; meaning, it binds with its aromatic domains to the voids between TM2 & 7 and TM4 & 6, and it forms a salt bridge to TM3 and weak non-ionic interactions to TM5 and 6. The protonated amino group of the ligand is salt bridged to the TM3 Asp103 (2.9 Å). Since class II antagonists are too large to bind into the D_1 class of dopamine receptors, the interaction with the TM5 serine network is not possible. The ligand clashes with Phe102 (3), which blocks the cavity, and as a result, the heteroatom is not in a position to interact with the serine networks. The remainder of the residues in the cavity form a mostly hydrophobic pocket for the ligand. The residues in the cavity include: Leu76 (2), Val77 (2), Trp80 (2), Lys81 (2), Trp99 (3), Val100 (3), Cys106 (3), Ser107 (3), Trp148 (4), Tyr194 (5), Ser198 (5), Ser199 (5), Ile201 (5),

Ser202 (5), Trp285 (6), Phe288 (6), Phe289 (6), Asn292 (6), Asp314 (7), Val317 (7), Trp318 (7), Phe319 (7), Gly320 (7), and Trp321 (7) (**Figure 3-12**).

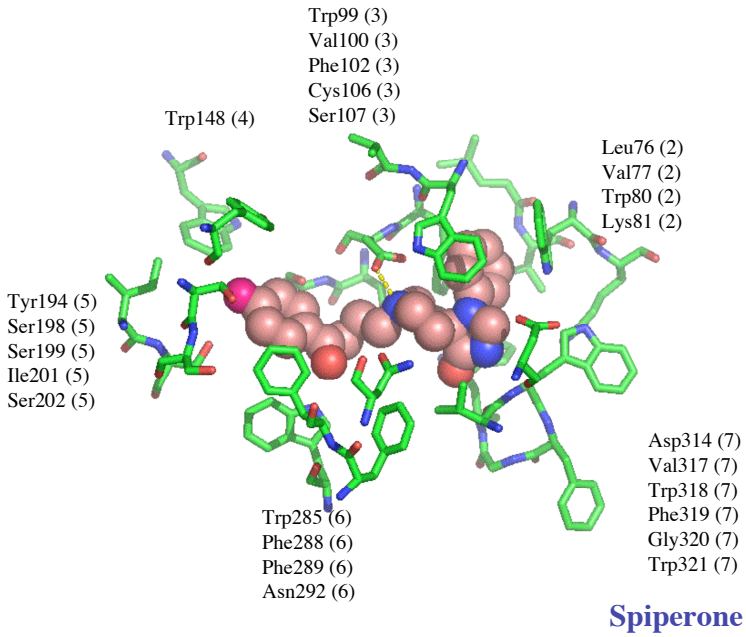

Figure 3-12. The 5.5 Å binding site of Spiperone to the human D_1 dopamine receptor. The numbers in the brackets indicate the TM helices to which the residues belong to.

Sulpiride: Sulpiride is a class I antagonist meaning it binds in the putative agonist binding site with minimal extension into the TM2, and 7 aromatic micro domain. Sulpiride has a salt bridge to the TM3 Asp103 (2.8 Å). Interestingly, the same aspartate is also hydrogen bonding to the amide hydrogen of Sulpiride (3.0 Å). This interaction is also found in all the Sulpiride-like ligands. Although the addition of the amide was introduced to decrease the lipophilicity of these drugs, the addition seems to fair well due to the interactions it has with the Asp103 in TM3. The sulfonamide portion of the ligand

interacts well with the sequence of Serines in TM5. There are two hydrogen bonds of 2.8 Å and 3.6 Å to Ser198 and Ser202, respectively. There is also a hydrogen bond between Tyr194 (5) and the sulfonamide group; this interaction is 3.3 Å long. The strength of these hydrogen bonds is, however, a different issue. The remainder of the residue provide a mostly hydrophobic pocket. The residues in close proximity include: Trp99 (3), Phe102 (3), Ser107 (3), Trp148 (4), Val152 (4), Phe156 (4), Ala195 (5), Ser199 (5), Ile201 (5), Trp285 (6), Phe288 (6), Phe289 (6), Asn292 (6), Asp314 (7), Val317 (7) (**Figure 3-13**).

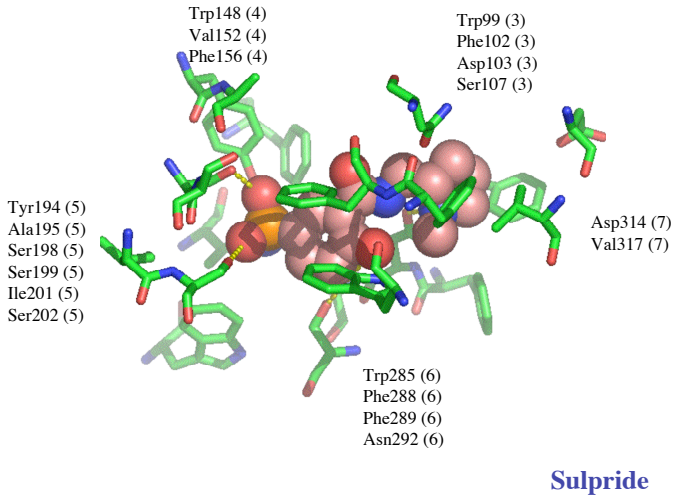

Figure 3-13. The 5.5 Å binding site of Sulpride to the human D_1 dopamine receptor. The numbers in the brackets indicate the TM helices to which the residues belong to.

Comparisons of Binding Site of Agonists vs. Antagonists: Experimental studies have outlined the binding site for agonists and antagonists. The putative agonist-binding site is located between TM3, 4, 5, & 6, and some residues in the EC2 loop (assuming this loop

closes during the process of activation). We have classified antagonists into two categories: Class I & II. Class I antagonists, such as Clozapine bind in the putative agonist binding pocket meaning they occupy the void between TM3, 4, 5 and 6. Class II antagonists, such as Haloperidol consists of two aromatic domains connected by a linker, which possess a protonated amino group. These antagonists bind in the cavity between TM2, 3, 4, 5, 6, and 7. There are two aromatic micro domains (pictures of aromatic micro domains goes here). The first aromatic micro-domain is located in TM4 and TM6, which is composed of the very symmetric Trp148 (4), Phe156 (4), Trp285 (6), Phe288 (6), and Phe289 (6). This aromatic micro-domain stabilizes one of the aromatic rings of the class II antagonists. TM3 provides the salt bridge to TM3 Asp103, which stabilizes the ligand in place. TM5 provides weak interactions with heteroatom functionalities such as halogens on the rings of class II antagonists. These interactions are weak but important in recognition of the correct aromatic domain for docking into the cavity. The second aromatic micro-domain composed of Trp90 (2), Trp318 (7), and Trp321 (7) stabilize the second aromatic ring group of the class II antagonists. It must be noted, however, that due to the presence of Phe102 (3) which blocks the cavity and does not allow for the longer ligands in class II to access the second aromatic micro-domain. Class II antagonists are not predicted to bind to this class of receptors.

Comparison of agonists binding site: There is very little difference in the putative agonist-binding site of different agonists. The agonists studied, (dopamine, 7-OH DPAT, and Apomorphine) all possess protonated amino groups, which are salt bridged to TM3 Asp103. All of these ligands studied form favorable hydrogen bonding interactions to a

network of TM5 serines, although this is not an absolute necessary for agonism. There is, in every case studied, favorable interaction from the first aromatic micro-domain located in TM4 and TM6. A residue that has not been appreciated in drug design is Asn292 (6). The presence of this residue contributes greatly to ligand binding, yet it appears that there few agonists utilize this residue effectively. It is important to note that the agonists studied effectively interact with both Ser198 and Ser202 in TM5. The interactions to Ser199, the third TM5 serine, are too long to be considered a hydrogen bond (on the order of ~ 5 Å). Under no circumstance, due to structural constraints, can all three serines effectively interact with the agonists studied. It appears that there could at most be two hydrogen bonds to the TM5 serines. Although in our structure Ser198 is not participating in any interactions, it is possible that in a slightly different structure, perhaps one resulting from activation, there could be interactions to Ser199 and Ser202 as opposed to Ser198 and Ser202. All agonists studied cause strong coupling of TM3 and 5. None of the agonists studied block TM3 and 6 motions. Based on structural studies of rhodopsin, it has been established that a motion between TM3 and 6 are essential for activation. The coupling of TM3 and 6 by agonists causes a decrease in distance between TM3 and 5 while allowing for motion between TM3 and 6.

Comparison of antagonists binding site: The antagonists studied were classified into two categories: Class I antagonists (exemplified by Clozapine), which bind in the putative agonist binding pocket; and class II antagonists (exemplified by Haloperidol), which bind in the cavity between TM2, 3, 4, 5, 6, and 7.

Class I Antagonists: the Clozapine-like antagonists salt bridge to the TM3 Asp103 with their protonated amino group. They do not have two aromatic rings and therefore only utilize the first aromatic micro-domain between TM4 and 6. As is the case with both Class I and class II antagonists, they form only one weak interaction with the TM5 serine network. In our models the interaction may be with Ser198 or Ser202. At first glance, it appears that both the number of and strength of the interactions with the TM5 serines may be important for activation. Interestingly, however, the situation is more complicated than it appears; Strange et al. have identified agonism from a non-hydroxylated form of the DPAT series. The critical distinguishing feature of an agonist vs. antagonist appears to be its relative position to TM6. Class I antagonists burry their aliphatic domain deep into the conserved TM6 WXXFF motif. Experimental studies of rhodopsin suggest that motion of TM3 and 6 is necessary for activation. The binding of antagonists at the TM6 WXXFF would prevent any motion, specifically the hinge motion between TM3 and TM6 that is necessary for activation. It appears that the presence of one hydroxyl/one hydrogen bond donor/acceptor is not an absolute necessity for antagonism. The class I antagonists are further stabilized by Trp99 in TM3.

Class II Antagonists: this class of antagonists is predicted to not bind effectively to this receptor. The Haloperidol-like antagonists salt bridge to TM3 Asp103 with their protonated amino group. Due to the presence of Phe102 (3) in the third transmembrane region, the ligands are not able to extend into the cavity between TM2 and 7 and therefore will not bind to this receptor. In most cases, only one of the aromatic rings is halogenated, and this is the ring that binds to the first aromatic micro-domain, with the

second ring would bind to the second aromatic micro-domain but Phe102 (3) does not allow for this binding in the second aromatic micro-domain. Since the ligand has little room to bind in the putative cavity, it fails to form adequate contacts to the TM5 serine network and is also expected to have lower efficacy as an antagonist. In some cases Asn292 (6) may also stabilize the class II antagonists. As is the case with the class I antagonists, class II antagonists prevent motion between TM3 and TM6 by burying their aliphatic portion between TM3 and TM6, thereby preventing interaction of these helices. There is very little difference between the binding sites of the class II antagonists, although some utilize the cavity better than others.

Ligand	**B.E. (Kcal/mol)**
7OHDPAT	-48.7
Apomorphine	-47.8
Clozapine	-41.8
Dopamine	-48.3
Fenoldopam	-48.8
Haldol	NA
Raclopride	NA
SCH	-60.6
SKF	-45.1
Spiperone	NA
Sulpiride	NA

Table 3-2. Binding energies in kcal/mol for a library of 11 ligands to the human D_1 dopamine receptor. Haldol and Raclopride do not bind this class of dopamine receptors due to the presence of TM3 Phe102 blocker.

D_1 Receptor Experimental Ranking:

SCH23390~SKF38393~Fenoldopam>Clozapine~Haldol~Spiperone~Apomorphine~Dop amine~7OHDPAT>Sulpiride~Raclopride

D_1 Receptor Ranking Theory:

SCH23390>SKF38393~Fenoldopam~Dopamine~Apomorphine~7OHDPAT~Clozapine>

Haldol~Raclopride~Spiperone~Sulpiride

Appendix IV: The Predicted Structure of the Human D_3 Dopamine Receptor

The Predicted Structure of the Human D_3 Dopamine Receptor

M. Yashar S. Kalani [§,*], Nagarajan Vaidehi[*] & William A. Goddard III[**]

* Materials and Process Simulation Center, Beckman Institute, California Institute of Technology, Pasadena, CA 91125

§ Johns Hopkins University School of Medicine, Baltimore, MD 21205

****To whom correspondence should be addressed (e-mail: wag@wag.caltech.edu)**

Results:

We have predicted the structure and binding site of 10 agonists and antagonists (Shown in **Figure 4-1**) in D_3DR using the methods detailed in the Methods and Materials section. **Figure 4-2** shows the 3D atomic resolution structure of the human D_3DR predicted based upon the model of the D_2DR obtained using the Membstruk procedure and the predicted binding site of dopamine determined using the HierDock procedure. We refer to this predicted structure as D_3DR. Using the D_3DR structure, we have identified the agonist and antagonist-binding sites for a library of 10 ligands (**Figure 4-1**), calculated their binding energies, and the criteria for agonist and antagonist activation of the receptor. The antagonists studied in this publication are divided into two classes: 1) class I antagonists that are bulky and bind in a similar location as agonists, exemplified by Clozapine; and, 2) class II antagonists that consists of two aromatic moieties connected by a flexible linker chain exemplified by haloperidol. In this paper we give details of the residues in the binding site of all the 10 ligands and analyze the similarities and differences in their binding sites.

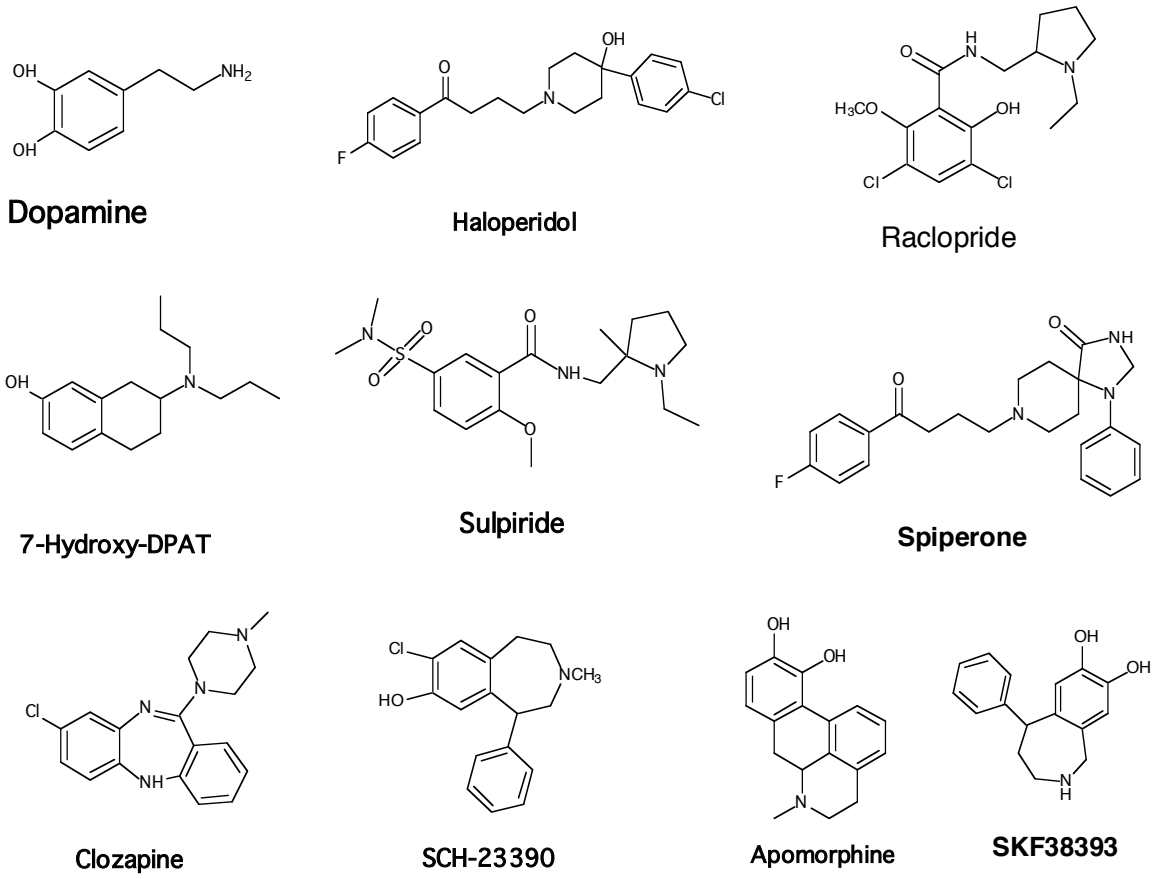

Figure 6-1. 10 agonists and antagonists studied for the human Dopamine D_3 receptor.

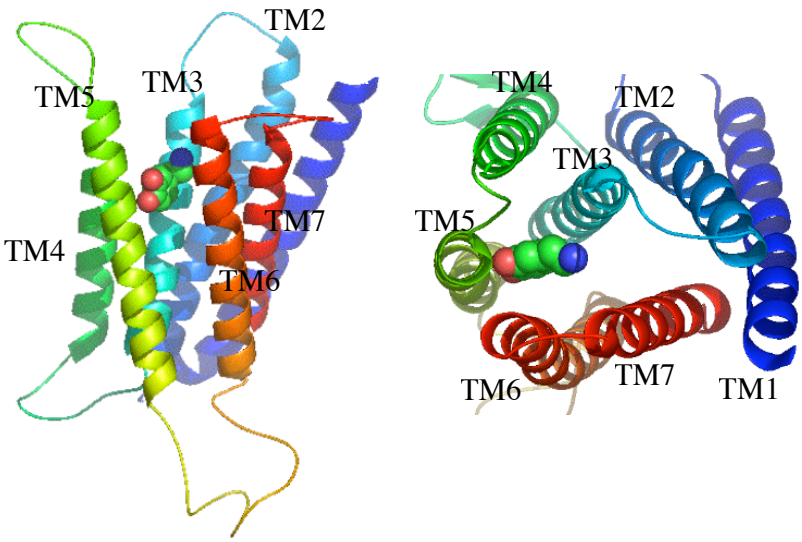

Figure 6-2. Predicted binding site of Dopamine (shown in sphere) in the predicted structure of human dopamine D_3 receptor.

In the preliminary studies, we have validated these methods for bovine rhodopsin, human ß-2 adrenergic receptor, human s1p (sphingolipid) and lpa (lysophosphatidic acid) receptors, and 10 mouse olfactory receptors (Vaidehi 2002, Floriano 2000, Floriano 2003, Hall 2003). The results are in good agreement with available experimental data, indicating a good description of the binding site and relative binding energies of various ligands.

Prediction of the Structure of Human D_3DR:

The Membstruk procedure used to predict the structure is detailed in Vaidehi 2002. The TM2nDs procedure (Vaidehi 2002, Trabanino 2003) was utilized to identify the transmembrane (TM) spanning regions based on a hydrophobic analysis of the sequence. A seven helical motif was identified (below) ranging from 19-29 residues per helix. The highlighted residues represent TM helices, while the intervening sequences are loop regions.

MASLSQLSSHLNYTCGAENSTGASQARPHAYYALSYCALILAIVFGNGLVCMAV
LKERALQTTTNYLVVSLAVADLLVATLVMPWVVYLEVTGGVWNFSRICCDVFV
TLDVMMCTASILNLCAISIDRYTAVVMPVHYQHGTGQSSCRRVALMITAVWVL
AFAVSCPLLFGFNTTGDPTVCSISNPDFVIYSSVVSFYLPFGVTVLVYARIYVVLK
QRRRKRILTRQNSQCNSVRPGFPQQTLSPDPAHLELKRYYSICQDTALGGPGFQE
RGGELKREEKTRNSLSPTIAPKLSLEVRKLSNGRLSTSLKLGPLQPRGVPLREKKA
TQMVAIVLGAFIVCWLPFFLTHVLNTHCQTCHVSPELYSATTWLGYVNSALNPVI
YTTFNIEFRKAFLKILSC

Scheme 4-1. Predicted transmembrane regions are highlighted below in the human D_3 dopamine receptor.

The TM prediction was utilized in building seven canonical □-helices and optimized using the procedure described in Vaidehi 2002. The helices were bundled in

explicit bilayer of dilaurylphosphatidylcholine lipid molecules to mimic the biological membrane. The structural factors such as helical bend, helical tilt etc., of the predicted structure of D_3DR structure compared to the crystal structure of rhodopsin are summarized in **Table 4-1**.

TM Helix	Helical Bend	Plane Tilt	HPM Angle	HPM Mag.	HPM Fit	Plane CM Dist.	Plane CM Angle	CM Fit
1	13.9	51.2	4.0	8.2	0.0	15.9	0.0	2.2527
2	8.8	32.9	109.5	5.8	0.0	10.0	34.5	0.4490
3	5.9	11.3	63.0	2.8	0.0	4.2	119.9	2.1168
4	2.1	11.4	-9.2	9.1	0.0	14.5	125.3	-2.0740
5	11.1	7.8	-21.8	7.0	0.0	14.1	187.7	2.2381
6	22.1	12.9	-157.9	9.6	0.0	11.7	244.4	2.2205
7	8.5	20.9	72.3	5.3	0.0	10.1	301.1	-6.3052

Centered Comparison Table

TM Helix	HPM Angle	HPM Magnitude	Helical Bend	P. Face Deg.

1	76.5	3.2	4.4	242
2	108.1	3.4	9.3	150
3	17.7	2.5	0.0	57
4	5.7	3.6	4.7	245
Helix 5	-17.0	3.3	17.2	219
Helix 6	-126.7	5.9	17.4	201
Helix 7	11.2	4.1	2.7	157

Table 4-1. Comparison of the D_3DR with the crystal structure of bovine rhodopsin

RMS height of TMR: 29.5

RMS radius of TMR: 12.1

From **Table 4-1** it is clear that the helical bends are very different for D_3DR compared to rhodopsin. The volume of the TM barrel for D_3DR is 13471.1 $Å^3$. There is one disulfide bond between Cys103 and Cys181 in EC2. Rhodopsin has a volume of 11,807.7 $Å^3$. The calculated RMS in the coordinates of the C_{α} atoms of the D_3DR

structure compared to the crystal structure of rhodopsin is 7.10 Å and a total residue RMS of 7.74 Å (all atoms).

Prediction of the putative binding site for dopamine in D_3DR: The Hierdock2.0 procedure (Vaidehi 2002) was utilized to scan all the D_3DR models as described in Materials and Methods section. We discuss the details of the predicted binding site in D_3DR model for all the 10 ligands studied in this paper.

Dopamine: Dopamine is the endogenous ligand of the dopamine receptors. It binds in the putative agonist binding site located between TM3, 4, 5, and 6. There are two main contacts that energetically stabilize dopamine in this docked conformation: 1) salt bridge between the TM3 Asp110 (bidentate, 2.8 Å and 2.8 Å), and 2) a network of hydrogen bonds to the TM5 Ser192, Ser193, and Ser196. In our structure Ser192 and Ser196 both have 2.8 Å interactions with the catechol hydroxyls. Ser193 is ~ 5 Å away and the interactions it has with the catechol hydroxyls are too far to be considered hydrogen bonds, although a rotation of TM5 will allow Ser193 to form excellent interactions with the catechol of dopamine. Under no circumstance can all three serines in TM5 form hydrogen bonds with reasonable distances and angles; at no time can there be more than 2 hydrogen bonds to the sequence of serines in TM5. Interaction between Ser193 and Ser196 may result during steps leading to or resulting from activation. Other residues in the binding pocket provide mostly hydrophobic packing for the ligand. These residues include Phe106 (3), Met113 (3), Cys114 (3), Phe162 (4), Phe188 (5), Val189 (5), Trp342

(6), Phe346 (6), His349 (6), and Thr369 (7). The first phenylalanine of the conserved WXXFF motif, Phe345 is slightly greater than 5.5 Å away from dopamine. His349 in TM6 is providing a very strong component of the binding energy of dopamine to the receptor. Assuming Asp110 forms a bidentate salt bridge, or a salt bridge and a hydrogen bond to the amino group of dopamine, the interaction with His349 fulfils the ability of the amino group to form favorable interactions with any other residues.

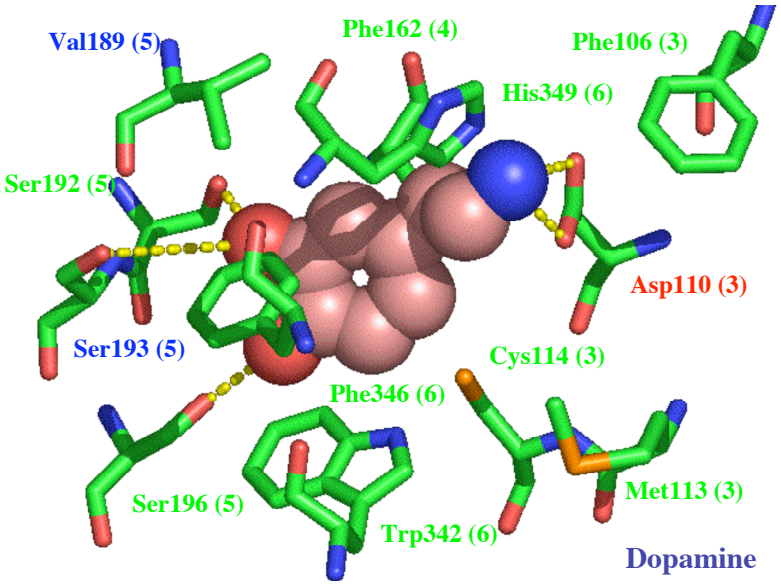

Figure 4-3. The 5.5 Å binding site of dopamine to the human D_3 dopamine receptor. The numbers in the brackets indicate the TM helices to which the residues belong to.

7-OH DPAT: The ligand binds in putative agonist binding site located between TM3, 4, 5, and 6. The protonated amino group of 7-OH DPAT is salt bridged to the TM3 Asp110 (2.8 Å). The other major polar contacts are to the conserved TM5 serines 192, 193 and 196. There are two hydrogen bonds, one 2.9 Å to Ser192 and 3.1 Å to Ser196. The

interaction to Ser193 is 5.8 Å and is too long to be considered a hydrogen bond. The remainder of the residues in the cavity are mainly hydrophobic residues that provide stabilization for the aromatic and aliphatic rings of the ligand. The residues in close hydrophobic contact of the ligands are Phe106 (3), Leu109 (3), Met113 (3), Cys114 (3), Phe162 (4), Asn185 (EC2), Val189 (5), Trp342 (6), Phe345 (6), Phe346 (6), His349 (6), Thr369 (7), and Tyr373 (7) (**Figure 4-4**) which provide a mainly hydrophobic pocket.

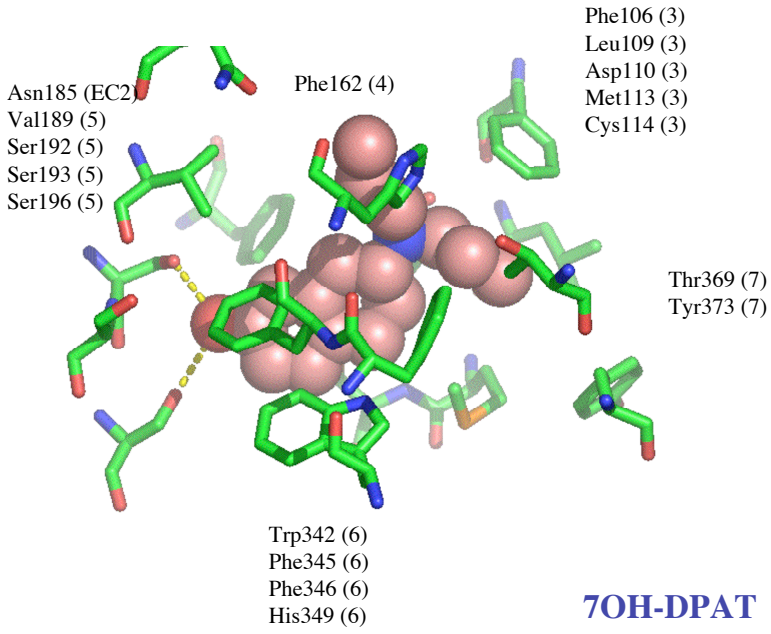

Figure 4-4. The 5.5 Å binding site of 7-OH DPAT to the human D_3 dopamine receptor. The numbers in the brackets indicate the TM helices to which the residues belong to.

Apomorphine: The ligand binds in the putative agonist binding site located between TM3, 4, 5, and 6. The protonated amino group of Apomorphine is salt bridged to the TM3 Asp110 (2.9 Å). The other major polar contacts are to the conserved TM5 serines

192, 193 and 196. There are as previously two hydrogen bonds to Ser192 (3.0 Å) and Ser196 (3.2 Å) both to the hydroxyl groups on Apomorphine. The contact to Ser193 is ~ 6 Å apart. Other residues form a most hydrophobic pocket around the ligand; these residues include: Phe106 (3), Met113 (3), Cys114 (3), Trp158 (4), Phe162 (4), Phe188 (5), Val189 (5), Phe338 (6), Trp342 (6), Phe345 (6), Phe346 (6), His349 (6), and Thr369 (7) (**Figure 4-5**). Mutational experiments have shown that Phe345Ala and Phe346Ala mutants show substantial reduction in binding constants for Apomorphine (Cho et al 1995). This shows that these residues are important in ligand recognition.

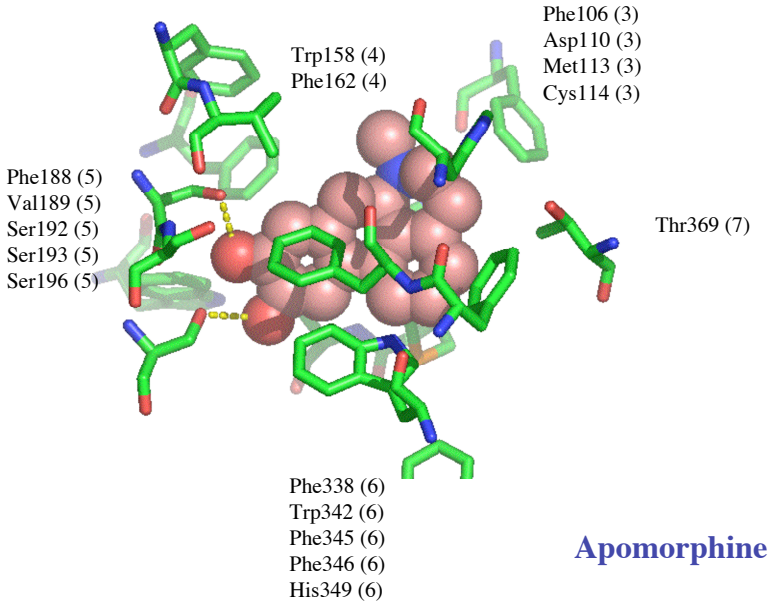

Figure 4-5. The 5.5 Å binding site of Apomorphine to the human D_3 dopamine receptor. The numbers in the brackets indicate the TM helices to which the residues belong to.

Clozapine: Clozapine is a class I antagonist, meaning it binds in the putative agonist binding site located between TM3, 4, 5, and 6. There is, as always, an amino group salt bridged to the TM3 Asp110 (2.8 Å). As is the case for all antagonists studied, there is a lone hydrogen bond to the sequence of TM5 serines. Although the hydrogen bond may be to either Ser192 or Ser196, in our structure, the more reasonable distance and angle are for the interaction between Ser192 and the heteroatom (3.2 Å). There is a third interaction, which although cannot be categorized as a hydrogen bond, is energetically significant; this is a 3.4 Å interaction between Trp342 in TM6 and the hydrogen of the ring in Clozapine. Cys114 is ~5 Å apart from the other nitrogen in the Clozapine ring. The remainder of the residues provide a mostly hydrophobic pocket for the ligand. The residues in close proximity of the Clozapine ligand are Trp85 (2), Phe106 (3), Leu109 (3), Met113 (3), Cys114 (3), Phe162 (4), Phe188 (5), Val189 (5), Phe338 (6), Phe345 (6), Phe346 (6), His349 (6), Thr369 (7), and Tyr373 (7) (**Figure 4-6**).

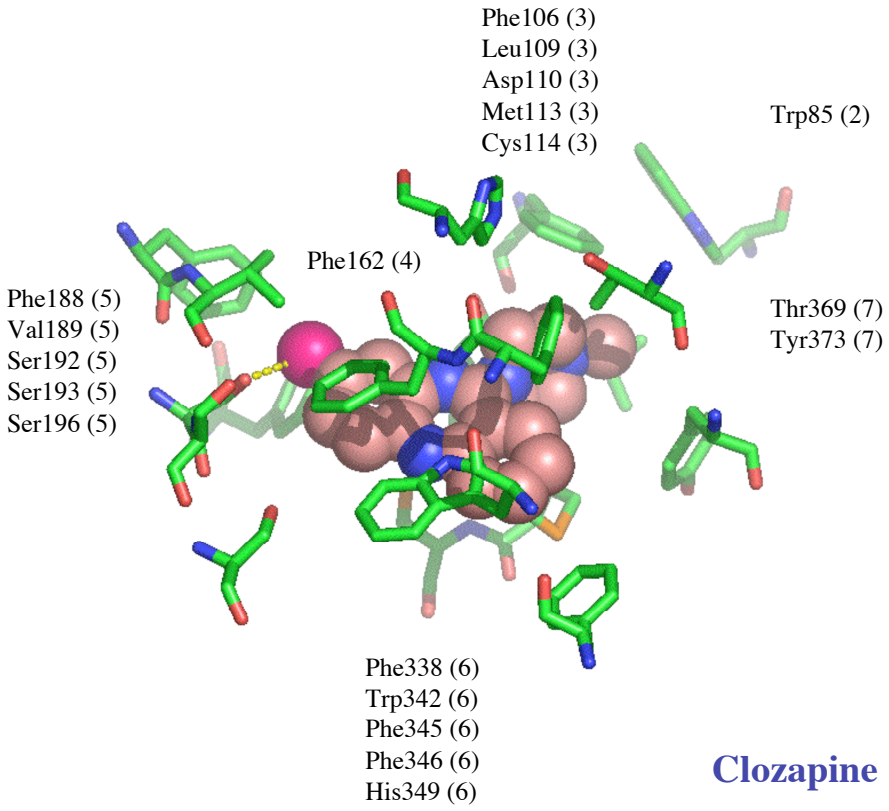

Figure 4-6. The 5.5 Å binding site of Clozapine to the human D_3 dopamine receptor. The numbers in the brackets indicate the TM helices to which the residues belong to.

Fenoldopam: Fenoldopam is an agonist, meaning it binds in the putative agonist binding site located between TM3, 4, 5, and 6. There is a bidentate salt bridge between Asp110 (TM3) with and the amino group with a distances of 2.6 and 2.8 Å. Cys114 (TM3) is hydrogen bonded to heteroatom with a length of 3.4 Å, although the strength of this hydrogen bond is much weaker than that present when serine in a similar position in the D_1-Like receptors interacts with this ligand. The catechol portion is hydrogen bonded to

the TM5 serine networks of Ser192, Ser193, and Ser196 (TM5). There is a 3.2 Å interaction and a 2.9 Å interaction to the catechol by Ser192 and Ser196, respectively. Ser193 is too far to form a hydrogen bond to the ligand. Interestingly, it is possible for the phenol group to be pi stacked between Phe345 and Phe346 (TM6) and for its hydroxyl group to interact via a hydrogen bond with His349 (6), although this interaction is again weaker than that present in the D_1-like receptor when there is an asparagine present. The remainder of the residues in the cavity provide a mostly hydrophobic pocket for the drug. These residues include: Phe106 (3), Val111 (3), Met113 (3), Cys114 (3), Trp158 (4), Phe162 (4), Val189 (5), Val195 (5), Phe338 (6), Trp342 (6), His349 (6), Thr369 (7), and Tyr373 (7) (**Figure 4-7**).

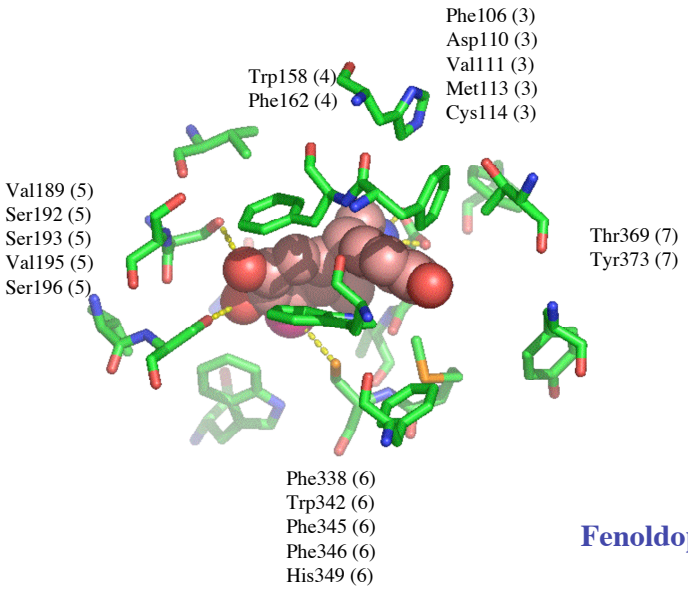

Figure 4-7. The 5.5 Å binding site of Fenoldopam to the human D_3 dopamine receptor. The numbers in the brackets indicate the TM helices to which the residues belong to.

Haloperidol: The ligand binds in the putative antagonist-binding site located between TM2, TM3, TM4, TM5, TM6, and TM7. Class II antagonists such as Haloperidol are composed of two aromatic domains connected by a linker domain, which has a protonated amino group. The protonated amino group of Haloperidol is salt bridged to the TM3 Asp110 (2.8 Å). There are several heteroatom contacts that are typically too weak to be considered hydrogen bonds. There is a weak interaction between the chlorine atom and TM5 Ser196 (3.2 Å). There is also a hydrogen bond between the hydroxyl of Haloperidol and TM6 Trp342 (3.4 Å). There is a third weak interaction between the fluorine atom on the second aromatic portion of Haloperidol and TM2 Trp85 (2.9 Å). Other residues form a mostly hydrophobic pocket around the ligand; these residues include: Val82 (2), Leu89 (2), Phe106 (3), Leu109 (3), Met113 (3), Cys114 (3), Trp158

(4), Phe162 (4), Phe188 (5), Val189 (5), Val195 (5), Trp342 (6), Phe345 (6), Phe346 (6), His349 (6), Ser366 (7), Ala367 (7), Thr369 (7), Trp370 (7), and Tyr373 (7) (**Figure 4-8**).

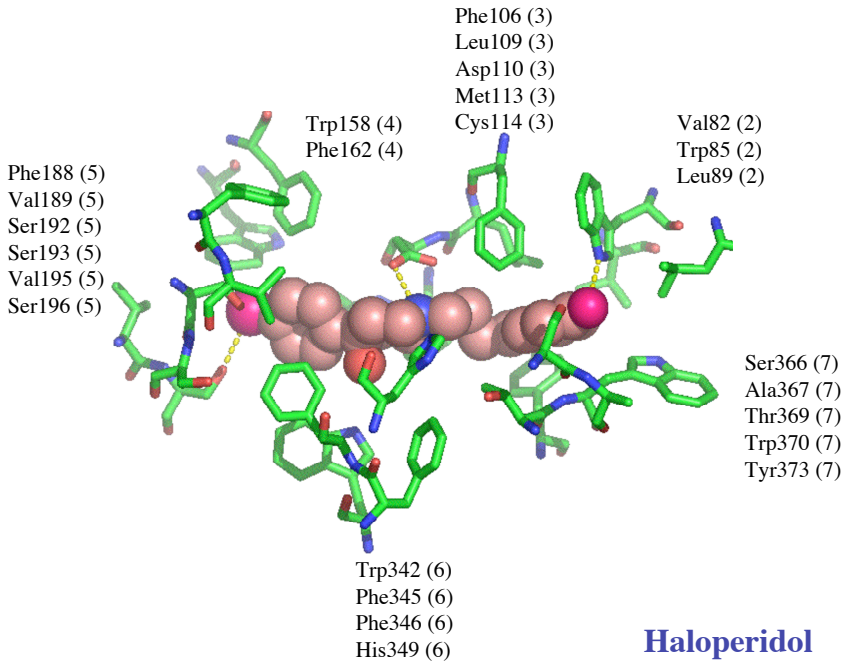

Figure 4-8. The 5.5 Å binding site of Haloperidol to the human D_3 dopamine receptor. The numbers in the brackets indicate the TM helices to which the residues belong to.

Raclopride: Raclopride binds in the class I antagonist-binding site, although it begins to extend to the TM2 and 7 aromatic micro-domain. The critical contact points are the salt bridge between TM3 Asp110 and the protonated amino group of the ligand (2.8 Å), and interactions with the TM3 Cys114 (3.6 Å) and Ser192 (3.8 Å) and Ser196 (3.9 Å), the latter of which is too long to be considered a hydrogen bond. The remainder of the residues provide a mainly hydrophobic pocket for the remainder of the ligand. The

residues in close proximity of the ligand include: Phe106 (3), Val107 (3), Met113 (3), Cys114 (3), Trp158 (4), Phe162 (4), Asn185 (EC2), Phe188 (5), Val189 (5), Trp342 (6), Phe345 (6), Phe346 (6), His349 (6), Ser366 (7), and Thr369 (7) (**Figure 4-9**).

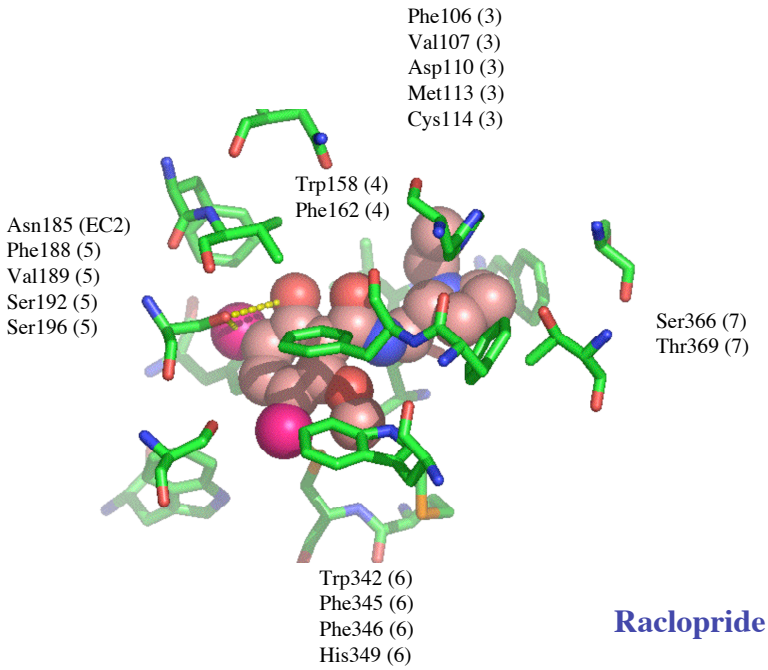

Figure 4-9. The 5.5 Å binding site of Raclopride to the human D_3 dopamine receptor. The numbers in the brackets indicate the TM helices to which the residues belong to.

SCH-23390: SCH-23390 is a class I antagonist. It forms a salt bridge with the TM3 Asp110 with a distance of 2.8 Å. There are two hydrogen bond contacts with the 5th transmembrane domain. There is a 3.0-Å interaction with Ser192 (5) and a 3.6 Å interaction with Ser196 (5). The remainder of the residues create a mostly hydrophobic pocket for the ligand, with Phe345 (6) and Phe346 (6) forming excellent Van der Waals interactions with the phenyl substituent of the ligand. Other amino acids in the cavity

include: Phe106 (3), Met113 (3), Cys114 (3), Trp158 (4), Phe162 (4), Asn185 (EC2), Phe188 (5), Val189 (5), Ser193 (5), Trp342 (6), His349 (6), Val350 (6), Thr353 (6), Thr369 (7) (**Figure 4-10**).

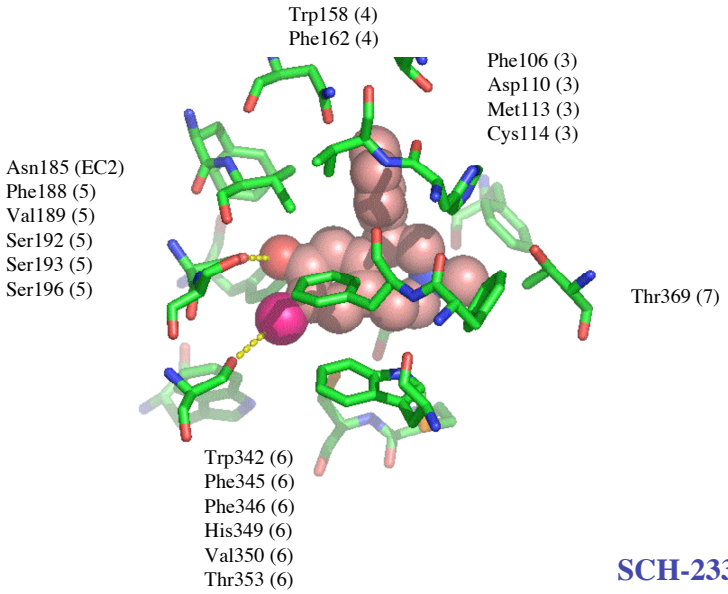

Figure 4-10. The 5.5 Å binding site of SCH-23390 to the human D_3 dopamine receptor. The numbers in the brackets indicate the TM helices to which the residues belong to.

SKF-38393: SKF-38393 is an agonist. It forms a bidentate salt bridge with Asp110 with a distance of 2.8 Å. There are two hydrogen bonds to Ser192 (3.0 Å) and Ser196 (3.8 Å). The phenyl substituent is pi stacked between Phe345 (6) and Phe346 (6). The remainder of the residues form a pocket around the ligand; these residues include: Phe106 (3), Met113 (3), Cys114 (3), Trp158 (4), Phe162 (4), Asn185 (EC2), Phe188 (5), Val189 (5), Ser193 (5), Trp342 (6), His349 (6), Val350 (6), Thr353 (6) (**Figure 4-10**).

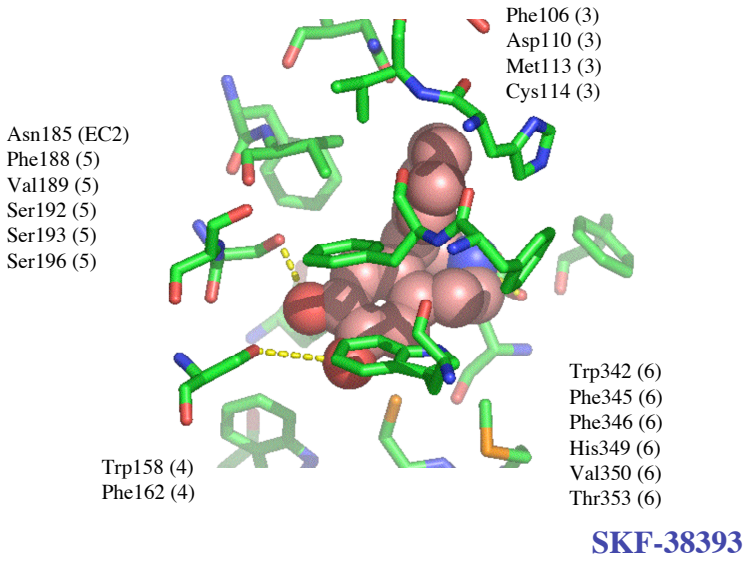

Figure 4-11. The 5.5 Å binding site of SKF-38393 to the human D_3 dopamine receptor. The numbers in the brackets indicate the TM helices to which the residues belong to.

Spiperone: Spiperone is a class II antagonist; meaning, it binds with its aromatic domains to the voids between TM2 & 7 and TM4 & 6, and it forms a salt bridge to TM3 and weak non-ionic interactions to TM5 and 6. The protonated amino group of the ligand is salt bridged to the TM3 Asp110 (2.9 Å). There is a hydrogen bond between the fluorine of the ligand and Ser192 (2.8 Å). Another weak, non-ionic interaction is to the TM6 Trp342 (3.0 Å). The remainder of the residues in the cavity create a mostly hydrophobic pocket for the aliphatic portions of the ligand. Residues present in the cavity include: Leu81 (2), Trp85 (2), Val105 (3), Phe106 (3), Val107 (3), Thr108 (3), Leu109 (3), Met113 (3), Cys114 (3), Trp158 (4), Phe162 (4), Val189 (5), Trp342 (6), Phe345 (6), Phe346 (6), His349 (6), Ser366 (7), Thr369 (7), Trp370 (7), Leu371 (7), Gly372 (7), Tyr373 (7) (**Figure 4-12**).

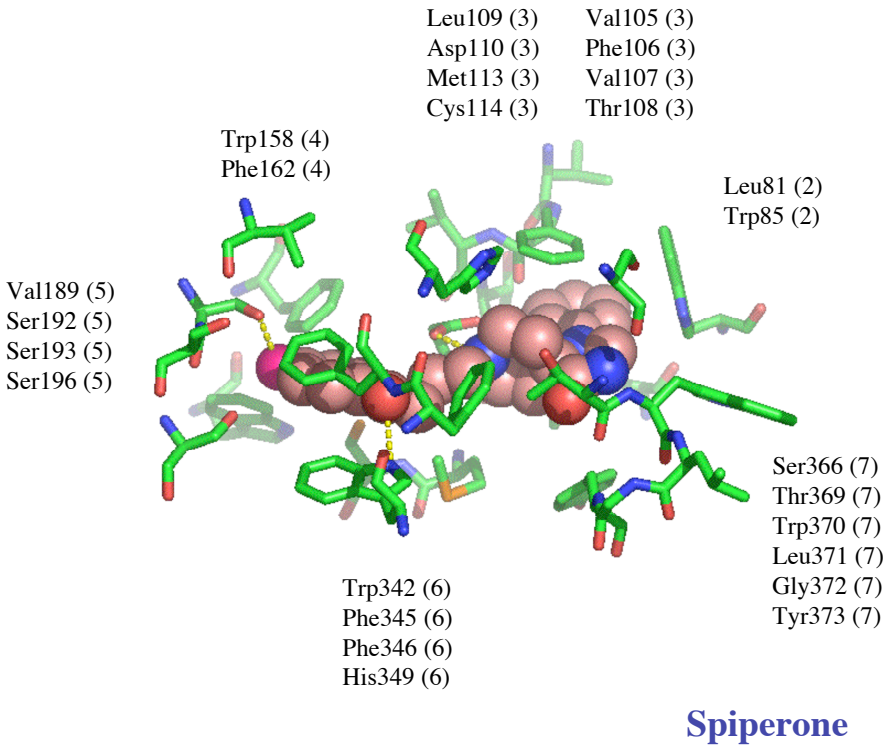

Figure 4-12. The 5.5 Å binding site of Spiperone to the human D_3 dopamine receptor. The numbers in the brackets indicate the TM helices to which the residues belong to.

Sulpiride: Sulpiride is a class I antagonist meaning it binds in the putative agonist binding site with minimal extension into the TM2 and 7 aromatic micro-domain. Sulpiride has a salt bridge to the TM3 Asp110 (2.8 Å). The sulfonamide portion of the ligand interacts well with the sequence of Serines in TM5. There are two hydrogen bonds of 2.9 Å and 3.5 Å to Ser192 and Ser196, respectively. The strength of these hydrogen bonds is, however, a different issue. The remainder of the residue provide a mostly hydrophobic pocket. The residues in close proximity include: Trp85 (2), Phe106 (3), Leu109 (3), Met113 (3), Cys114 (3), Trp158 (4), Phe162 (4), Phe188 (5), Val189 (5),

Ser193 (5), Trp342 (6), Phe345 (6), Phe346 (6), His349 (6), Ser366 (7), Thr369 (7), Trp370 (7), and Tyr373 (7) (**Figure 4-13**).

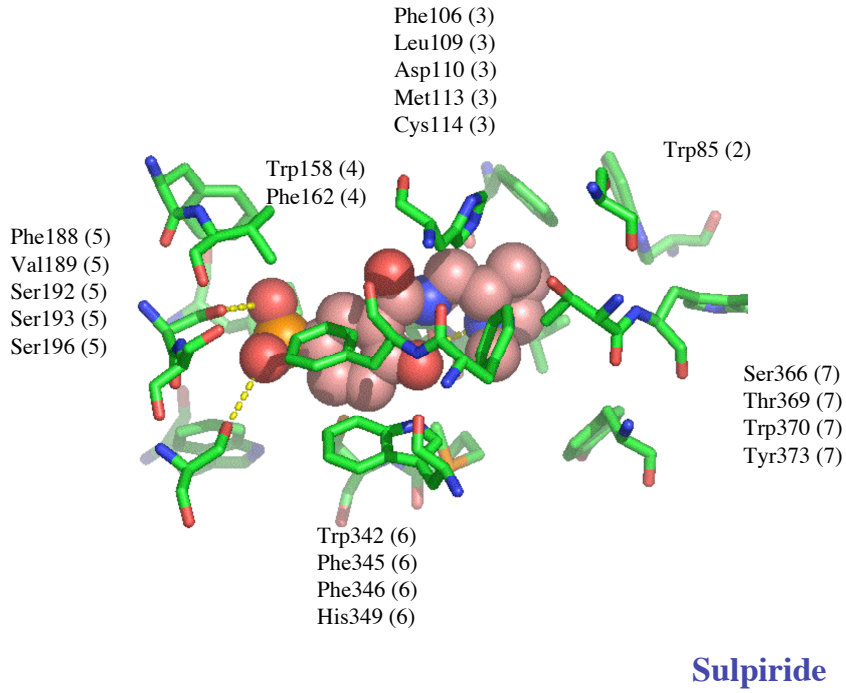

Figure 4-13. The 5.5 Å binding site of dopamine to the human D_3 dopamine receptor. The numbers in the brackets indicate the TM helices to which the residues belong to.

Comparisons of Binding Site of Agonists vs. Antagonists: Experimental studies have outlined the binding site for agonists and antagonists. The putative agonist-binding site is located between TM3, 4, 5, & 6, and some residues in the EC2 loop (assuming this loop closes during the process of activation). We have classified antagonists into two categories: Class I & II. Class I antagonists, such as Clozapine bind in the putative agonist binding pocket meaning they occupy the void between TM3, 4, 5 and 6. Class II antagonists, such as Haloperidol consists of two aromatic domains connected by a linker,

which possess a protonated amino group. These antagonists bind in the cavity between TM2, 3, 4, 5, 6, and 7. There are two aromatic micro domains (pictures of aromatic micro domains goes here). The first aromatic micro-domain is located in TM4 and TM6, which is composed of the very symmetric Trp158 (4), Phe162 (4), Trp342 (6), and Phe346 (6). This aromatic micro-domain stabilizes one of the aromatic rings of the class II antagonists. TM3 provides the salt bridge to TM3 Asp110, which stabilizes the ligand in place. TM5 provides weak interactions with heteroatom functionalities such as halogens on the rings of class II antagonists. These interactions are weak but important in recognition of the correct aromatic domain for docking into the cavity. The second aromatic micro-domain composed of Trp85 (2), Phe106 (3), Trp370 (7), and Tyr373 (7) stabilize the second aromatic ring group of the class II antagonists.

Comparison of agonists binding site: There is very little difference in the putative agonist-binding site of different agonists. The agonists studied, (dopamine, 7-OH DPAT, Apomorphine, and) all possess protonated amino groups, which are salt bridged to TM3 Asp110. All of these ligands studied form favorable hydrogen bonding interactions to a network of TM5 serines, although this is not an absolute necessary for agonism. There is, in every case studied, favorable interaction from the first aromatic micro-domain located in TM4 and TM6. A residue that has not been appreciated in drug design is His349 (6). The presence of this residue contributes greatly to ligand binding, yet it appears that there few agonists utilize this residue effectively. It is important to note that the agonists studied effectively interact with both Ser192 and Ser196 in TM5. The interactions to Ser193, the third TM5 serine, are too long to be considered a hydrogen bond (on the

order of ~ 5 Å). Under no circumstance, due to structural constraints, can all three serines effectively interact with the agonists studied. It appears that there could at most be two hydrogen bonds to the TM5 serines. Although in our structure Ser193 is not participating in any interactions, it is possible that in a slightly different structure, perhaps one resulting from activation, there could be interactions to Ser193 and Ser196 as opposed to Ser192 and Ser196. All agonists studied cause strong coupling of TM3 and 5. None of the agonists studied block TM3 and 6 motions. Based on structural studies of rhodopsin, it has been established that a motion between TM3 and 6 are essential for activation. The coupling of TM3 and 6 by agonists causes a decrease in distance between TM3 and 5 while allowing for motion between TM3 and 6.

Comparison of antagonists binding site: The antagonists studied were classified into two categories: Class I antagonists (exemplified by Clozapine), which bind in the putative agonist binding pocket; and class II antagonists (exemplified by Haloperidol), which bind in the cavity between TM2, 3, 4, 5, 6, and 7.

Class I Antagonists: the Clozapine-like antagonists salt bridge to the TM3 Asp110 with their protonated amino group. They do not have two aromatic rings and therefore only utilize the first aromatic micro-domain between TM4 and 6. As is the case with both class I and class II antagonists, they form only one weak interaction with the TM6 serine network. In our models the interaction may be with Ser192 or Ser196. At first glance, it appears that both the number of and strength of the interactions with the TM5 serines may be important for activation. Interestingly, however, the situation is more complicated

than it appears; Strange et al. have identified agonism from a non-hydroxylated form of the DPAT series. The critical distinguishing feature of an agonist vs. an antagonist appears to be its relative position to TM6. Class I antagonists burry their aliphatic domain deep into the conserved TM6 WXXFF motif. Experimental studies of rhodopsin suggest that motion of TM3 and 6 is necessary for activation. The binding of antagonists at the TM6 WXXFF would prevent any motion, specifically the hinge motion between TM3 and TM6 that is necessary for activation. It appears that the presence of one hydroxyl/one hydrogen bond donor/acceptor is not an absolute necessity for antagonism. The class I antagonists are further stabilized by Phe106 in TM3.

Class II Antagonists: the Haloperidol-like antagonists salt bridge to TM3 Asp110 with their protonated amino group. They possess two aromatic ring units. In most cases, only one of the aromatic rings is halogenated, and this is the ring that binds to the first aromatic micro-domain, with the second ring binding in the second aromatic micro-domain. The halogenated ring binds effectively into the cavity between TM4 and 6 and forms weak interactions with either Ser192 or Ser196 in TM5. It gains stability from the presence of TM4 Trp158 and Phe162 and TM6 Trp343 and Phe346. In some cases His349 (6) may also stabilize the class II antagonists. The non-halogenated aromatic domain is located in the void between TM2 and TM7. It gains stabilization from Trp85 (2), Phe106 (3), Trp370 (7), and Tyr373 (7). As is the case with the class I antagonists, class II antagonists prevent motion between TM3 and TM6 by burying their aliphatic portion between TM3 and TM6, thereby preventing interaction of these helices. There is very little difference between the binding sites of the class II antagonists, although some utilize the cavity better than others.

Ligand	B.E. (Kcal/mol)
7OHDPAT	-95
Apomorphine	-107.4
Clozapine	-79.8
Dopamine	-91.9
Fenoldopam	-92.2
Haldol	-123.5
Raclopride	-108.4
SCH	-102.3
SKF	-96.9
Spiperone	-121.2
Sulpiride	-107.9

Table 4-2. Binding energies in kcal/mol for a library of 11 ligands to the human D_3 dopamine receptor.

D_3 Receptor Experimental Ranking:

Raclopride~Spiperone~7-OHDPAT>Haldol~Sulpiride~Dopamine~Apomorphine>

Clozapine~SCH23390~SKF38393

D_3 Receptor Ranking Theory:

Haldol~Spiperone~Raclopride~Apomorphine~Sulpiride>SCH23390~SKF38393~7-

OHDPAT~Fenoldopam~Dopamine~Clozapine

Appendix V: The Predicted Structure of the Human D_4 Dopamine Receptor

The Predicted Structure of the Human D_4 Dopamine Receptor

M. Yashar S. Kalani [§,*], Nagarajan Vaidehi[*] & William A. Goddard III[**]

* Materials and Process Simulation Center, Beckman Institute, California Institute of Technology, Pasadena, CA 91125

§ Johns Hopkins University School of Medicine, Baltimore, MD 21205

****To whom correspondence should be addressed (e-mail: wag@wag.caltech.edu)**

Results:

We have predicted the structure and binding site of 10 agonists and antagonists (Shown in **Figure 5-1**) in D_4DR using the methods detailed in the Methods and Materials section. **Figure 5-2** shows the 3D atomic resolution structure of the human D_4DR modeled from the predicted structure of D_2DR using the Membstruk procedure and the predicted binding site of dopamine determined using the HierDock procedure. We refer to this predicted structure as D_4DR. Using the D_4DR structure, we have identified the agonist and antagonist-binding sites for a library of 10 ligands (**Figure 5-1**), calculated their binding energies, and the criteria for agonist and antagonist activation of the receptor. The antagonists studied in this publication are divided into two classes: 1) class I antagonists that are bulky and bind in a similar location as agonists, exemplified by Clozapine; and, 2) class II antagonists that consists of two aromatic moieties connected by a flexible linker chain exemplified by Haloperidol. In this paper we give details of the

residues in the binding site of all the 10 ligands and analyze the similarities and differences in their binding sites.

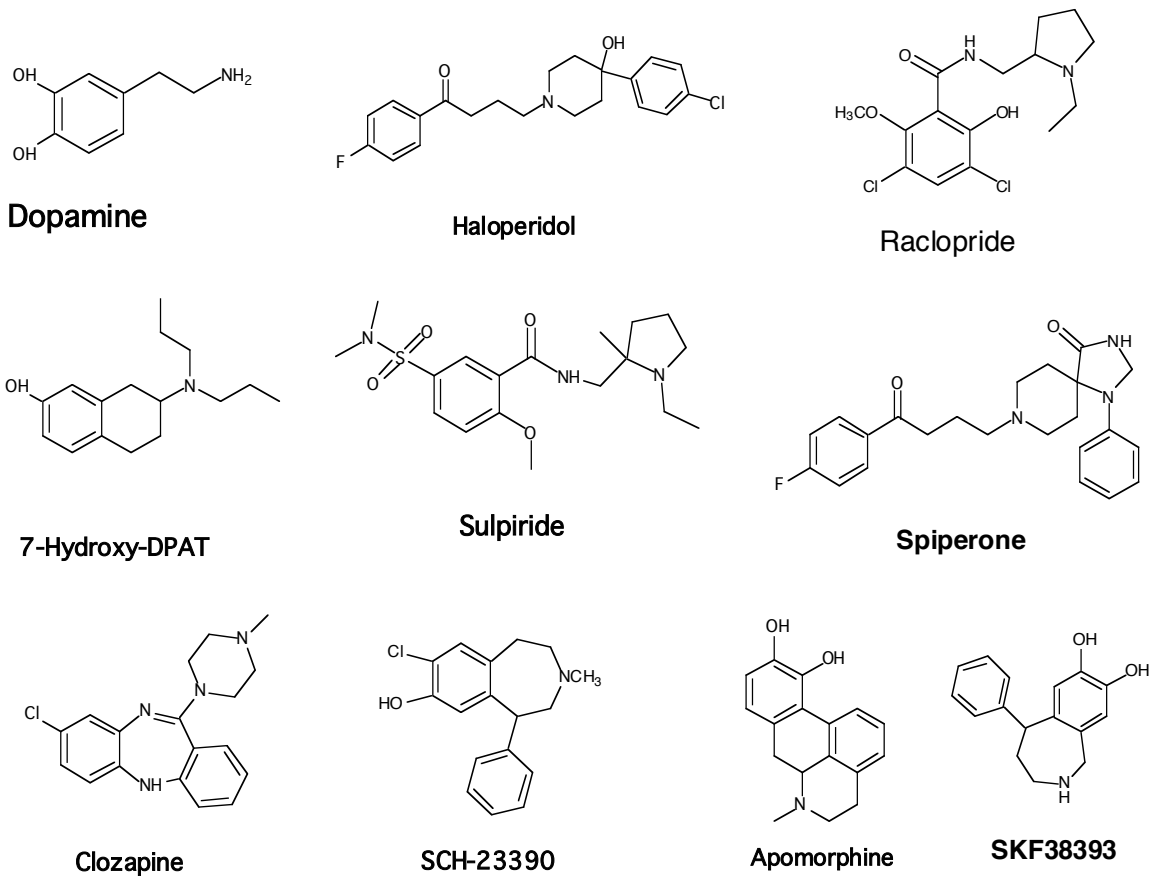

Figure 5-1. 10 agonists and antagonists studied for the human Dopamine D_4 receptor.

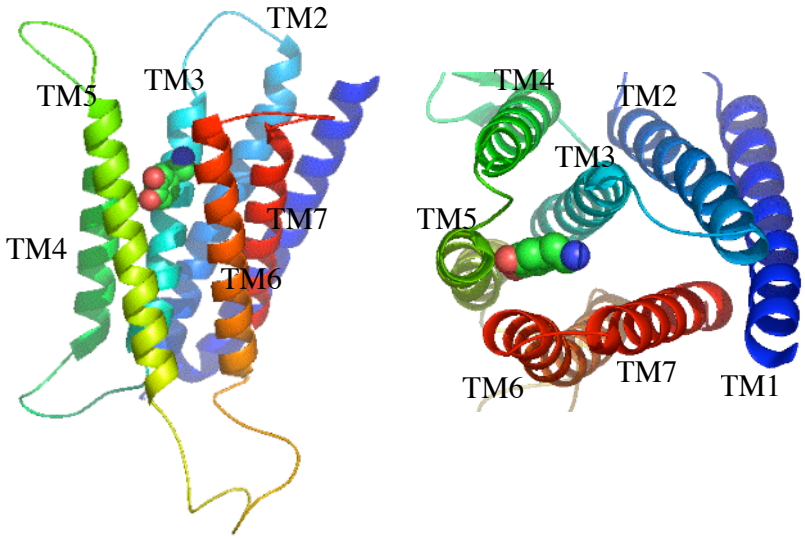

Figure 5-2. Predicted binding site of Dopamine (shown in sphere) in the predicted structure of human dopamine D_4 receptor.

In the preliminary studies, we have validated these methods for bovine rhodopsin, human ß-2 adrenergic receptor, human s1p (sphingolipid) and lpa (lysophosphatidic acid) receptors, and 10 mouse olfactory receptors (Vaidehi 2002, Floriano 2000, Floriano 2003, Hall 2003). The results are in good agreement with available experimental data, indicating a good description of the binding site and relative binding energies of various ligands.

Prediction of the Structure of Human D_4DR:

The Membstruk procedure used to predict the structure is detailed in Vaidehi 2002. The TM2nDs procedure (Vaidehi 2002, Trabanino 2003) was utilized to identify the transmembrane (TM) spanning regions based on a hydrophobic analysis of the sequence. A seven helical motif was identified (below) ranging from 19-29 residues per helix. The highlighted residues represent TM helices, while the intervening sequences are loop regions.

MGNRSTADADGLLAGRGPAAGASAGASAGLAGQGAAALVGGVLLIGAVLAGN
SLVCVSVATERALQTPTNSFIVSLAAADLLLALLVLPLFVYSEVQGGAWLLSPRL
CDALMAMDVMLCTASIFNLCAISVDRFVAVAVPLRYNRQGGSRRQLLLIGATW
LLSAAVAAPVLCGLNDVRGRDPAVCRLEDRDYVVYSSVCSFFLPCPLMLLLYW
ATFRGLQRWEVARRAKLHGRAPRRPSGPGPPSPTPPAPRLPQDPCGPDCAPPAPG
LPRGPCGPDCAPAAPGLPPDPCGPDCAPPAPGLPQDPCGPDCAPPAPGLPRGPCG
PDCAPPAPGLPQDPCGPDCAPPAPGLPPDPCGSNCAPPDAVRAAALPPQTPPQTR
RRRRAKITGRERKAMRVLPVVVGAFLLCWTPFFVVHITQALCPACSVPPRLVSA
VTWLGYVNSALNPVIYTVFNAEFRNVFRKALRACC

Scheme 5-1. Predicted transmembrane regions are highlighted below in the human D_4 dopamine receptor.

The TM prediction was utilized in building seven canonical α-helices and optimized using the procedure described in Vaidehi 2002. The helices were bundled in explicit bilayer of dilaurylphosphatidylcholine lipid molecules to mimic the biological membrane. The structural factors such as helical bend, helical tilt etc., of the predicted structure of D_4DR structure compared to the crystal structure of rhodopsin are summarized in **Table 5-1**.

TM Helix	Helical Bend	Plane Tilt	HPM Angle	HPM Mag.	HPM Fit	Plane CM Dist.	Plane CM Angle	CM Fit
1	10.1	32.3	-89.0	9.1	0.0	15.9	0.0	1.3762
2	14.6	33.0	-12.1	7.3	0.0	10.2	37.0	0.6935
3	3.9	13.4	9.0	2.8	0.0	3.9	124.1	2.7529
4	4.5	4.5	-81.7	8.2	0.0	14.5	127.0	-2.9960
5	8.7	10.4	-110.0	7.3	0.0	14.1	189.6	2. 6744
6	21.8	15.5	87.4	7.9	0.0	11.7	246.8	1.9452
7	4.0	18.9	-39.2	6.0	0.0	9.6	304.8	-6.4462

Centered Comparison Table

TM Helix	HPM Angle	HPM Mag.	Helical Bend	P. Face Deg.
1	-65.7	3.1	21.8	238
2	33.2	3.8	10.8	165
3	5.5	3.0	0.0	68
4	-69.1	4.1	3.5	242
5	24.4	3.8	15.3	221
6	-153.4	5.5	15.2	202
7	-11.6	3.9	2.3	141

Table 5-1. Comparison of the D_4DR with the crystal structure of bovine rhodopsin.

RMS height of TMR: 30.4

RMS radius of TMR: 12.0

From **Table 5-1** it is clear that the helical bends are very different for D_4DR compared to rhodopsin. The volume of the TM barrel for D_4DR is 13810.2 $Å^3$. There is

one disulfide bond between Cys108 and Cys185 in EC2. Rhodopsin has a volume of 11,807.7 $Å^3$. The calculated RMS in the coordinates of the C_α atoms of the D_4DR structure compared to the crystal structure of rhodopsin is 6.81 Å and a total residue RMS of 7.39 Å (all atoms).

Prediction of the putative binding site for dopamine in D4DR: The Hierdock2.0 procedure (Vaidehi 2002) was utilized to scan all the D_4DR models as described in Materials and Methods section. We discuss the details of the predicted binding site in D_4DR model for all the 10 ligands studied in this paper.

Dopamine: Dopamine is the endogenous ligand of the dopamine receptors. It binds in the putative agonist binding site located between TM3, 4, 5, and 6. There are two main contacts that energetically stabilize dopamine in this docked conformation; 1) salt bridge between the TM3 Asp115 (bidentate, 2.8 Å and 2.9 Å), and 2) a network of hydrogen bonds to the TM5 Ser196, Ser197, and Ser200. In our structure Ser196 and Ser200 have 3.0 and 3.2 Å interactions with the catechol hydroxyls, respectively. Ser197 is ~ 5 Å away and the interactions it has with the catechol hydroxyls are too far to be considered hydrogen bonds, although a rotation of TM5 will allow Ser197 to form excellent interactions with the catechol of dopamine. Under no circumstance can all three serines in TM5 form hydrogen bonds with reasonable distances and angles; at no time can there be more than 2 hydrogen bonds to the sequence of serine in TM5. Interaction between Ser196 and Ser200 may result during steps leading to or resulting from activation. Other

residues in the binding pocket provide mostly hydrophobic packing for the ligand. These residues include Leu113 (3), Leu118 (3), Cys119 (3), Val193 (5), Trp407 (6), Phe411 (6), His414 (6), Ile415 (6), and Thr434 (7) (**Figure 5-3**). The first phenylalanine of the conserved WXXFF motif, Phe410 is slightly greater than 5.5 Å away from dopamine. His414 in TM6 is providing a very strong component of the binding energy of dopamine to the receptor. Assuming Asp115 forms a bidentate salt bridge, or a salt bridge and a hydrogen bond to the amino group of dopamine, the interaction with His414 fulfils the ability of the amino group to form favorable interactions with any other residues. It is essential to know that a Phe-Ala164 mutation in TM4 has removed the stabilization of the aliphatic/aromatic portions of the ring. Additionally, Trp160 (4), usually present in the binding site of dopamine and other ligands is absent in this bound conformation.

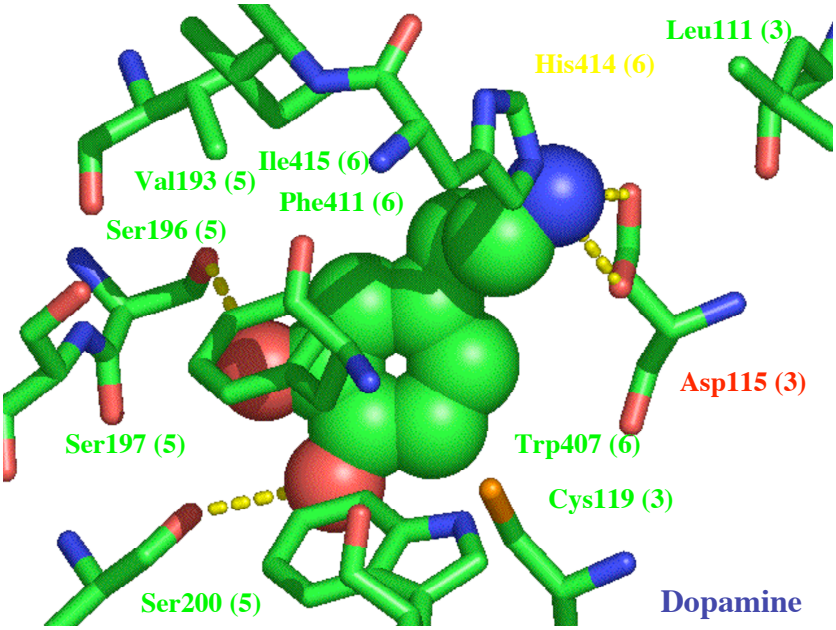

Figure 5-3. The 5.5 Å binding site of dopamine to the human D_4 dopamine receptor. The numbers in the brackets indicate the TM helices to which the residues belong to.

7-OH DPAT: The ligand binds in putative agonist binding site located between TM3, 4, 5, and 6. The protonated amino group of 7-OH DPAT is salt bridged to the TM3 Asp115 (2.8 Å). The other major polar contacts are to the conserved TM5 serines 196, 197 and 200. There are two hydrogen bonds, both 3.0 Å to Ser196 and 200. The interaction to Ser197 is 5.2 Å and is too long to be considered a hydrogen bond. The remainder of the residues in the cavity are mainly hydrophobic residues that provide stabilization for the aromatic and aliphatic rings of the ligand. The residues in close hydrophobic contact of the ligands are Leu111 (3), Met114 (3), Leu118 (3), Cys119 (3), Val193 (5), Trp407 (6), Phe410 (6), Phe411 (6), His414 (6), Ile415 (6), Thr434 (7), and Tyr438 (7), (**Figure 5-4**) which provide a mainly hydrophobic pocket.

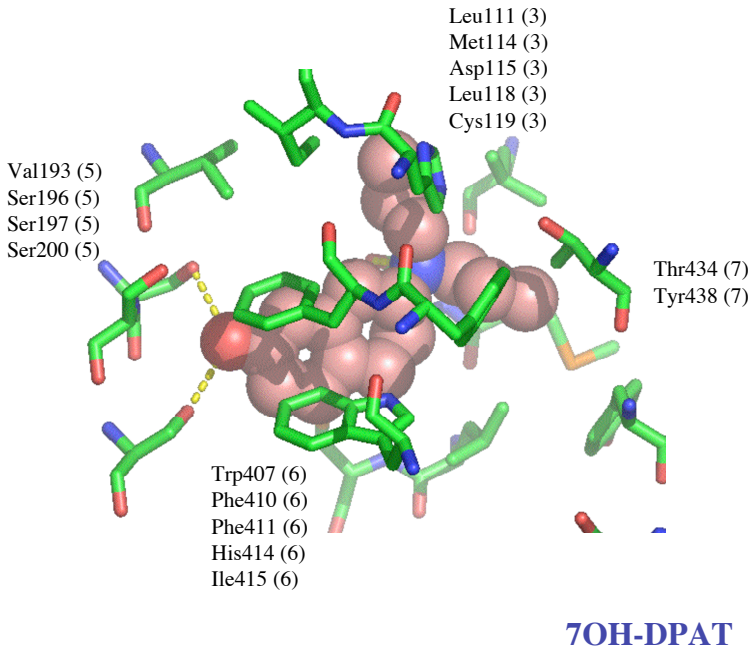

Figure 5-4. The 5.5 Å binding site of 7-OH DPAT to the human D_4 dopamine receptor. The numbers in the brackets indicate the TM helices to which the residues belong to.

Apomorphine: The ligand binds in the putative agonist binding site located between TM3, 4, 5, and 6. The protonated amino group of Apomorphine is salt bridged to the TM3 Asp115 (2.9 Å). The other major polar contacts are to the conserved TM5 serines 196, 197 and 200. There are as previously two hydrogen bonds to Ser196 (3.1 Å) and Ser200 (3.2 Å) both to the hydroxyl groups on Apomorphine. The contact to Ser197 is ~ 6 Å apart. Other residues form a most hydrophobic pocket around the ligand; these residues include: Leu111 (3), Leu118 (3), Cys119 (3), Trp160 (4), Val193 (5), Phe403 (6), Trp407 (6), Phe410 (6), Phe411 (6), His414 (5), Ile415 (6), Trp434 (7) (**Figure 5-5**). Mutational experiments have shown that Phe410Ala and Phe411Ala mutants show substantial reduction in binding constants for Apomorphine (Cho et al 1995). This shows that these residues are important in ligand recognition.

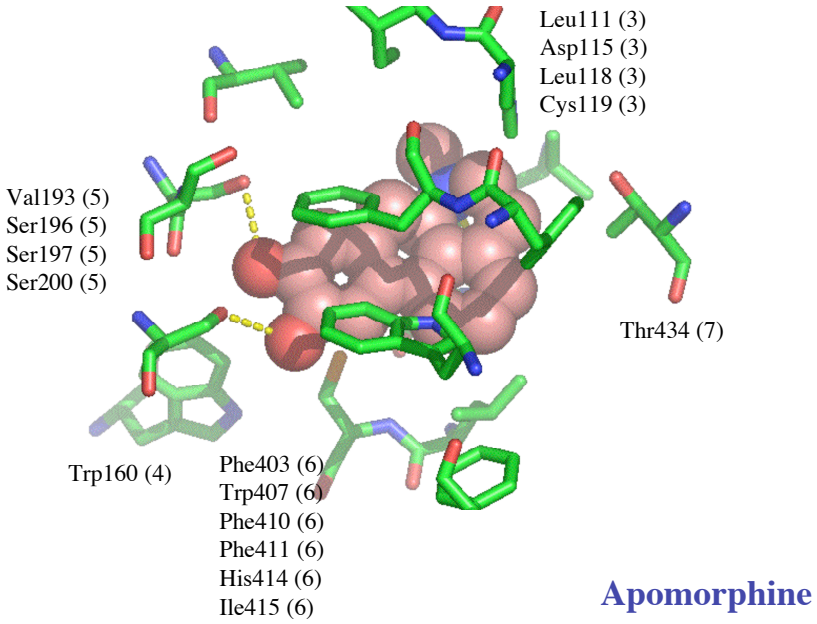

Figure 5-5. The 5.5 Å binding site of Apomorphine to the human D_4 dopamine receptor. The numbers in the brackets indicate the TM helices to which the residues belong to.

Clozapine: Clozapine is a class I antagonist, meaning it binds in the putative agonist binding site located between TM3, 4, 5, and 6. There is, as always, an amino group salt bridged to the TM3 Asp115 (2.8 Å). As is the case for all antagonists studied, there is a lone hydrogen bond to the sequence of TM5 serines. Although the hydrogen bond may be to either Ser196 or Ser200, in our structure, the more reasonable distance and angle are for the interaction between Ser196 and the heteroatom (3.2 Å). Cys119 is 4.2 Å apart from the ring nitrogen in the Clozapine ring. The remainder of the residues provide a mostly hydrophobic pocket for the ligand. The residues in close proximity of the Clozapine ligand are Leu90 (2), Leu111 (3), Met114 (3), Leu118 (3), Cys119 (3), Ser122 (3), Tyr192 (5), Val193 (5), Phe403 (7), Trp407 (7), Phe410 (7), Phe411 (7), His414 (6), Thr434 (7), and Tyr438 (7) (**Figure 5-6**).

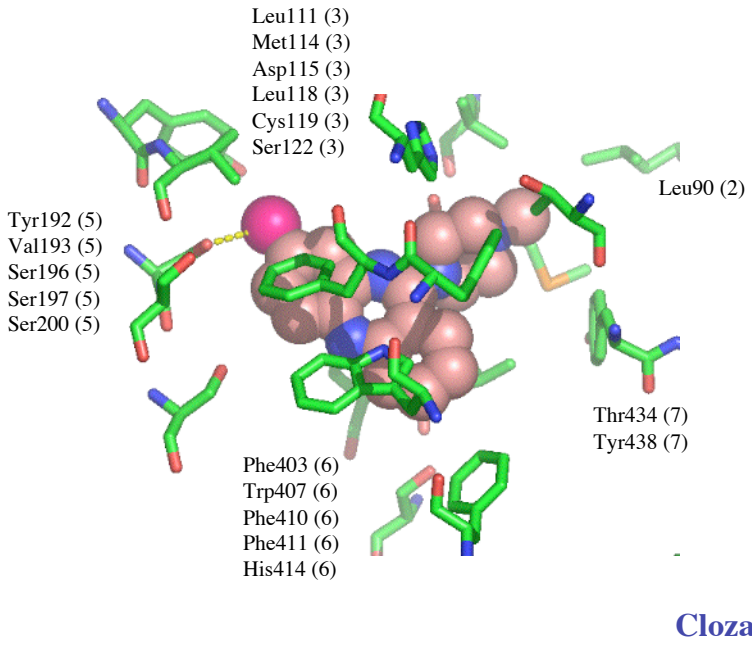

Figure 5-6. The 5.5 Å binding site of Clozapine to the human D_4 dopamine receptor. The numbers in the brackets indicate the TM helices to which the residues belong to.

Fenoldopam: Fenoldopam is an agonist, meaning it binds in the putative agonist binding site located between TM3, 4, 5, and 6. There is a bidentate salt bridge between Asp115 (TM3) with and the amino group with distances of 2.6 and 2.8 Å. Cys119 (TM3) is hydrogen bonded to heteroatom with a length of 3.5 Å. The catechol portion is hydrogen bonded to the TM5 serine networks of Ser196, Ser197, and Ser200 (TM5). There is a 3.2 Å interaction and a 2.9 Å interaction to the catechol by Ser196 and Ser200, respectively. Ser197 is too far to form a hydrogen bond to the ligand. Interestingly, it is possible for the phenol group to be pi stacked between Phe410 and Phe411 (TM6) and for its hydroxyl group to interact via a hydrogen bond with His414 (TM6). The remainder of the residues in the cavity provide a mostly hydrophobic pocket for the drug. These residues include: Val116 (3), Leu118 (3), Trp160 (4), Val193 (5), Cys199 (5), Phe403 (6), Trp407 (6), and Thr434 (7) (**Figure 5-7**).

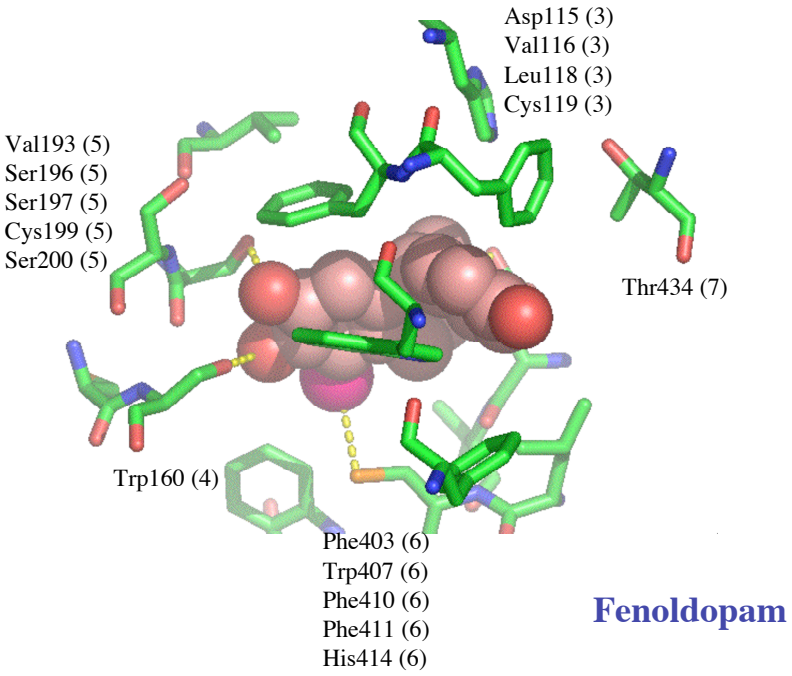

Figure 5-7. The 5.5 Å binding site of Fenoldopam to the human D_4 dopamine receptor. The numbers in the brackets indicate the TM helices to which the residues belong to.

Haloperidol: The ligand binds in the putative antagonist-binding site located between TM2, TM3, TM4, TM5, TM6, and TM7. Class II antagonists such as Haloperidol are composed of two aromatic domains connected by a linker domain, which has a protonated amino group. The protonated amino group of Haloperidol is salt bridged to the TM3 Asp115 (2.8 Å). There are several heteroatom contacts that are typically too weak to be considered hydrogen bonds. There is a weak interaction between the chlorine atom and TM5 Ser200 (3.2 Å). There is also a weak interaction between the hydroxyl of Haloperidol and TM6 Trp407 (4.1 Å). There is a third weak interaction between the fluorine atom on the second aromatic portion of Haloperidol and TM2 Ser431 (2.9 Å). In

cases where there is a TM2 trypthopan, the interaction with the fluorine is provided by the tryptophan. Other residues form a mostly hydrophobic pocket around the ligand; these residues include: Leu90 (2), Phe91 (2), Ser94 (2), Leu111 (3), Met114 (3), Leu118 (3), Cys119 (3), Trp160 (4), Val193 (5), Cys199 (5), Trp407 (6), Phe410 (6), Phe411 (6), His414 (6), Ile415 (6), Val430 (7), Ser431 (7), Ala432 (7), Thr434 (7), Trp435 (7), Tyr438 (7) (**Figure 5-8**).

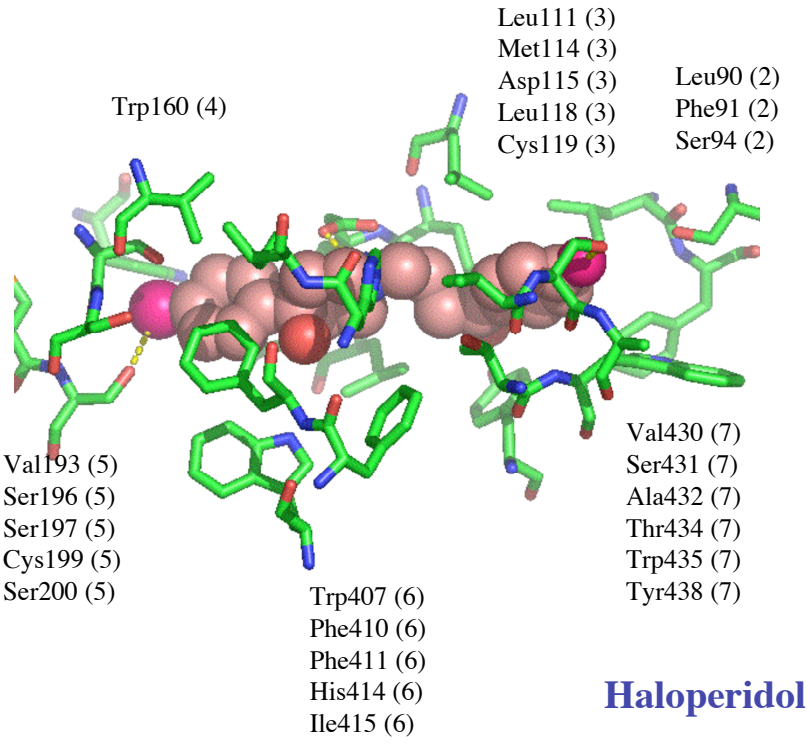

Figure 5-8. The 5.5 Å binding site of Haloperidol to the human D_4 dopamine receptor. The numbers in the brackets indicate the TM helices to which the residues belong to.

Raclopride: Raclopride binds in the class I antagonist-binding site, although it begins to extend to the TM2 and 7 aromatic micro-domain. The critical contact points are the salt bridge between TM3 Asp115 and the protonated amino group of the ligand (2.9 Å), and interactions with the TM3 Cys119 (4.3 Å) and Ser200 (3.8 Å) both of which is too long to be considered a hydrogen bond. The remainder of the residues provide a mainly hydrophobic pocket for the remainder of the ligand. The residues in close proximity of the ligand include: Leu111 (3), Met112 (3), Leu118 (3), Trp160 (4), Ala164 (4), Phe192 (5), Val193 (5), Trp407 (6), Phe410 (6), Phe411 (6), His414 (6), Ile415 (6), and Thr434 (7) (**Figure 5-9**).

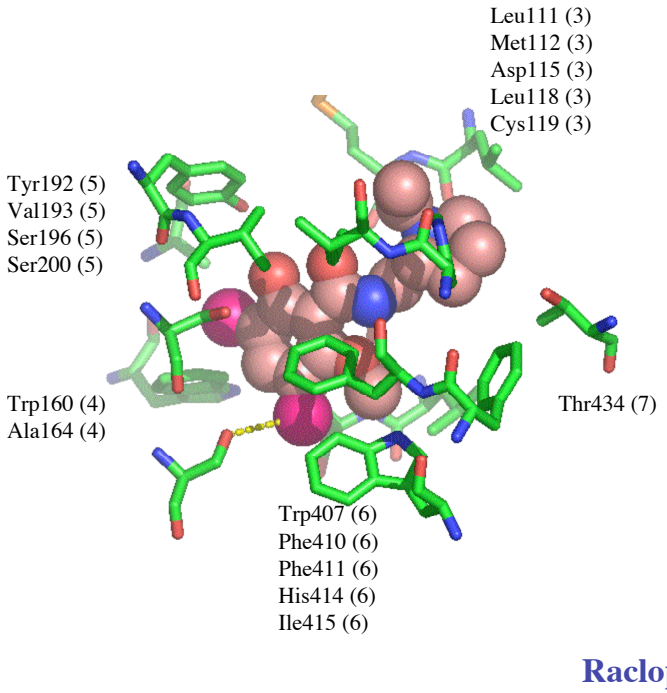

Figure 5-9. The 5.5 Å binding site of Raclopride to the human D_4 dopamine receptor. The numbers in the brackets indicate the TM helices to which the residues belong to.

SCH-23390: SCH-23390 is a class I antagonist. It forms a salt bridge with the TM3 Asp115 with a distance of 2.9 Å. There are two hydrogen bond contacts with the 5th transmembrane domain. There is a 3.1-Å interaction with Ser196 (5); there is a second interaction, which is too weak to be considered a hydrogen bond with Ser200 (5) with a distance of 3.8 Å. The remainder of the residues create a mostly hydrophobic pocket for the ligand, with Phe410 (6) and Phe411 (6) forming excellent Van der Waals interactions with the phenyl substituent of the ligand. Other amino acids in the cavity include: Leu111 (3), Met112 (3), Leu118 (3), Cys119 (3), Phe192 (5), Val193 (5), Ser197 (5), Trp407 (6), His414 (6), Ile415 (6), and Thr434 (7) (**Figure 5-10**).

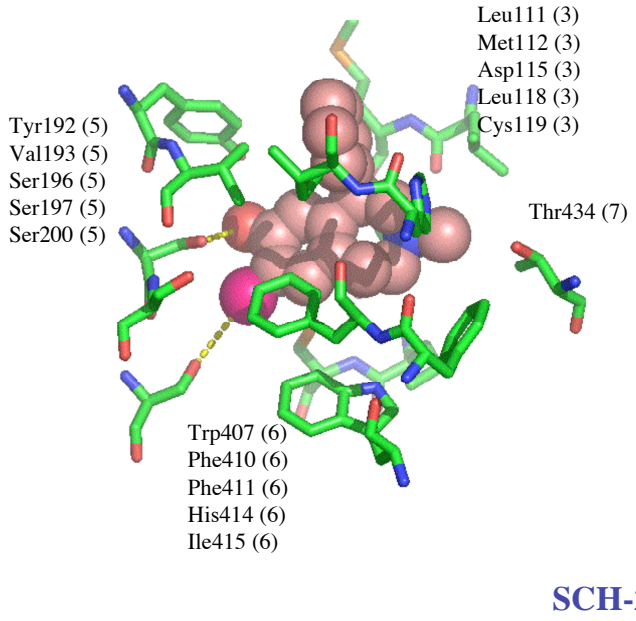

Figure 7-10. The 5.5 Å binding site of SCH-23390 to the human D_4 dopamine receptor. The numbers in the brackets indicate the TM helices to which the residues belong to.

SKF-38393: SKF-38393 is an agonist. It forms a bidentate salt bridge with Asp115 with a distance of 2.8 Å. There are two hydrogen bonds to Ser196 (3.0 Å) and Ser200 (3.3 Å). The phenyl substituent is pi stacked between Phe410 (6) and Phe411 (6). The remainder of the residues form a pocket around the ligand; these residues include: Leu111 (3), Leu118 (3), Cys119 (3), Phe192 (5), Val193 (5), Ser197 (5), Trp407 (5), His414 (6), and Ile415 (6) (**Figure 5-11**).

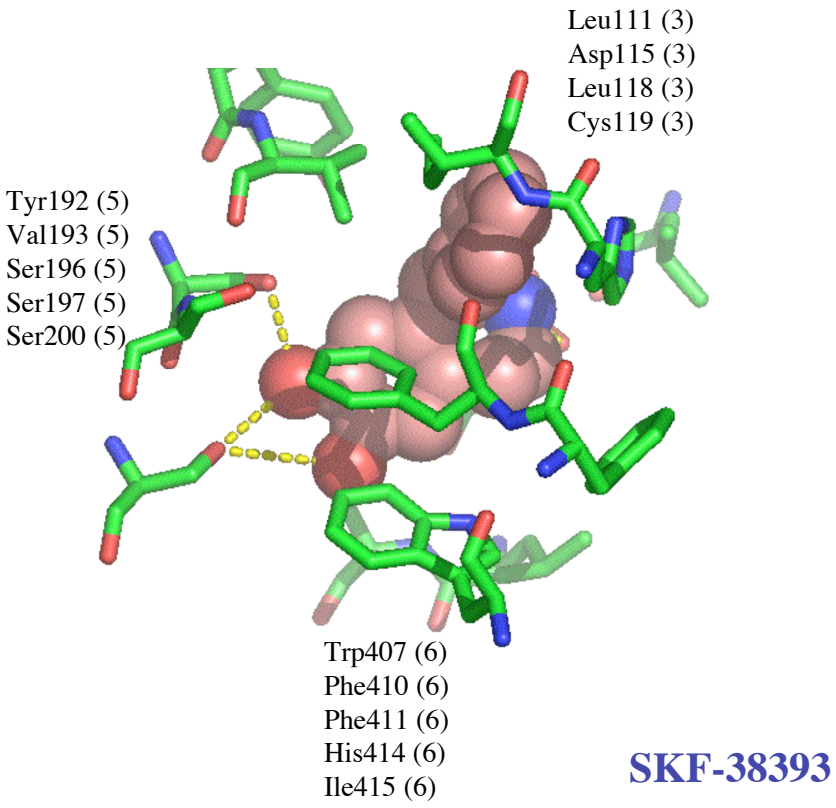

Figure 5-11. The 5.5 Å binding site of SKF-38393 to the human D_4 dopamine receptor. The numbers in the brackets indicate the TM helices to which the residues belong to.

Spiperone: Spiperone is a class II antagonist; meaning, it binds with its aromatic domains to the voids between TM2 & 7 and TM4 & 6, and it forms a salt bridge to TM3 and weak non-ionic interactions to TM5 and 6. The protonated amino group of the ligand is salt bridged to the TM3 Asp115 (2.9 Å). There is a hydrogen bond between the fluorine of the ligand and Ser196 (2.9 Å). Another weak, non-ionic interaction is to the TM6 Trp407 (3.0 Å). The remainder of the residues in the cavity create a mostly hydrophobic pocket for the aliphatic portions of the ligand. Residues present in the cavity include: Leu86 (2), Val87 (2), Leu90 (2), Phe91 (2), Ser94 (2), Leu111 (3), Met112 (3), Met114 (3), Leu118 (3), Cys119 (3), Trp160 (4), Val193 (5), Ser197 (5), Ser200 (5), Trp407 (6), Phe410 (6), Phe411 (6), His414 (6), Ser431 (7), Thr434 (7), Trp435 (7), and Tyr438 (7) (**Figure 5-12**).

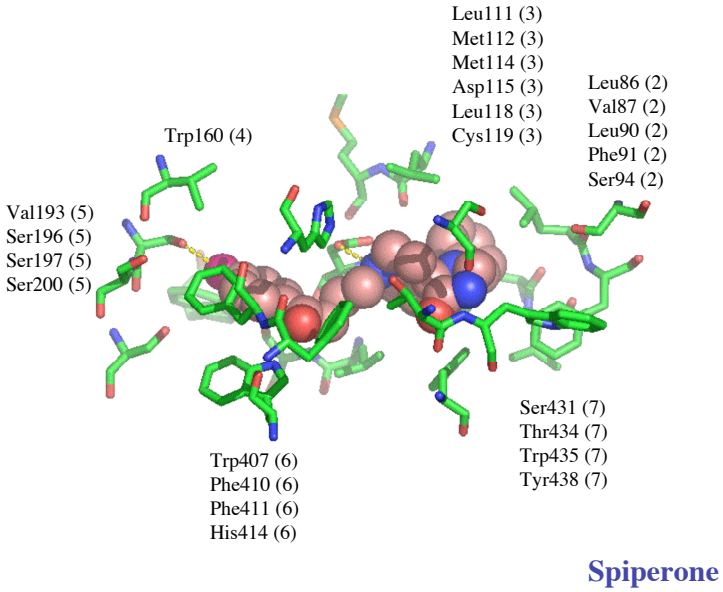

Figure 5-12. The 5.5 Å binding site of Spiperone to the human D_4 dopamine receptor. The numbers in the brackets indicate the TM helices to which the residues belong to.

Sulpiride: Sulpiride is a class I antagonist meaning it binds in the putative agonist binding site with minimal extension into the TM2 and 7 aromatic micro-domain. Sulpiride has a salt bridge to the TM3 Asp115 (2.9 Å). The sulfonamide portion of the ligand interacts well with Ser196 in TM5. There are two hydrogen bonds of 2.8 Å and 3.1 Å. Cys119 is interacting with the ligand; the hydrogen bond is 3.3 Å. The strength of these hydrogen bonds is, however, a different issue. The remainder of the residue provide a mostly hydrophobic pocket. The residues in close proximity include: Leu111 (3), Met114 (3), Val416 (3), Leu118 (3), Cys119 (3), Trp160 (4), Tyr192 (5), Val193 (5), Ser197 (5), Ser200 (5), Trp407 (6), Phe410 (6), Phe411 (6), His414 (6), Ile415 (6), and Thr434 (7) (**Figure 5-13**).

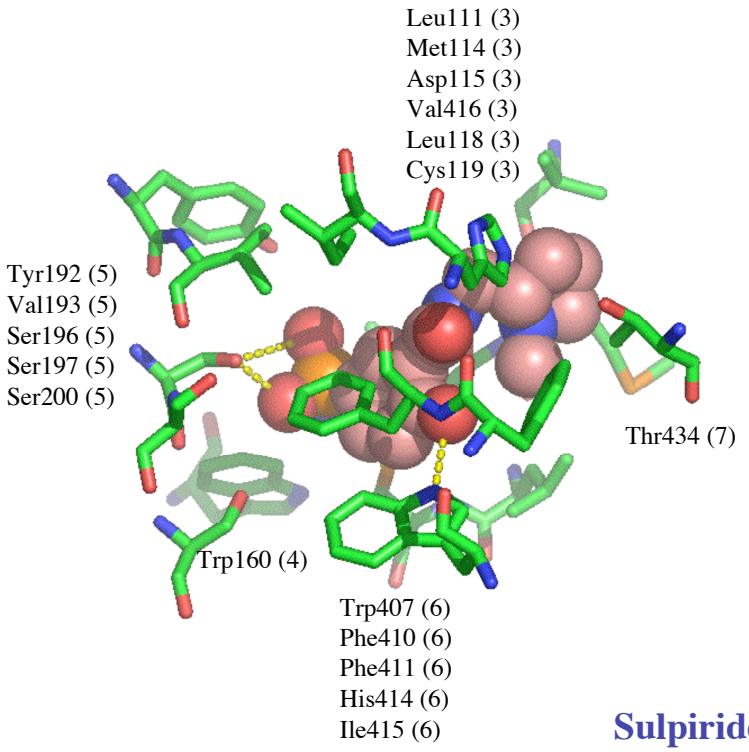

Figure 5-13. The 5.5 Å binding site of Sulpiride to the human D_4 dopamine receptor. The numbers in the brackets indicate the TM helices to which the residues belong to.

Comparisons of Binding Site of Agonists vs. Antagonists: Experimental studies have outlined the binding site for agonists and antagonists. The putative agonist-binding site is located between TM3, 4, 5, & 6, and some residues in the EC2 loop (assuming this loop closes during the process of activation). We have classified antagonists into two categories: Class I & II. Class I antagonists, such as Clozapine bind in the putative agonist binding pocket meaning they occupy the void between TM3, 4, 5 and 6. Class II antagonists, such as Haloperidol consists of two aromatic domains connected by a linker, which possess a protonated amino group. These antagonists bind in the cavity between

TM2, 3, 4, 5, 6, and 7. There are two aromatic micro domains (pictures of aromatic micro domains goes here). The first aromatic micro-domain is located in TM4 and TM6, which is composed of the very symmetric Trp160 (4), Ala164 (mutated in this receptor) (4), Trp407 (6), and Phe411 (6). This aromatic micro-domain stabilizes one of the aromatic rings of the class II antagonists. TM3 provides the salt bridge to TM3 Asp115, which stabilizes the ligand in place. TM5 provides weak interactions with heteroatom functionalities such as halogens on the rings of class II antagonists. These interactions are weak but important in recognition of the correct aromatic domain for docking into the cavity. The second aromatic micro-domain composed of Phe91 (2), Leu111 (mutated in this receptor) (3), Trp435 (7), and Tyr438 (7) stabilize the second aromatic ring group of the class II antagonists.

Comparison of agonists binding site: There is very little difference in the putative agonist-binding site of different agonists. The agonists studied, (dopamine, 7-OH DPAT, Apomorphine) all possess protonated amino groups, which are salt bridged to TM3 Asp115. All of these ligands studied form favorable hydrogen bonding interactions to a network of TM5 serines, although this is not an absolute necessary for agonism. There is, in every case studied, favorable interaction from the first aromatic micro-domain located in TM4 and TM6. A residue that has not been appreciated in drug design is His414 (6). The presence of this residue contributes greatly to ligand binding, yet it appears that there few agonists utilize this residue effectively. It is important to note that the agonists studied effectively interact with both Ser196 and Ser200 in TM5. The interactions to Ser197, the third TM5 serine, are too long to be considered a hydrogen bond (on the

order of ~ 5 Å). Under no circumstance, due to structural constraints, can all three serines effectively interact with the agonists studied. It appears that there could at most be two hydrogen bonds to the TM5 serines. Although in our structure Ser197 is not participating in any interactions, it is possible that in a slightly different structure, perhaps one resulting from activation, there could be interactions to Ser197 and Ser200 as opposed to Ser196 and Ser200. All agonists studied cause strong coupling of TM3 and 5. None of the agonists studied block TM3 and 6 motions. Based on structural studies of rhodopsin, it has been established that a motion between TM3 and 6 are essential for activation. The coupling of TM3 and 6 by agonists causes a decrease in distance between TM3 and 5 while allowing for motion between TM3 and 6.

Comparison of antagonists binding site: The antagonists studied were classified into two categories: Class I antagonists (exemplified by Clozapine), which bind in the putative agonist binding pocket; and class II antagonists (exemplified by Haloperidol), which bind in the cavity between TM2, 3, 4, 5, 6, and 7.

Class I Antagonists: the Clozapine-like antagonists salt bridge to the TM3 Asp115 with their protonated amino group. They do not have two aromatic rings and therefore only utilize the first aromatic micro-domain between TM4 and 6. As is the case with both Class I and II antagonists, they form only one weak interaction with the TM6 serine network. In our models the interaction may be with Ser196 or Ser200. At first glance, it appears that both the number of and strength of the interactions with the TM5 serines

may be important for activation. Interestingly, however, the situation is more complicated than it appears; Strange et al. have identified agonism from a non-hydroxylated form of the DPAT series. The critical distinguishing feature of an agonist vs. an antagonist appears to be its relative position to TM6. Class I antagonists burry their aliphatic domain deep into the conserved TM6 WXXFF motif. Experimental studies of rhodopsin suggest that motion of TM3 and 6 is necessary for activation. The binding of antagonists at the TM6 WXXFF would prevent any motion, specifically the hinge motion between TM3 and TM6 that is necessary for activation. It appears that the presence of one hydroxyl/one hydrogen bond donor/acceptor is not an absolute necessity for antagonism. The class I antagonists are further stabilized by Leu111 in TM3.

Class II Antagonists: the Haloperidol-like antagonists salt bridge to TM3 Asp115 with their protonated amino group. They possess two aromatic ring units. In most cases, only one of the aromatic rings is halogenated, and this is the ring that binds to the first aromatic micro-domain, with the second ring binding in the second aromatic micro-domain. The halogenated ring binds effectively into the cavity between TM4 and 6 and forms weak interactions with either Ser193 or Ser197 in TM5. It gains stability from the presence of TM4 Trp160 and Ala164 and TM6 Trp407 and Phe411. In some cases His414 (6) may also stabilize the class II antagonists. The non-halogenated aromatic domain is located in the void between TM2 and TM7. It gains stabilization from Phe91 (2), Leu111 (3), Trp435 (7), and Tyr438 (7). As is the case with the class I antagonists, class II antagonists prevent motion between TM3 and TM6 by burying their aliphatic portion between TM3 and TM6, thereby preventing interaction of these helices. There is

very little difference between the binding sites of the class II antagonists, although some utilize the cavity better than others.

Ligand	B.E. (Kcal/mol)
7OHDPAT	-38.8
Apomorphine	-50.1
Clozapine	-33.1
Dopamine	-47
Fenoldopam	-33.9
Haldol	-65.5
Raclopride	-39.5
SCH	-46.6
SKF	-35.7
Spiperone	-56.5
Sulpiride	-49.8

Table 5-2. Binding energies in kcal/mol for a library of 10 ligands to the human D_4 dopamine receptor.

D_4 Receptor Experimental Ranking:

Spiperone~Haldol~Apomorphine>Clozapine~Sulpiride~Dopamine~Fenoldopam>

Raclopride~SCH23390~7-OHDPAT~SKF38393

D_4 Receptor Theory Ranking:

Haldol~Spiperone~Apomorphine>Sulpiride~SCH23390~Dopamine>Fenoldopam~

SKF38393~Clozapine~Raclopride~7-OHDPAT

Appendix VI: The Predicted Structure of the Human D_5 Dopamine Receptor

The Predicted Structure of the Human D_5 Dopamine Receptor

M. Yashar S. Kalani [§,*], Nagarajan Vaidehi[*] & William A. Goddard III[**]

* Materials and Process Simulation Center, Beckman Institute, California Institute of Technology, Pasadena, CA 91125

§ Johns Hopkins University School of Medicine, Baltimore, MD 21205

****To whom correspondence should be addressed (e-mail: wag@wag.caltech.edu)**

Results:

We have predicted the structure and binding site of 10 agonists and antagonists (Shown in **Figure 6-1**) in D_5DR using the methods detailed in the Methods and Materials section. **Figure 6-2** shows the 3-D atomic resolution structure of the human D_5DR modeled from the predicted D_2DR structure obtained using the Membstruk procedure and the predicted binding site of dopamine determined using the HierDock procedure. We refer to this predicted structure as D_5DR. Using the D_5DR structure, we have identified the agonist and antagonist-binding sites for a library of 11 ligands (**Figure 6-1**), calculated their binding energies, and the criteria for agonist and antagonist activation of the receptor. The antagonists studied in this publication are divided into two classes: 1) class I antagonists that are bulky and bind in a similar location as agonists, exemplified by Clozapine, and 2) class II antagonists that consists of two aromatic moieties connected by a flexible linker chain exemplified by haloperidol. In this paper we give details of the

residues in the binding site of all the 10 ligands and analyze the similarities and differences in their binding sites.

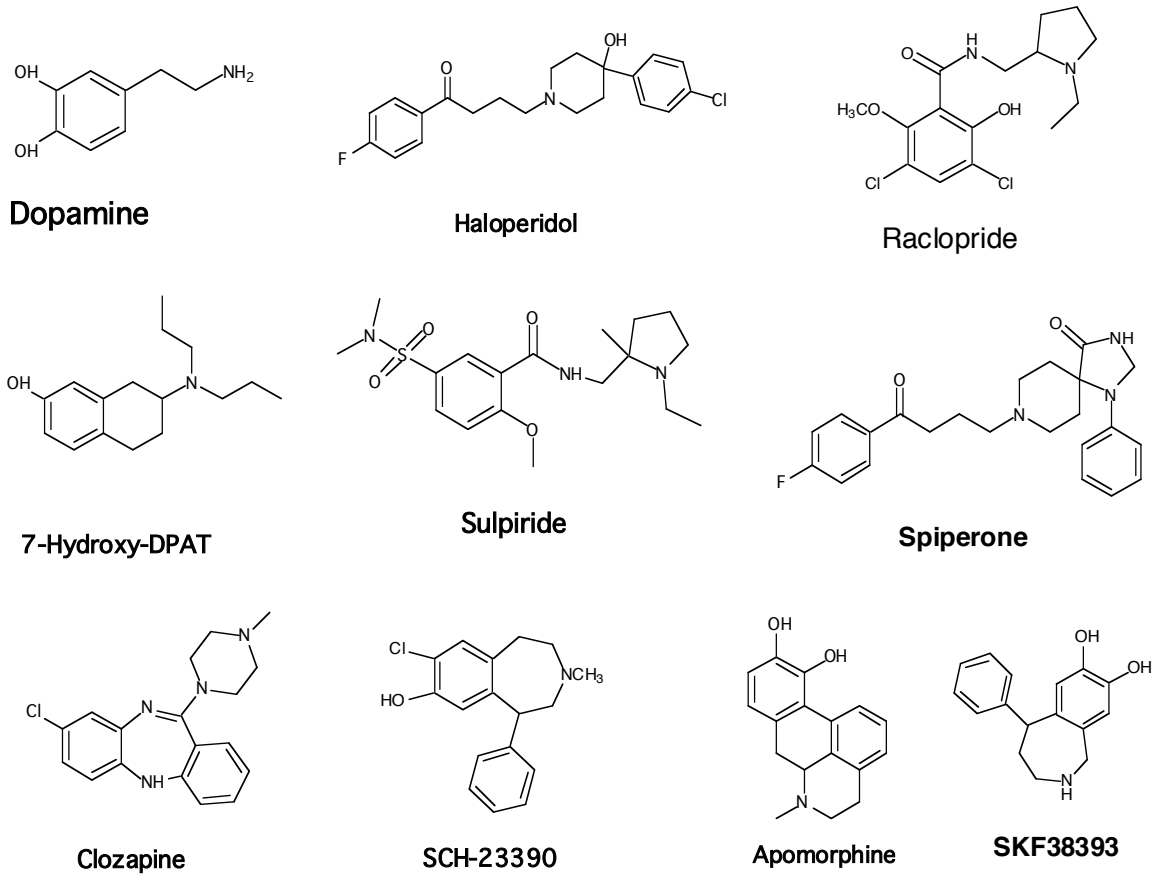

Figure 6-1. 10 agonists and antagonists studied for the human Dopamine D_5 receptor.

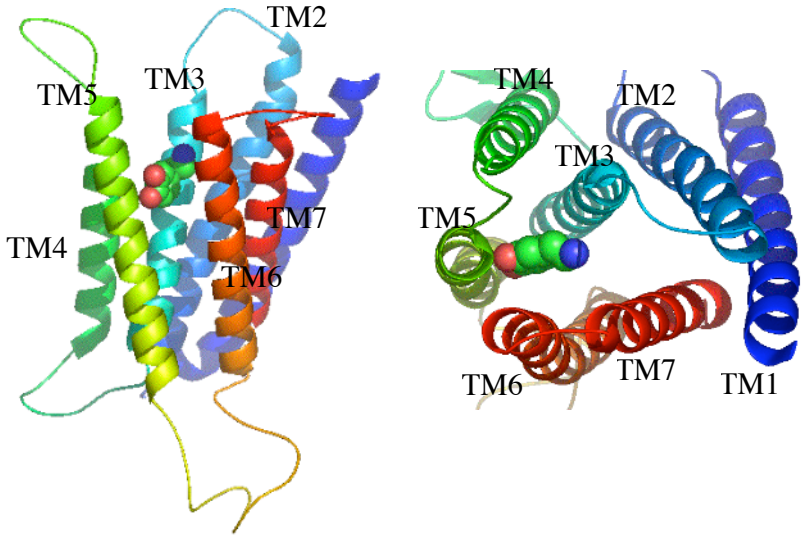

Figure 6-2. Predicted binding site of Dopamine (shown in sphere) in the predicted structure of human dopamine D_5 receptor.

In the preliminary studies, we have validated these methods for bovine rhodopsin, human ß-2 adrenergic receptor, human s1p (sphingolipid) and lpa (lysophosphatidic acid) receptors, the human D2 dopamine receptor (Kalani 2003), and 10 mouse olfactory receptors (Vaidehi 2002, Floriano 2000, Floriano 2003, Hall 2003). The results are in good agreement with available experimental data, indicating a good description of the binding site and relative binding energies of various ligands.

Prediction of the Structure of Human D_5DR:

The Membstruk procedure used to predict the structure is detailed in Vaidehi 2002. The homology modeling procedure used to model the structure of the D_5 receptor based on the D_2 (MS) structure is outlined elsewhere. The TM2nDs procedure (Vaidehi 2002, Trabanino 2003) was utilized to identify the transmembrane (TM) spanning regions based on a hydrophobic analysis of the sequence. A seven helical motif was identified (below) ranging from 19-29 residues per helix. The highlighted residues represent TM helices, while the intervening sequences are loop regions. The same transmembrane predictions were used in the alignment to the human D_2 structure to perform homology modeling.

MLPPGSNGTAYPGQFALYQQLAQGNAVGGSAGAPPLGPSQVVTACLLTLLIIWT
LLGNVLVCAAIVRSRHLRANMTNVFIVSLAVSDLFVALLVMPWKAVAEVAGYW
PFGAFCDVWVAFDIMCSTASILNLCVISVDRYWAISRPFRYKRKMTQRMALVMV
GLAWTLSILISFIPVQLNWHRDQAASWGGLDLPNNLANWTPWEEDFWEPDVNA
ENCDSSLNRTYAISSSLISFYIPVAIMIVTYTRIYRIAQVQIRRISSLERAAEHAQSCR
SSAACAPDTSLRASIKKETKVLKTLSVIMGVFVCCWLPFFILNCMVPFCSGHPEGP
PAGFPCVSETTFDVFVWFGWANSSLNPVIYAFNADFQKVFAQLLGCSHFCSRTPV
ETVNISNELISYNQDIVFHKEIAAAYIHMMPNAVTPGNREVDNDEEEGPFDRMFQ
IYQTSPDGDPVAESVWELDCEGEISLDKITPFTPNGFH

Scheme 6-1. Predicted transmembrane regions are highlighted below in the human D_5 dopamine receptor. (the n-termini are not completely clear).

The TM prediction was utilized in building seven canonical α-helices and optimized using the procedure described in Vaidehi 2002. The helices were bundled in explicit bilayer of dilaurylphosphatidylcholine lipid molecules to mimic the biological membrane. The structural factors such as helical bend, helical tilt etc., of the predicted structure of D_5DR (homology) structure compared to the crystal structure of rhodopsin are summarized in **Table 6-1**.

TM Helix	Helical Bend	Plane Tilt	HPM Angle	HPM Mag.	HPM Fit	Plane CM Dist.	Plane CM Angle	CM Fit
1	6.2	39.0	73.5	10.1	0.0	15.5	0.0	3.1251
2	9.9	36.1	29.4	6.8	0.0	9.9	31.9	0.0536
3	4.8	13.8	15.3	3.6	0.0	4.4	120.6	2.0260
4	31.2	23.4	72.3	11.3	0.0	14.1	114.9	-4.1285
5	10.5	8.1	-99.6	9.3	0.0	14.9	182.7	5.0534
6	24.9	12.5	-177.4	7.5	0.0	11.7	236.5	1.9978
7	35.1	24.9	169.9	4.7	0.0	12.6	296.0	-8.1273

Centered Comparison Table

TM Helix	HPM Angle	HPM Mag.	Helical Bend	P. Face Deg.
Helix 1	92.6	4.1	3.2	252
Helix 2	51.9	4.0	9.1	151
Helix 3	-16.2	2.5	0.0	69
Helix 4	-89.4	2.4	10.5	243
Helix 5	-65.3	4.9	21.5	222
Helix 6	-158.7	5.0	19.7	174
Helix 7	-26.0	1.6	29.2	147

Table 6-1. Comparison of the D_4DR with the crystal structure of bovine rhodopsin.

RMS height of TMR: 30.8

RMS radius of TMR: 12.4

From **Tables 6-1** it is clear that the helical bends are very different for D_5DR compared to rhodopsin. The volume of the TM barrel for D_5DR is 14857.9 $Å^3$. There is one disulfide bond between Cys113 and Cys217 in EC2. Rhodopsin has a volume of

11,807.7 $Å^3$. The calculated RMS in the coordinates of the C_{α} atoms of the D_5DR structure compared to the crystal structure of rhodopsin is 6.94 Å and a total residue RMS of 7.74 Å (all atoms).

Prediction of the putative binding site for dopamine in D_5DR: The Hierdock2.0 procedure (Vaidehi 2002) was utilized to scan all the D_5DR models as described in Materials and Methods section. We discuss the details of the predicted binding site in D_5DR (homology) model for all the 11 ligands studied in this paper to capture the same binding as those identified in the D_2 (MS) for comparison reasons and explanations of receptor specificity in future chapters.

Dopamine: Dopamine is the endogenous ligand of the dopamine receptors. It binds in the putative agonist binding site located between TM3, 4, 5, and 6. There are two main contacts that energetically stabilize dopamine in this docked conformation: 1) salt bridge between the TM3 Asp120 (bidentate, 2.8 Å and 2.9 Å), and 2) a network of hydrogen bonds to the TM5 Ser229, Ser230, and Ser233. In our structure Ser229 and Ser233 both have 2.9 Å interactions with the catechol hydroxyls. Ser230 is ~ 5 Å away and the interactions it has with the catechol hydroxyls are too far to be considered hydrogen bonds, although a rotation of TM5 will allow Ser230 to form excellent interactions with the catechol of dopamine. Under no circumstance can all three serines in TM5 form hydrogen bonds with reasonable distances and angles; at no time can there be more than 2 hydrogen bonds to the sequence of serines in TM5. Interaction between Ser229 and

Ser230 may result during steps leading to or resulting from activation. Other residues in the binding pocket provide mostly hydrophobic packing for the ligand. These residues include Trp116, and Ser124 (TM3), Phe173 (TM4), Tyr225, and Ala226 (TM5), Trp309, Phe313, and Asn316 (TM6). The first phenylalanine of the conserved WXXFF motif, Phe312, is slightly greater than 5.5 Å away from dopamine. Asn316 in TM6 is providing a very strong component of the binding energy of dopamine to the receptor. Assuming Asp120 forms a bidentate salt bridge, or a salt bridge and a hydrogen bond to the amino group of dopamine, the interaction with Asn316 fulfils the ability of the amino group to form favorable interactions with any other residues. It must be noted, however, that the presence of Trp116 (3) may be the reason why dopamine exhibits reduced binding to the D_5 subtype of the receptor compared to the D_2 receptor. The presence of the Trp116 (3) provides Asp120 (3) an alternate hydrogen bond donor, meaning the aspartate will share its electron density between the protonated amino group and the indole and will not interact as efficiently with the primary amino group. Interestingly, I predict that tertiary amino groups should have enhanced binding to this receptor since the presence of a single proton will not cause for competition for the aspartate electron density.

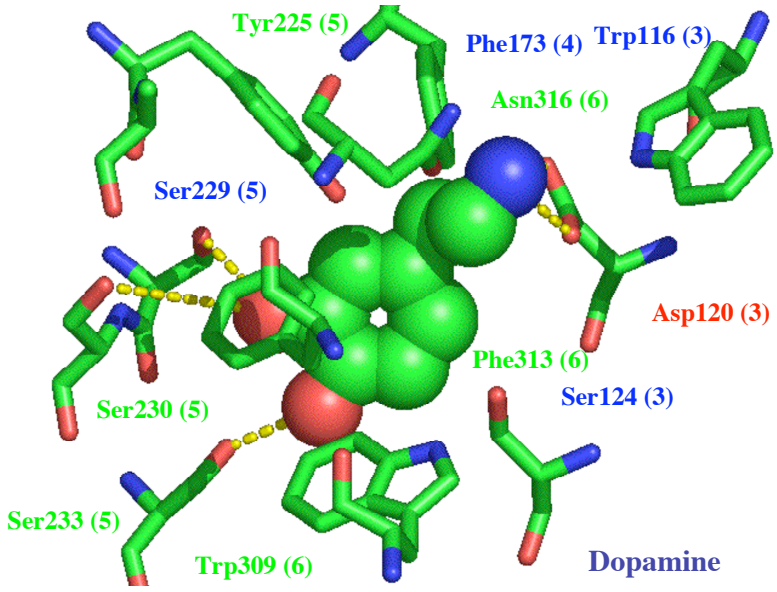

Figure 6-3. The 5.5 Å binding site of dopamine to the human D_5 dopamine receptor. The numbers in the brackets indicate the TM helices to which the residues belong to.

7-OH DPAT: The ligand binds in putative agonist binding site located between TM3, 4, 5, and 6. The protonated amino group of 7-OH DPAT is salt bridged to the TM3 Asp120 (2.8 Å). The other major polar contacts are to the conserved TM5 serines 229, 230 and 233. There are two hydrogen bonds, one 4.3 Å to Ser229 and 2.9 Å to Ser233. The interaction to Ser230 is ~ 6 Å and is too long to be considered a hydrogen bond. The remainder of the residues in the cavity are mainly hydrophobic residues that provide stabilization for the aromatic and aliphatic rings of the ligand. The residues in close hydrophobic contact of the ligands are Trp116, Phe119, Cys123, Ser124, Ile128 (all in TM3), Trp165 and Phe173 (TM4), Tyr225, Ile232 (both in TM5), Trp309, Phe312,

Phe313, Asn316 (all TM6), Val345, Trp349 (both in TM7) (**Figure 6-4**) which provide a mainly hydrophobic pocket.

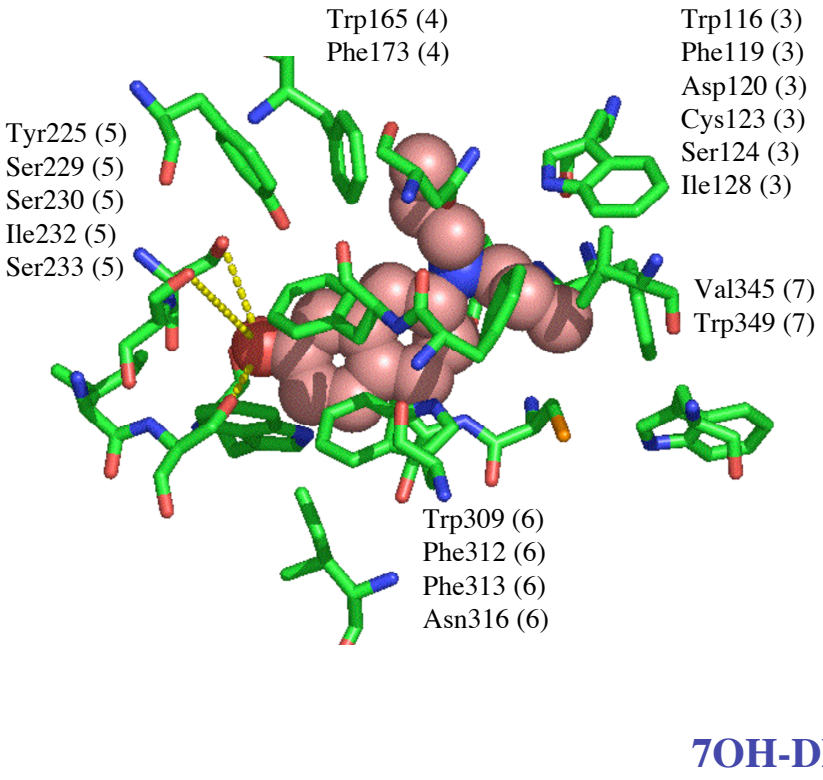

Figure 6-4. The 5.5 Å binding site of 7-OH DPAT to the human D_5 dopamine receptor. The numbers in the brackets indicate the TM helices to which the residues belong to.

Apomorphine: The ligand binds in the putative agonist binding site located between TM3, 4, 5, and 6. The protonated amino group of Apomorphine is salt bridged to the TM3 Asp120 (2.8 Å). The other major polar contacts are to the conserved TM5 serines 229, 230 and 233. There are three hydrogen bonds: Ser299 (4.1 Å) and Ser233 (3.1 and 2.8 Å) to the hydroxyl groups on Apomorphine. The contact to Ser230 is ~ 6 Å apart. Other residues form a most hydrophobic pocket around the ligand; these residues include: Trp116, Phe119, Cys123, Ser124, Ile128 (all in TM3), Trp165 and Phe173 (TM4),

Tyr225, Ile232 (both in TM5), Trp309, Phe312, Phe313, Asn316 (all TM6), Val345 (TM7) (**Figure 6-5**), which provide a mainly hydrophobic pocket. Mutational experiments have shown that Phe312Ala and Phe313Ala mutants show substantial reduction in binding constants for Apomorphine (Cho et al 1995). This shows that these residues are important in ligand recognition.

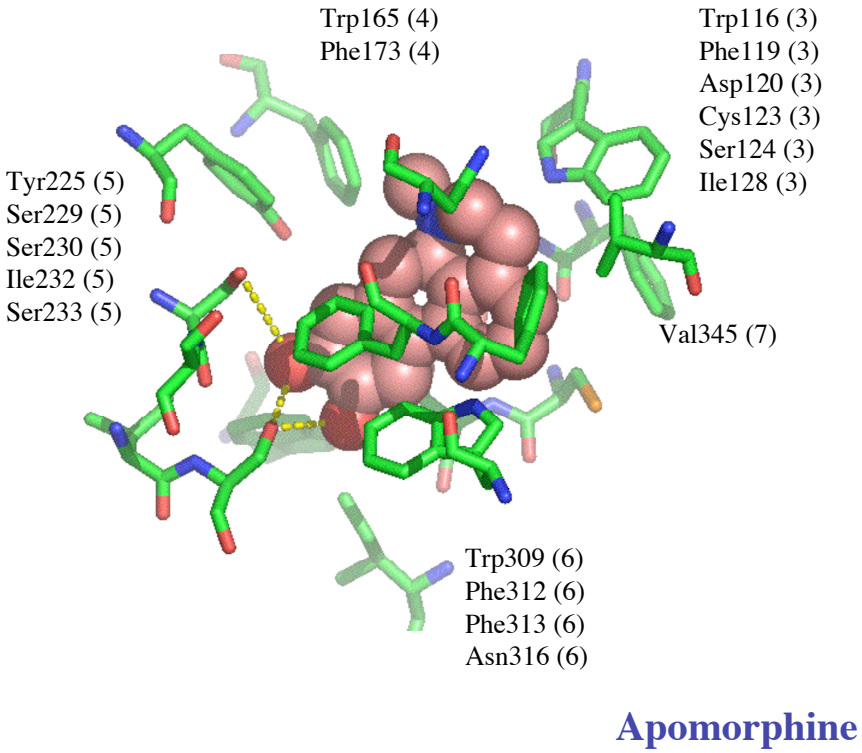

Figure 6-5. The 5.5 Å binding site of Apomorphine to the human D_5 dopamine receptor. The numbers in the brackets indicate the TM helices to which the residues belong to.

Clozapine: Clozapine is a class I antagonist, meaning it binds in the putative agonist binding site located between TM3, 4, 5, and 6. There is, as always, an amino group salt

bridged to the TM3 Asp120 (2.8 Å). As is the case for all antagonists studied, there is a lone hydrogen bond to the sequence of TM5 serines. Although the hydrogen bond may be to either Ser229 or Ser233, in our structure, the more reasonable distance and angle are for the interaction between Ser229 and the heteroatom (3.2 Å). There is a third interaction, which although cannot be categorized as a hydrogen bond, is energetically significant; this is a 3.2 Å interaction between Trp309 in TM6 and the hydrogen of the ring in Clozapine. Ser124 is ~5 Å apart from the other nitrogen in the Clozapine ring. The remainder of the residues provide a mostly hydrophobic pocket for the ligand. There residues in close proximity of the Clozapine ligand are Trp116, Phe119, Cys123, Ser124, Ile128 (all in TM3), Trp165 and Phe173 (TM4), Tyr225, Ile232 (both in TM5), Trp309, Phe312, Phe313, Asn316 (all TM6), Val345, Trp349 (both in TM7) (**Figure 6-6**) which provide a mainly hydrophobic pocket.

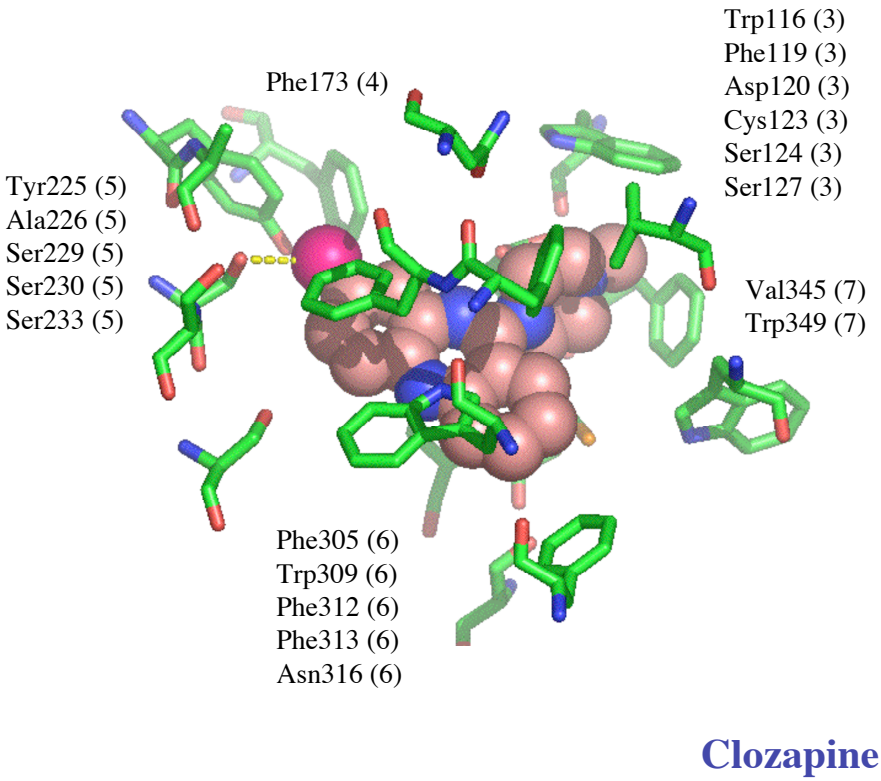

Figure 6-6. The 5.5 Å binding site of Clozapine to the human D_5 dopamine receptor. The numbers in the brackets indicate the TM helices to which the residues belong to.

Fenoldopam: Fenoldopam is an agonist, meaning it binds in the putative agonist binding site located between TM3, 4, 5, and 6. There is a bidentate salt bridge between Asp120 (TM3) with and the amino group with distances of 2.6 and 2.8 Å. Ser124 (TM3) is hydrogen bonded to heteroatom with a length of 3.2 Å. The catechol portion is hydrogen bonded to the TM5 serine networks of Ser229, Ser230, and Ser233 (TM5). There is a 3.1 Å interaction and a 2.8 Å interaction to the catechol by Ser229 and Ser233, respectively. Ser230 is too far to form a hydrogen bond to the ligand. Interestingly, it is possible for the phenol group to be pi stacked between Phe312 and Phe313 (TM6) and for its

hydroxyl group to interact via a hydrogen bond with Asn316 (TM6). The remainder of the residues in the cavity provide a mostly hydrophobic pocket for the drug. These residues include: Trp116 (3), Ile121 (3), Ile128 (3), Trp165 (4), Ile169 (4), Phe173 (4), Tyr225 (5), Ala226 (5), Ile232 (5), Phe305 (6), Trp309 (6), and Val345 (7) (**Figure 6-7**).

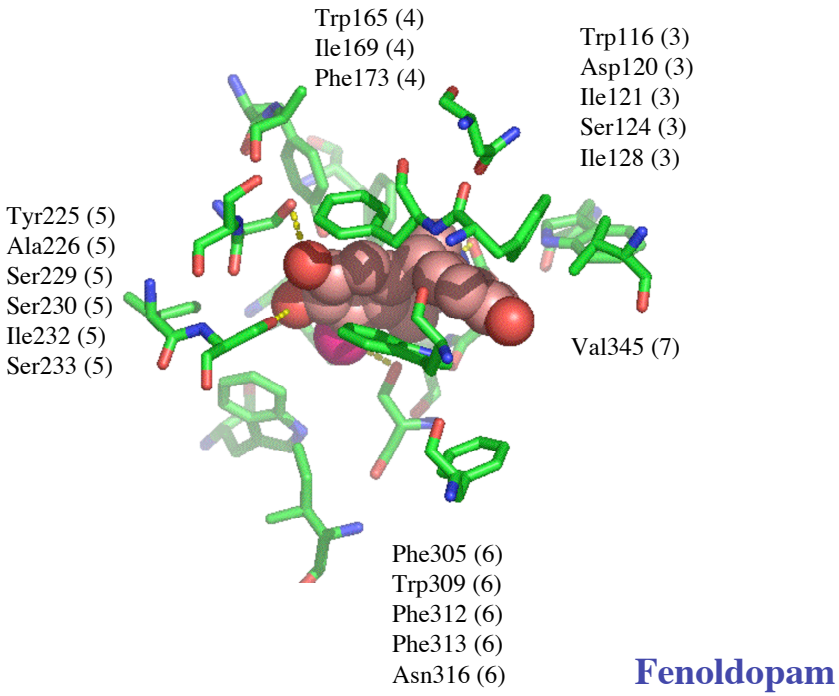

Figure 6-7. The 5.5 Å binding site of Fenoldopam to the human D_5 dopamine receptor. The numbers in the brackets indicate the TM helices to which the residues belong to.

Haloperidol: The ligand binds in the putative antagonist-binding site located between TM2, TM3, TM4, TM5, TM6, and TM7. Class II antagonists such as Haloperidol are composed of two aromatic domains connected by a linker domain, which has a protonated amino group. The protonated amino group of Haloperidol is salt bridged to the TM3 Asp120 (2.9 Å). There are several heteroatom contacts that are typically too weak

to be considered hydrogen bonds. There is a long hydrogen bond between the hydroxyl of Haloperidol and TM6 Trp309 (4.0 Å). Haloperidol and other class II antagonists are predicted to have low affinities to the D_1 receptor; and, indeed experimental studies are in accordance with this prediction. The presence of Phe119 (TM3) blocks the cavity usually occupied by the linker and the second aromatic domain. The blocking of the cavity causes the ligand to contort on itself and not fit properly in the cavity. As a result the interaction with the serine network is absent. The absence of contacts with the serine network is deemed unimportant for the function of the antagonist, and as a result Haloperidol would continue to function as an antagonist, but it would have significantly reduced affinity to this receptor. The class I antagonist, apparently, would bind with a greater affinity to this receptor. Other residues form a mostly hydrophobic pocket around the ligand; these residues include: Trp97 (2), Lys298 (2), Trp116 (3), Cys123 (3), Ser124 (3), Trp165 (4), Ile169 (4), Phe173 (4), Tyr225 (5), Ser229 (5), Ser230 (5), Ile232 (5), Ser233 (5), Phe312 (6), Phe313 (6), Asn316 (6), Asp342 (7), Val343 (7), Val345 (7), Trp346 (7), Trp349 (7), Ala350 (7) (**Figure 6-8**).

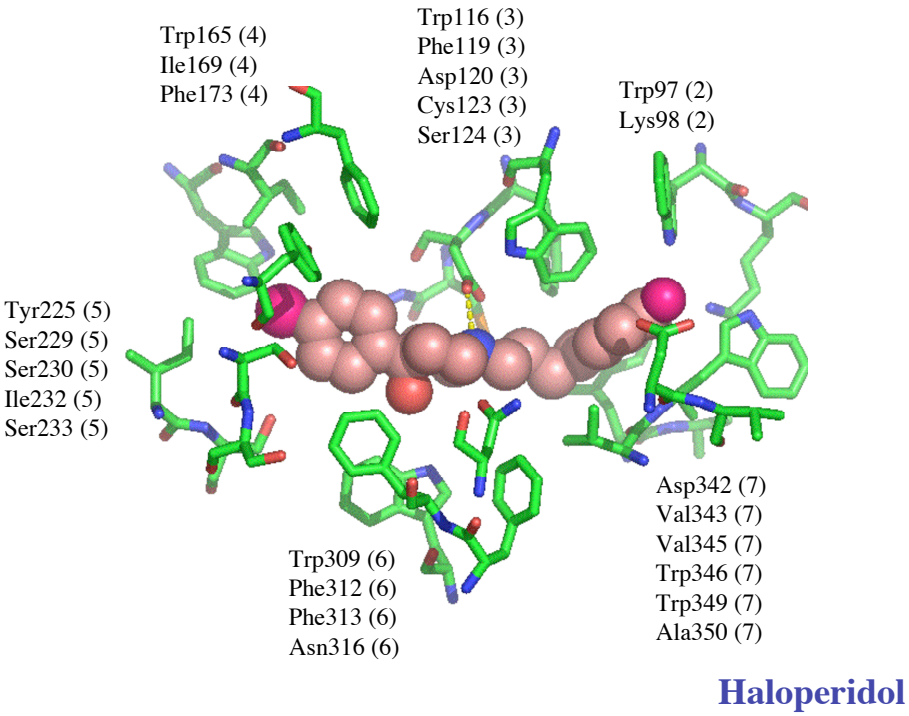

Figure 6-8. The 5.5 Å binding site of Haloperidol to the human D_5 dopamine receptor. The numbers in the brackets indicate the TM helices to which the residues belong to.

Raclopride: Raclopride binds in the class I antagonist-binding site, although it begins to extend to the TM2 and 7 aromatic micro-domain. The critical contact points are the salt bridge between TM3 Asp120 and the protonated amino group of the ligand (2.8 Å), and interactions with the TM3 Ser124 (3.9 Å) and TM5 Ser299 (3.8 Å) and Ser233 (3.8 Å), the latter of which are too weak to be considered a hydrogen bond. Tyr225 in TM5 is in proximity of heteroatom of the ligand and may form weak hydrogen bonds with the ligand. The remainder of the residues provide a mainly hydrophobic pocket for the remainder of the ligand. The residues in close proximity of the ligand include: Trp116 (3), Ser127 (3), Ile128 (3), Trp165 (4), Ile169 (4), Phe173 (4), Tyr225 (5), Ser229 (5), Ser230 (5), Ile232 (5), Ser233 (5), Trp309 (6), Phe312 (6), Phe313 (6), Asn316 (6),

Asp342 (7), and Val345 (7) (**Figure 6-9**). Raclopride fits nicely into the cavity and does not clash with Phe119 in TM3. It is predicted that the shorter antagonists, Clozapine and the likes, will have higher affinity than the class II antagonists to this class of the receptors.

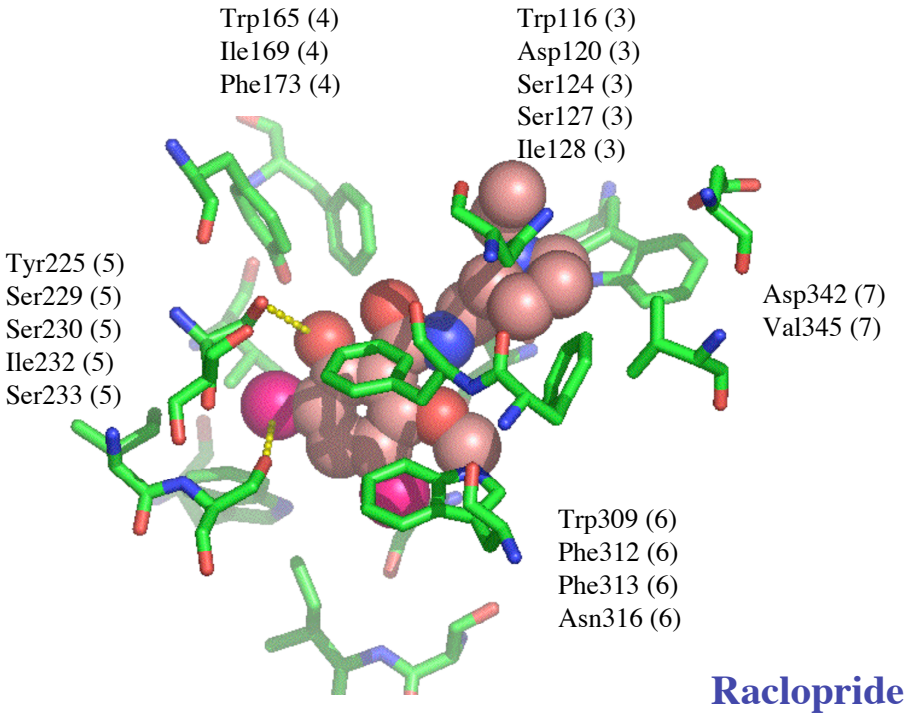

Figure 6-9. The 5.5 Å binding site of Raclopride to the human D_5 dopamine receptor. The numbers in the brackets indicate the TM helices to which the residues belong to.

SCH-23390: SCH-23390 is a class I antagonist. It forms a salt bridge with the TM3 Asp120 with a distance of 2.8 Å. There are two hydrogen bond contacts with the 5th transmembrane domain. There are two 3.3 Å interaction with Ser2229 and Ser233 (5). Tyr225 (5) is in close proximity of ligand heteroatom and can hydrogen bond with them.

The remainder of the residues create a mostly hydrophobic pocket for the ligand, with Phe312 (6) and Phe313 (6) forming excellent Van der Waals interactions with the phenyl substituent of the ligand. Other amino acids in the cavity include: Trp116 (3), Phe119 (3), Ser124 (3), Phe173 (4), Ala226 (5), Ser230 (5), Trp309 (6), Asn316 (6), Cys317 (6), Val345 (7) (**Figure 6-10**). There is no clash between the ligand and Phe119 (3) since the ligand does not extend into the domain between TM2 and TM7.

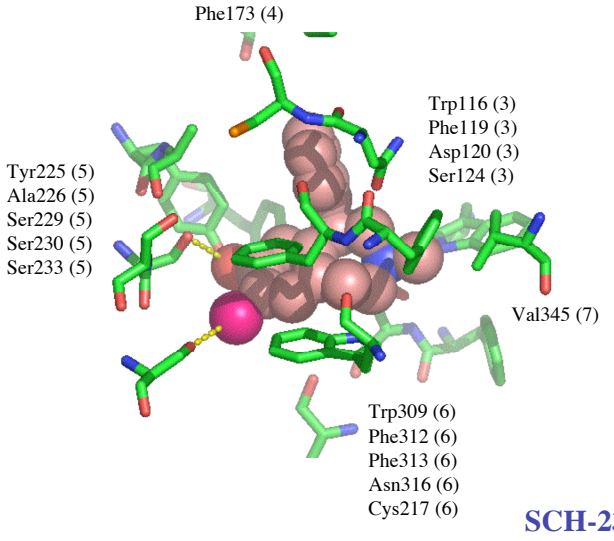

Figure 6-10. The 5.5 Å binding site of SCH-23390 to the human D_5 dopamine receptor. The numbers in the brackets indicate the TM helices to which the residues belong to.

SKF-38393: SKF-38393 is an agonist. It forms a bidentate salt bridge with Asp120 with a distance of 2.8 Å. There are three hydrogen bonds to Ser229 (3.1 Å) and Ser233 (3.0 and 3.4 Å). The phenyl substituent is pi stacked between Phe312 (6) and Phe313 (6). The remainder of the residues form a pocket around the ligand; these residues include: Trp116

(3), Ser124 (3), Phe173 (4), Tyr225 (5), Ala226 (5), Ser230 (5), Ile232 (5), Trp309 (6), Asn316 (6), Cys317 (6), Val345 (7) (**Figure 6-11**).

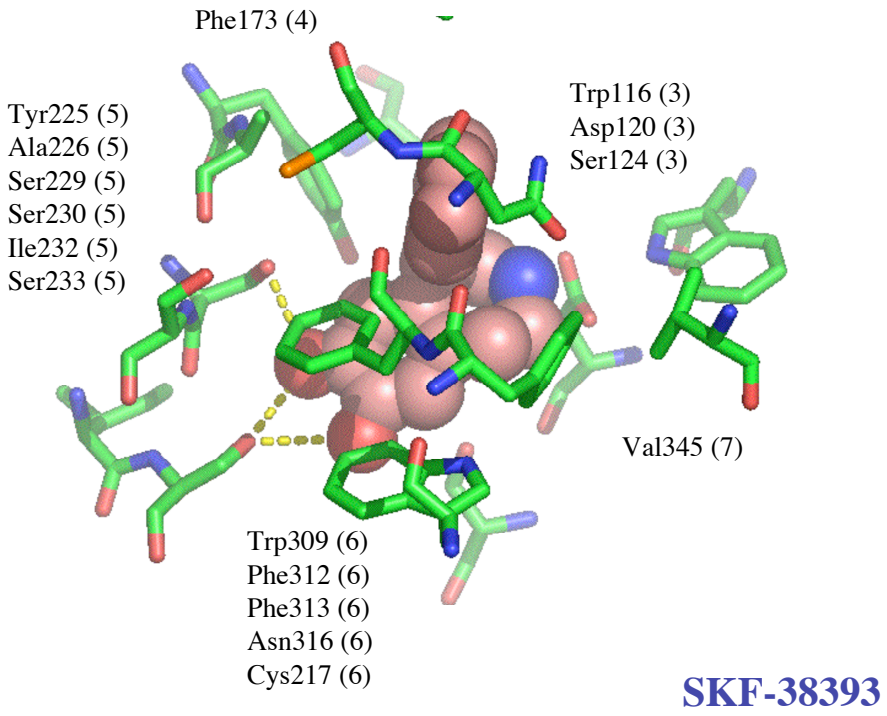

Figure 6-11. The 5.5 Å binding site of SKF-38393 to the human D_5 dopamine receptor. The numbers in the brackets indicate the TM helices to which the residues belong to.

Spiperone: Spiperone is a class II antagonist; meaning, it binds with its aromatic domains to the voids between TM2 & 7 and TM4 & 6, and it forms a salt bridge to TM3 and weak non-ionic interactions to TM5 and 6. The protonated amino group of the ligand

is salt bridged to the TM3 Asp120 (2.9 Å). Since class II antagonists are too large to bind into the D_5 class of dopamine receptors, the interaction with the TM5 serine network is not possible. The ligand clashes with Phe119 (3), which blocks the cavity, and as a result, the heteroatom is not in a position to interact with the serine networks. The remainder of the residues in the cavity form a mostly hydrophobic pocket for the ligand. The residues in the cavity include: Trp97 (2), Lys298 (2), Trp116 (3), Cys123 (3), Ser124 (3), Trp165 (4), Tyr225 (5), Ser229 (5), Ser230 (5), Ile232 (5), Ser233 (5), Trp309 (6), Phe312 (6), Phe313 (6), Asn316 (6), Asp342 (7), Val345 (7), Trp346 (7), Phe347 (7), Gly348 (7), Trp349 (7) (**Figure 6-12**).

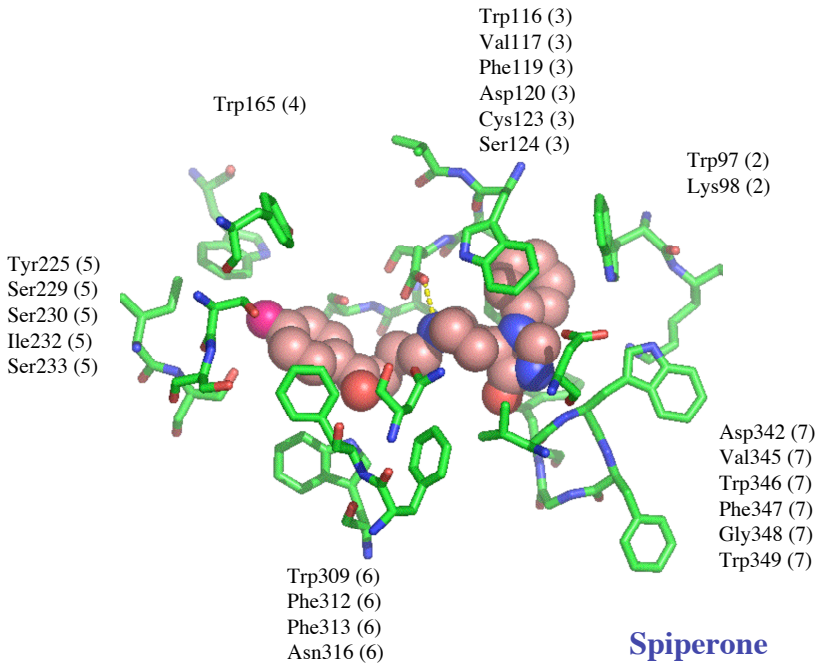

Figure 6-12. The 5.5 Å binding site of dopamine to the human D_5 Spiperone receptor. The numbers in the brackets indicate the TM helices to which the residues belong to.

Sulpiride: Sulpiride is a class I antagonist meaning it binds in the putative agonist binding site with minimal extension into the TM2 and 7 aromatic micro-domain. Sulpiride has a salt bridge to the TM3 Asp120 (2.8 Å). There is also the potential for a hydrogen bond between Asp120 and the amide hydrogen of the ligand. This interaction is also found in all the Sulpiride-like ligands. Although the addition of the amide was introduced to decrease the lipophilicity of these drugs, the addition seems to fair well due to the interactions it has with the Asp120 in TM3. The sulfonamide portion of the ligand interacts well with the sequence of serines in TM5. There are two hydrogen bonds of 2.8 Å and 3.8 Å to Ser229 and Ser233, respectively. There is also a hydrogen bond between Tyr225 (5) and the sulfonamide group; this interaction is 3.3 Å long. The strength of these hydrogen bonds is, however, a different issue. The remainder of the residue provide a mostly hydrophobic pocket. The residues in close proximity include: Trp116 (3), Phe119 (3), Ile121 (3), Ser124 (3), Ile128 (3), Trp165 (4), Ile169 (4), Phe173 (4), Tyr225 (5), Ser230 (5), Ile232 (5), Trp309 (6), Phe312 (6), Phe313 (6), Asn316 (6), Asp342 (7), Val345 (7) (**Figure 6-13**).

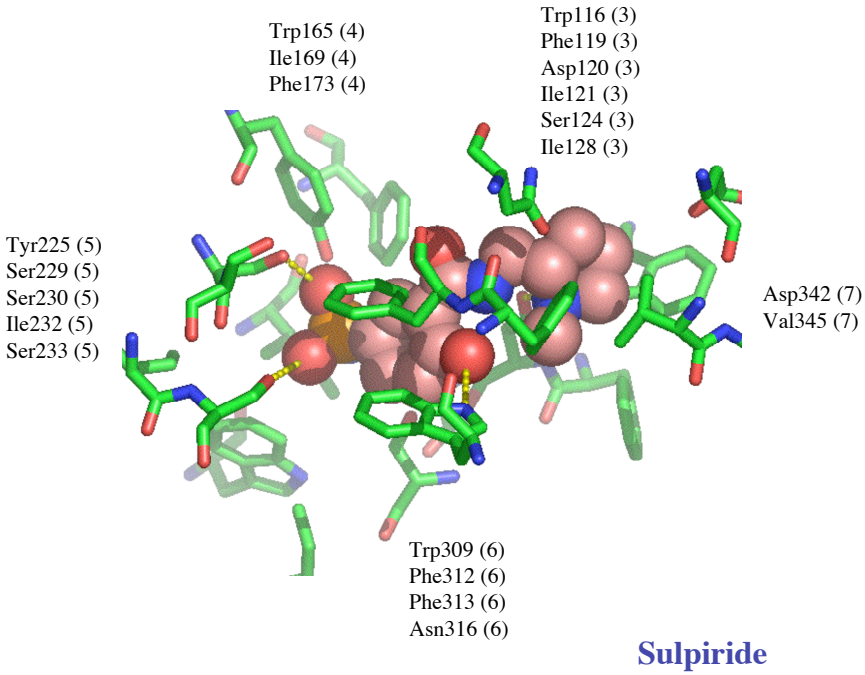

Figure 6-13. The 5.5 Å binding site of Sulpiride to the human D_5 dopamine receptor. The numbers in the brackets indicate the TM helices to which the residues belong to.

Comparisons of Binding Site of Agonists vs. Antagonists: Experimental studies have outlined the binding site for agonists and antagonists. The putative agonist-binding site is located between TM3, 4, 5, & 6, and some residues in the EC2 loop (assuming this loop closes during the process of activation). We have classified antagonists into two categories: Class I & II. Class I antagonists, such as Clozapine bind in the putative agonist binding pocket meaning they occupy the void between TM3, 4, 5 and 6. Class II antagonists, such as Haloperidol consists of two aromatic domains connected by a linker, which possess a protonated amino group. These antagonists bind in the cavity between TM2, 3, 4, 5, 6, and 7. There are two aromatic micro-domains. The first aromatic micro-domain is located in TM4 and TM6, which is composed of the very symmetric Trp165 (4), Phe173 (4), Trp309 (6), Phe312 (6), and Phe313 (6). This aromatic micro-domain

stabilizes one of the aromatic rings of the class II antagonists. TM3 provides the salt bridge to TM3 Asp120, which stabilizes the ligand in place. TM5 provides weak interactions with heteroatom functionalities such as halogens on the rings of class II antagonists. These interactions are weak but important in recognition of the correct aromatic domain for docking into the cavity. The second aromatic micro-domain composed of Trp97 (2), Trp346 (7), and Trp349 (7) stabilize the second aromatic ring group of the class II antagonists. It must be noted, however, that due to the presence of Phe119 (3) which blocks the cavity and does not allow for the longer ligands in class II to access the second aromatic micro-domain. Class II antagonists are not predicted to bind to this class of receptors.

Comparison of agonists binding site: There is very little difference in the putative agonist-binding site of different agonists. The agonists studied, (dopamine, 7-OH DPAT, and Apomorphine) all possess protonated amino groups, which are salt bridged to TM3 Asp120. All of these ligands studied form favorable hydrogen bonding interactions to a network of TM5 Serines, although this is not an absolute necessary for agonism. There is, in every case studied, favorable interaction from the first aromatic micro-domain located in TM4 and TM6. A residue that has not been appreciated in drug design is Asn316 (6). The presence of this residue contributes greatly to ligand binding, yet it appears that there few agonists utilize this residue effectively. It is important to note that the agonists studied effectively interact with both Ser229 and Ser233 in TM5. The interactions to Ser230, the third TM5 serine, are too long to be considered a hydrogen bond (on the order of ~ 5 Å). Under no circumstance, due to structural constraints, can all three serines

effectively interact with the agonists studied. It appears that there could at most be two hydrogen bonds to the TM5 serines. Although in our structure Ser229 is not participating in any interactions, it is possible that in a slightly different structure, perhaps one resulting from activation, there could be interactions to Ser230 and Ser233 as opposed to Ser229 and Ser233. All agonists studied cause strong coupling of TM3 and 5. None of the agonists studied block TM3 and 6 motions. Based on structural studies of rhodopsin, it has been established that a motion between TM3 and 6 are essential for activation. The coupling of TM3 and 6 by agonists causes a decrease in distance between TM3 and 5 while allowing for motion between TM3 and 6.

Comparison of antagonists binding site: The antagonists studied were classified into two categories: Class I antagonists (exemplified by Clozapine), which bind in the putative agonist binding pocket; and class II antagonists (exemplified by Haloperidol), which bind in the cavity between TM2, 3, 4, 5, 6, and 7.

Class I Antagonists: the Clozapine-like antagonists salt bridge to the TM3 Asp120 with their protonated amino group. They do not have two aromatic rings and therefore only utilize the first aromatic micro-domain between TM4 and 6. As is the case with both class I and II antagonists, they form only one weak interaction with the TM5 serine network. In our models the interaction may be with Ser229 or Ser233. At first glance, it appears that both the number of and strength of the interactions with the TM5 serines may be important for activation. Interestingly, however, the situation is more complicated

than it appears; Strange et al. have identified agonism from a non-hydroxylated form of the DPAT series. The critical distinguishing feature of an agonist vs. an antagonist appears to be its relative position to TM6. Class I antagonists burry their aliphatic domain deep into the conserved TM6 WXXFF motif. Experimental studies of rhodopsin suggests that motion of TM3 and 6 is necessary for activation. The binding of antagonists at the TM6 WXXFF would prevent any motion, specifically the hinge motion between TM3 and TM6 that is necessary for activation. It appears that the presence of one hydroxyl/one hydrogen bond donor/acceptor is not an absolute necessity for antagonism. The class I antagonists are further stabilized by Trp116 in TM3.

Class II Antagonists: this class of antagonists are predicted to not bind effectively to this receptor. The Haloperidol-like antagonists salt bridge to TM3 Asp120 with their protonated amino group. Due to the presence of Phe119 (3) in the third transmembrane region, the ligands are not able to extend into the cavity between TM2 and 7 and therefore will not bind to this receptor. In most cases, only one of the aromatic rings is halogenated, and this is the ring that binds to the first aromatic micro-domain, with the second ring would bind to the second aromatic micro-domain but Phe119 (3) does not allow for this binding in the second aromatic micro-domain. Since the ligand has little room to bind in the putative cavity, it fails to form adequate contacts to the TM5 serine network and is also expected to have lower efficacy as an antagonist. In some cases Asn316 (6) may also stabilize the class II antagonists. As is the case with the class I antagonists, class II antagonists prevent motion between TM3 and TM6 by burying their aliphatic portion between TM3 and TM6, thereby preventing interaction of these helices.

There is very little difference between the binding sites of the class II antagonists, although some utilize the cavity better than others.

Ligand	B.E. (Kcal/mol)
7OHDPAT	-153
Apomorphine	-176.2
Clozapine	-146
Dopamine	-165.7
Fenoldopam	-154.6
Haldol	NA
Raclopride	NA
SCH	-169.3
SKF	-159.2
Spiperone	NA
Sulpiride	NA

Table 6-2. Binding energies in kcal/mol for a library of 10 ligands to the human D_5 dopamine receptor. Due to the presence of the TM3 phenylalanine, long class II antagonists are unable to bind to this class of receptor.

D_5 Receptor Experimental Ranking:

SCH23390~SKF38393~Fenoldopam>Clozapine~Haldol~Apomorphine~Dopamine>Spiperone~Sulpiride

D_5 Receptor Theory Ranking:

Apomorphine~SCH23390~SKF38393~Fenoldopam~Dopamine~7-OHDPAT~Clozapine>Haldol~Raclopride~Spiperone~Sulpiride